personal buildup for

Force Motors Limited Library

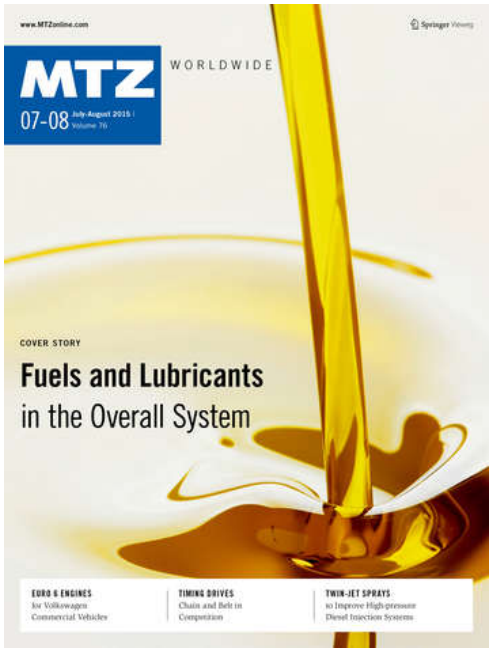

mtzw 7/2015, as epaper released on 12.06.2015
http://http:www.mtz-worldwide.com

content:

www.MTZonline.com

Springer Vieweg

MTZ WORLDWIDE

07-08 July-August 2015 | Volume 76

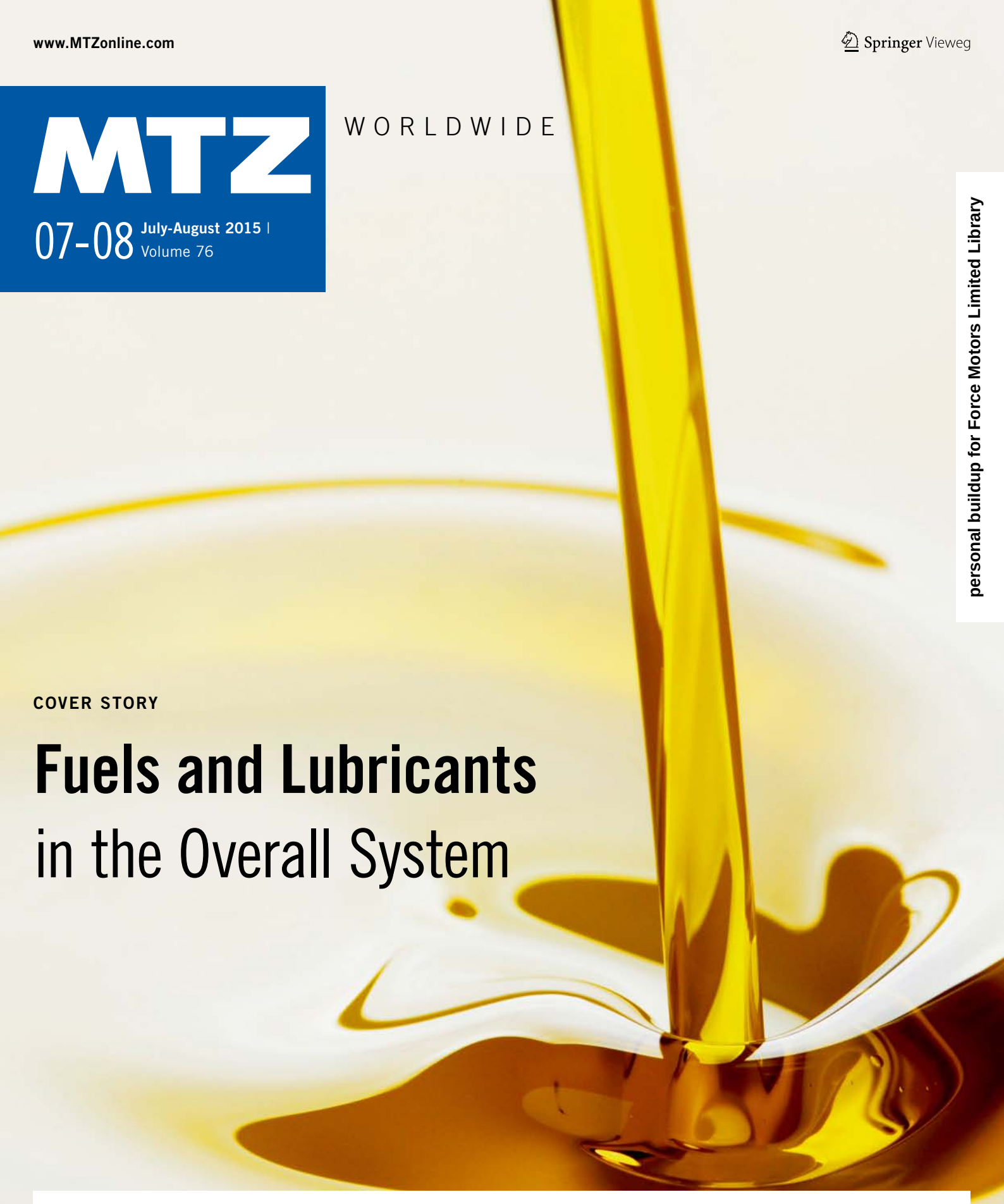

COVER STORY

Fuels and Lubricants in the Overall System

EURO 6 ENGINES
for Volkswagen Commercial Vehicles

TIMING DRIVES
Chain and Belt in Competition

TWIN-JET SPRAYS
to Improve High-pressure Diesel Injection Systems

CONTENTS

COVER STORY

Fuels and Lubricants in the Overall System

When it comes to cutting CO_2 emissions, every single gram will count in the future. In this context in the further development of the internal combustion engine, engineers are increasingly focusing on fuels, lubricants and the lubrication system. For example, many new combustion concepts to reduce CO_2 and emissions reach their full potential only when they are perfectly matched to the existing fuel.

COVER FIGURE © yellowj | Fotolia
FIGURE ABOVE [M] © Romolo Tavani | Fotolia

Time Wasted

Dear Reader,

once again this year, the Vienna Motor Symposium was an important indicator of the state of engine development. A wide range of interesting papers provided information on new engines, efficiency and alternative fuels. To put it briefly: the kaleidoscope of solutions and new approaches remains as broad as ever. The strict CO_2 targets in the key global markets, which will become even tighter over the coming decade, clearly define the objectives. It is not a question of which strategies are promising and efficient, but of which approaches will lead to sustainable success as quickly as possible in practice.

The problem is not the automotive industry, which has once again created significant efficiency potentials with the new generation of internal combustion engines, even though this is becoming increasingly difficult. The trend towards a greater use of electrically powered auxiliary units is a further component. The right strategies have been and are being applied when it comes to the electrification of the powertrain, with 48 V technology finally making its breakthrough, above all in lower vehicle classes. The mild hybrid, already virtually written off, is also back on the agenda. But the greatest potentials are without doubt to be found in plug-in hybrid technology. A very interesting aspect is the networking of the powertrain with telemetric data. By using an electronic horizon generated via the navigation system, route profiles and traffic conditions can be calculated, thus allowing the driving strategy to be optimised. This is an important stepping stone into the hybrid age that we are rapidly approaching.

The main worries, however, are still battery-electric vehicles and alternative fuels. The power output of battery stacks is still too low to get anywhere near the driving range of internal combustion engines. It remains to be seen whether the doubling of the range that is predicted for the next battery generation can actually be achieved. But at least there seems to be a glimmer of hope. On the other hand, the situation regarding a speedy market launch of alternative fuels is currently frustrating. As we reported in the last MTZ, the technology has been well-researched and tested. Biomass to Liquid (BtL) is one of the most promising options for the automotive sector. Actually, there would be nothing preventing their rapid introduction onto the market as a really globally sustainable means of reducing CO_2 – if only politicians had not repeatedly changed the general framework for renewable forms of energy. What is more, this year sees the ending of tax relief for "particularly eligible fuels". That hardly seems like political confidence building to promote the necessary willingness to invest. Valuable time is being wasted.

Best regards,

Dr. Alexander Heintzel
Editor in Chief

Octane Requirements of Modern Downsized Boosted Gasoline Engines

Over the past 15 years, Shell has published the results of various studies which show that for modern downsized gasoline engines, a high research octane number (RON) increases engine efficiency in the regions of the operating range where combustion is limited by engine knock. However for a given level of RON there is no advantage to having a fuel with a high motor octane number (MON), and there can even be a disadvantage. This can be explained from an analysis of the chemical kinetics of gasoline autoignition in the specific temperature and pressure regimes of a modern downsized boosted engine. In the following Shell summarises findings from three recent collaborative projects which support this emerging understanding.

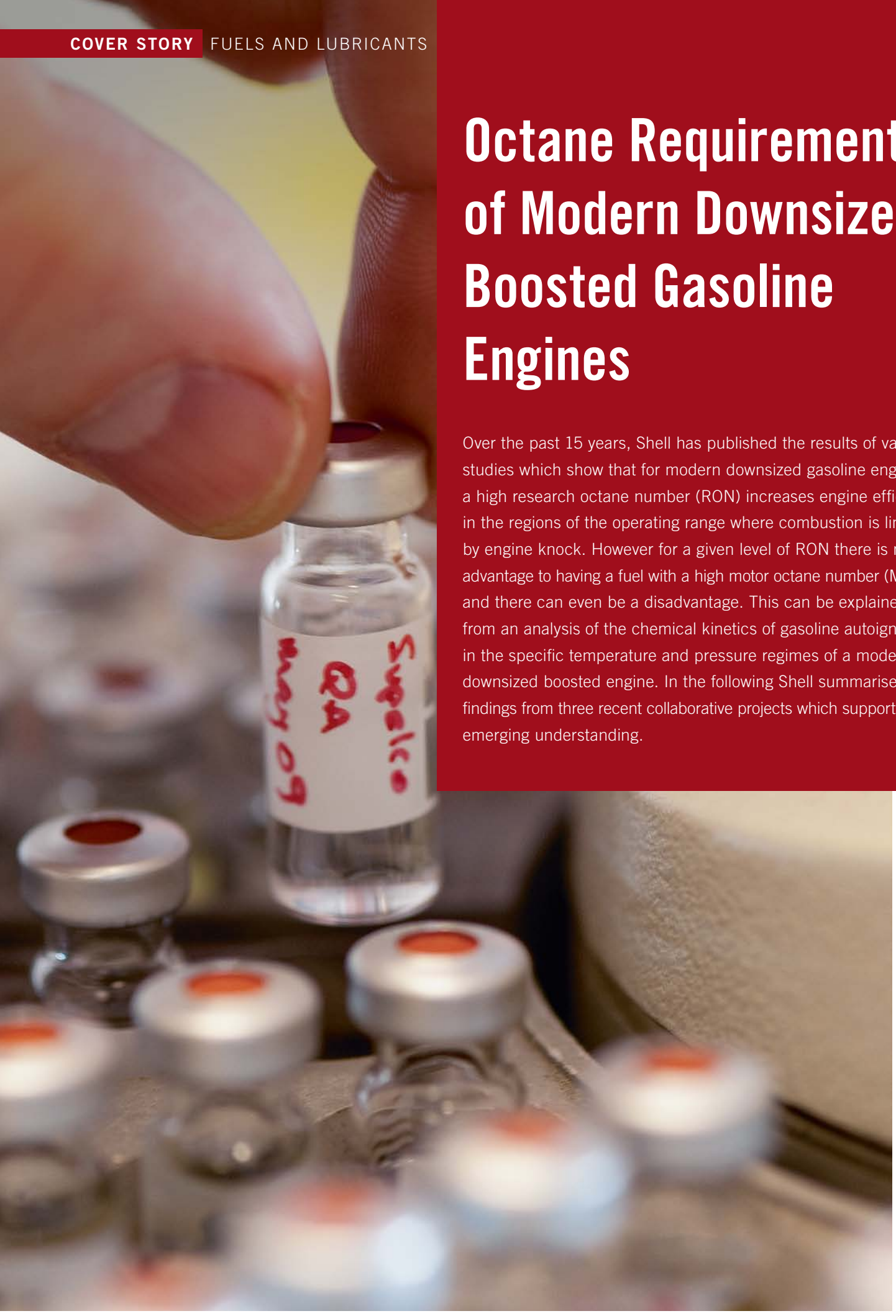

EFFICIENCY LOSS BY KNOCKING

Recent trends in gasoline engine development have been driven by the balance between customer demand for vehicle performance and meeting increasingly ambitious global targets for fleet-average CO_2 emissions – such as 130 g/km by 2015 and 95 g/km by 2020 in Europe [1]. A key area of engine research hence relies on improving combustion efficiency and reducing losses to meet fuel consumption targets without compromising performance. Though various technologies have been developed to this aim, the use of more aggressively downsized and boosted engines is a major industry trend that enables improved efficiency at a given engine torque and speed via reduced friction and pumping losses, achieved by operating the engine at a higher specific output [2].

Engine knock occurs when the end-gas in the combustion chamber auto-ignites ahead of the flame front. It leads to pressure oscillations, which if severe enough can cause damage to the engine. Modern vehicles are fitted with a knock sensor, which can automatically retard the timing at which the spark fires in the engine cycle, thereby avoiding the knock. However, retarding the spark in this way leads to a loss of engine efficiency, since the movement of the piston during the power stroke of the engine is no longer synchronised with the expansion of the hot gases.

A fuel's knock resistance is historically characterised by the research octane number (RON) and motor octane number (MON) as determined in a Cooperative Fuels Research (CFR) engine test that dates back to the 1930s. RON and MON are assigned by determining the volume percent of iso-octane in a binary mixture with n-heptane (the resulting mixture being known as a primary reference fuel (PRF)) which has the same propensity to knock at a given engine compression as the real fuel. The MON test uses a higher temperature, lower manifold pressure and higher engine speed condition than the RON test.

However inter-cooling in boosted engines and use of EGR can lead to a much lower temperature for a given pressure in a real engine as compared to a CFR engine. These differences in pressure and temperature regimes can lead to subtle but important differences in the chemical reactions that lead to gasoline autoignition. This is illustrated in **FIGURE 1**. During 2014, Shell published research carried out separately with three automotive manufacturers. In each case, the findings were consistent with a fundamental chemical kinetic interpretation of gasoline autoignition.

CHEMICAL KINETICS OF AUTOIGNITION AND THE K VALUE

Techniques such as shock tubes, rapid compression machines and jet stirred reactors have been used comprehensively over the last four to five decades to gain an understanding of the low and intermediate temperature oxidation chemistry of gasoline components [4]. This has led to the development of chemical kinetic mechanisms for the oxidation of surrogates for gasoline. Both shock tubes and rapid compression machines allow measurement of the autoignition delay time, τ, which defines the time interval between a fuel/air mixture being rapidly compressed and heated to a given temperature and pressure, and the occurrence of a rapid sustained rise in temperature.

FIGURE 2 shows the ignition delay time for a surrogate "realistic" gasoline (RON = 95, MON = 85) and two PRF mixtures: PRF 95 denotes a mixture with 95 % by volume of iso-octane and 5 % by volume of n-heptane, which by definition has an octane number of 95 and PRF 85 is defined in an analogous fashion.

For the surrogate "realistic" gasoline, the autoignition delay time decreases monotonically with increasing temperature. However for the PRF fuels, there is a region of the curve in which the autoignition delay can show an inflection and some cases even increase with increased temperature; this is a phenomenon known as "Negative Temperature Coefficient" (NTC) behaviour. Unfortunately this

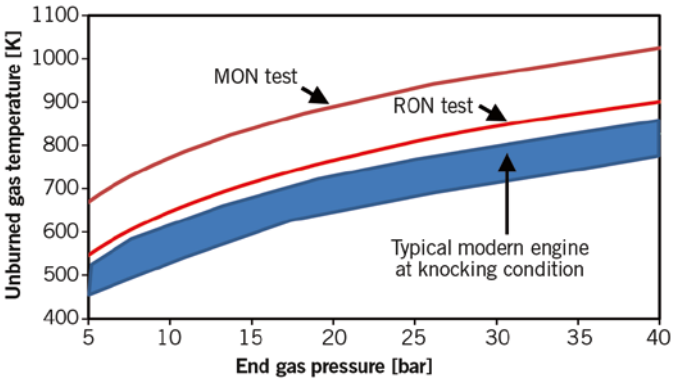

FIGURE 1 Indicative pressure versus temperature chart for unburned gas (adapted from [3])

AUTHORS

Prof. Roger Cracknell
is Principal Scientist, Retail Fuels Technology, at Shell Global Solutions (UK) Ltd. in Manchester (UK).

Dr. Wolfgang Warnecke
is Chief Scientist for Mobility at the Shell Global Solutions Deutschland GmbH in Hamburg (Germany).

Jan-Hendrik Redmann
is Scientist, Retail Fuels Technology, at the Shell Global Solutions Deutschland GmbH in Hamburg (Germany).

Dr. Tor Kit Goh
is Scientist, Retail Fuels Technology, at the Shell Global Solutions Deutschland GmbH in Hamburg (Germany).

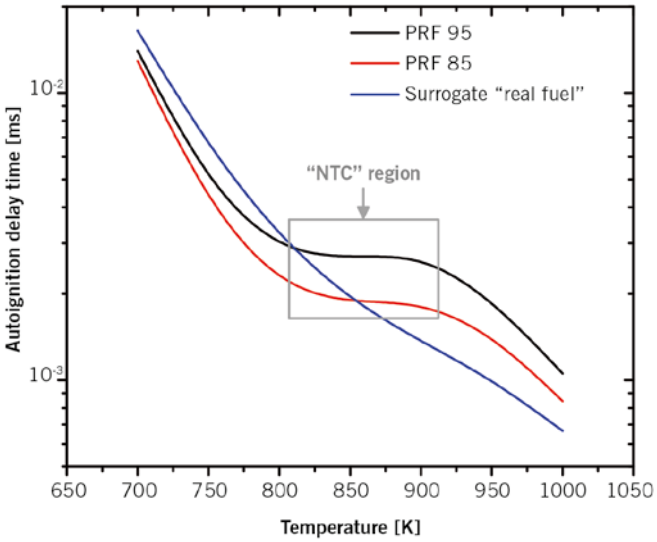

FIGURE 2 Calculated autoignition delay times at 40 bar for a surrogate gasoline (95 RON, 85 MON) comprising 62 vol. % toluene, 16 vol. % i-octane, 22 vol. % n-heptane as well as PRF 95 and PRF 85 (surrogate compositions were computed based on the work of [5], all simulations were carried out for stoichiometric fuel/air mixtures using the chemical kinetic mechanism from [6])

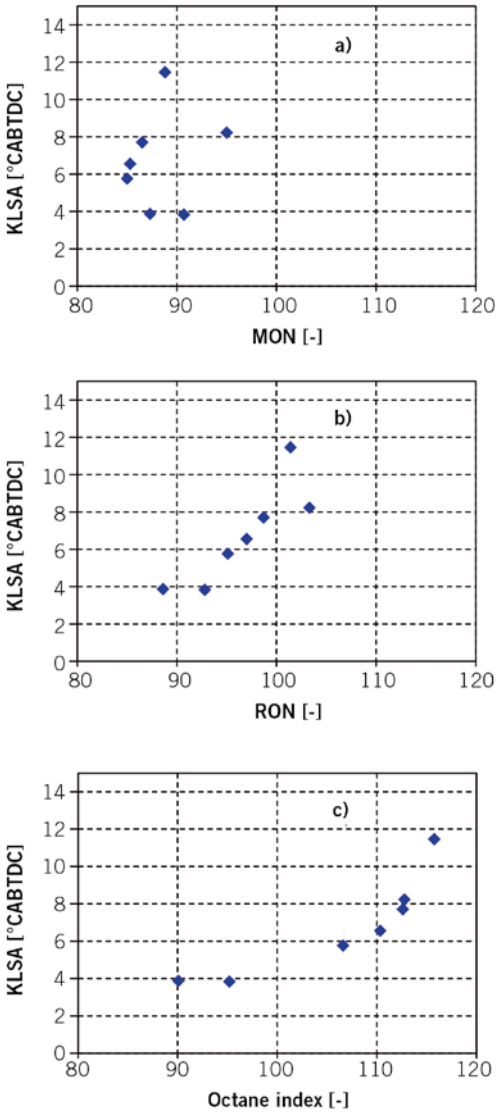

FIGURE 3 Results from Ultraboost project: KLSA versus octane at 2000 rpm, 30 bar BMEP and 10 % EGR for MON (a), RON (b) and octane index (K = -1.1) (c) (data from [12])

NTC region corresponds with the temperature and pressure regime found in the RON and MON tests.

At temperatures lower than the NTC region, it can be seen that the surrogate "realistic" gasoline is more resistant to autoignition than either PRF 95 or PRF 85. Approaching the NTC region, the line for the surrogate "real fuel" crosses over the curve for PRF 95 and then at higher temperatures it crosses the curve for PRF 85. The temperatures at which the surrogate intersects the PRF 95 and PRF 85 curves respectively can be thought of (at least in a qualitative sense) as representing the conditions in the RON and MON tests. The presence of the pronounced NTC behaviour in the primary reference fuels is the main reason why the RON of a real fuel is typically around ten numbers higher than the MON [7].

As illustrated in **FIGURE 1**, the temperature for a given pressure tends to be lower at a boosted condition in a modern engine than for a CFR engine. It can be seen from **FIGURE 2**, that a fuel can have an octane rating of 95 RON and 85 MON, but at temperatures lower than the RON test, it will be much more resistant to autoignition than PRF 95.

Moreover it is the gradient of the autoignition delay with respect to temperature for the surrogate "realistic" gasoline that determines the extent to which it is more resistant to autoignition at lower temperatures than would be suggested by its RON value alone. This gradient depends on the difference between RON and MON, known as the sensitivity. Thus chemical kinetic considerations would suggest that for a given RON level, fuels with high sensitivity would have a higher resistance to autoignition at temperatures lower than the conditions in the RON test.

A practical approach to quantify the octane appetite of modern engines [8, 9] is to define an octane index (OI) as a linear combination of RON and MON with an engine condition dependent weighting factor, K, such that

Eq. 1	$OI = K \cdot MON + (1 - K) \cdot RON$

This can also be written as:

Eq. 2	$OI = RON - KS$

where S is the sensitivity (RON-MON). The K value is thought to be dependent only on the in-cylinder temperature and pressure conditions in the end-gas prior to the onset of autoignition.

The definition of octane in the US is based on the original assumption that MON and RON are equally important and putting K = 0.5 gives OI = (RON+MON)/2 which is the definition of the US Anti Knock Index (AKI). Mittal and Heywood [10] have shown a progressive decrease in K over the last 50 years and results obtained by Shell on passenger vehicles from the last 20 years suggests that the best fit for OI is to have K less than zero, which means mathematically that for a given RON, a high MON value can indeed be disadvantageous.

THE ULTRABOOST PROJECT

The objective of the Ultraboost project was to develop a downsized, boosted engine technology capable of achieving a 35 % CO_2 emissions reduction over the New European Drive Cycle (NEDC) in a 2010 model year Range Rover vehicle, whilst maintaining performance, relative to a baseline naturally aspirated V8 production engine. A 60 % downsized engine was developed, requiring air charging up to 3.5 bar absolute [11].

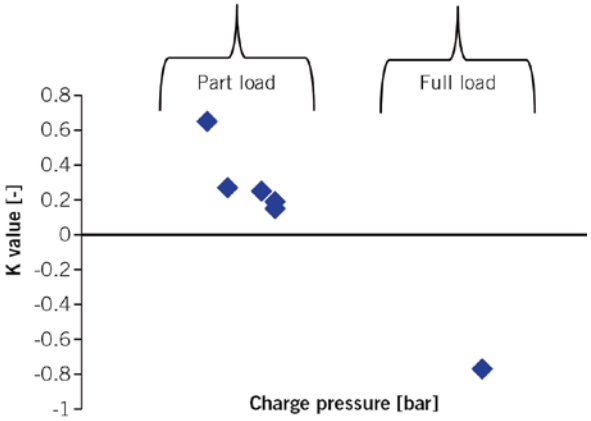

FIGURE 4 Relationship between K value and charge pressure at full and part load accelerations in a Pontiac Solstice (partly schematical, redrawn from [13])

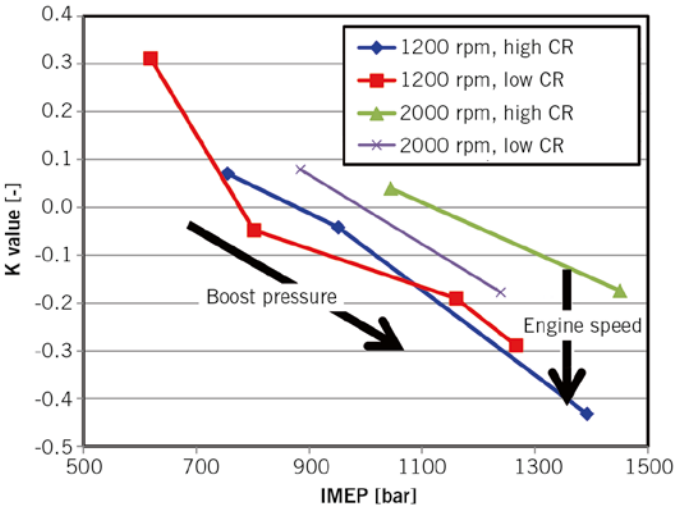

FIGURE 5 K values become more negative as engine speed decreases and boost pressure increases [14] (CR: compression ratio)

In order to determine the octane appetite for this engine, a matrix of seven fuels with decorrelated RON and MON was tested. The results for the 2000 rpm and 30 bar BMEP condition are shown in **FIGURE 3**. It can be seen that there is no correlation between knock limited spark advance (KLSA) and MON, and only a limited correlation between KLSA and RON. If however KLSA is plotted against Eq. 1, then the best fit value is found to be K = -1.1 [12]. This is amongst the most negative K values ever reported, reflecting the extreme levels of charge pressure employed in this engine.

MEASUREMENTS ON A PONTIAC SOLSTICE

A Pontiac Solstice, kindly provided by GM was run on a Shell internal cycle used for fuel economy estimation using a matrix of fuels with decorrelated RON and MON. The part load accelerations tended to have positive K values while the full load operation (where knock is a much more significant constraint) gave a K value of -0.75 [13], **FIGURE 4**. The results show a clear link between charge pressure and K value. This is consistent with our interpretation that a higher charge pressure will mean a lower temperature for a given pressure.

NISSAN COLLABORATION

A similar pattern emerges in a collaborative study conducted between Shell and Nissan [14] using a single cylinder engine (400 cm³ displacement, port fuel injection and external boosting) running at different engine speeds and boost pressures. It was found that K decreased with engine load which for a given compression ratio (CR) depends on boost pressure. Interestingly lower engine speed also promotes a lower K value. This is illustrated in **FIGURE 5**.

CONCLUSIONS

Shell has published research carried out separately with three automotive manufacturers representing different types of gasoline engine technology. In each case, in the regions of the engine operating map where knock is really critical, a negative K value is observed. This means that for a given level of RON, a high MON value can actually be disadvantageous. Higher levels of charge pressure appear to accentuate this effect which is changing the octane requirements of modern downsized boosted gasoline engines.

REFERENCES

[1] European Commission: Climate Action: Reducing CO_2 emissions from passenger cars. http://ec.europa.eu/clima/policies/transport/vehicles/cars/index_en.htm, Jan. 2013
[2] Davies, T.; Cracknell, R.; Lovett, G.; Cruff, L.; Fowler, J.: Fuel Effects in a Boosted DISI Engine. SAE Technical Paper 2011-01-1985
[3] Kalghatgi, G. T.: Fuel Engine Interactions. SAE International, Warrendale PA, 2014
[4] Battin-Leclerc, F.: Detailed chemical kinetic models for the low-temperature combustion of hydrocarbons with application to gasoline and diesel fuel surrogates. In: Prog. Energy Combust. Sci. 34 (2008), No. 4, pp. 440-498
[5] Morgan, N.; Smallbone, A.; Bhave, A.; Kraft, M.; Cracknell, R.; Kalghatgi, G.: Mapping surrogate gasoline compositions into RON/MON space. In: Combust. Flame 157 (2010), No. 6, pp. 1122-1131
[6] Andrae, J. C. G.; Head, R. A.: HCCI experiments with gasoline surrogate fuels modeled by a semidetailed chemical kinetic model. In: Combust. Flame 156 (2009), No. 4, pp. 842–851
[7] Leppard, W.: The Chemical Origin of Fuel Octane Sensitivity. SAE Technical Paper 902137 (1990)
[8] Kalghatgi, G. T.: Fuel Anti-Knock Quality – Part I. Engine Studies. SAE Technical Paper 2001-01-3584 (2001)
[9] Kalghatgi, G. T.: Fuel Anti-Knock Quality – Part II. Vehicle Studies – How Relevant is Motor Octane Number (MON) in Modern Engines? SAE Technical Paper 2001-01-3585 (2001)
[10] Mittal, V.; Heywood, J. B.: The shift in relevance of fuel RON and MON to knock onset in modern SI engines over the last 70 years. SAE Technical Paper 2009-01-2622 (2009)
[11] Turner, J. W. G. et al.: Ultra Boost for Economy: Extending the Limits of Extreme Engine Downsizing. SAE Technical Paper 2014-01-1185 (2014)
[12] Remmert, S. et al: The Relevance of a Lower Limit to the MON Specification in a Downsized, Highly Boosted DISI Engine. SAE Technical Paper 2014-01-2718 (2014)
[13] Orlebar, C.; Joedicke A.; Studzinksi, W.: The Effects of Octane, Sensitivity and K on the Performance and Fuel Economy of a Direct Injection Spark Ignition Vehicle. SAE Technical Paper 2014-01-1216 (2014)
[14] Kassai, M.; Shiraishi, T.; Teraji, A.; Wakefield, S.; Goh, T.; Doyle, D.; Wilbrand K.; Shibuya, M.: The Effect of fuel properties on knocking performance of boosted downsized engines. Conference "Advanced Fuels for Sustainable Mobility", Nuerburgring, Germany, 2014

Combined Oil-Vacuum Pump

In view of stricter CO_2 targets, further optimisation of frictional loss in the powertrain is necessary. This includes not only reducing engine friction, caused among others by the piston group or the bearing journals themselves, but also lowering the power consumption of engine accessories. In this article, Mahle illustrates how combining a pendulum-slider oil pump and a vacuum pump into a single module provides potential weight and package savings besides the benefits of highly efficient and wear-resistant operating map control of the oil pump.

AUTHORS

Holger Conrad
is Head of Pump Systems Predevelopment at the Mahle Filtersysteme GmbH in Auengrund (Germany).

Dr. Martin Janssen
is Head of Global Predevelopment at the Mahle Filtersysteme GmbH in Stuttgart (Germany).

Dr. Peter Wieske
is Head of Concepts and Systems in Corporate Advanced Engineering at the Mahle International GmbH in Stuttgart (Germany).

MORE COMPACT DESIGN

Besides driving the vehicle, the power produced by the combustion engine is needed in order to operate the engine accessories, such as the oil pump. Engine accessories are often designed on the basis of the maximum requirements in the operating map, causing unnecessarily high frictional losses at the other operating points. The ongoing development of engine accessories that can be controlled to meet demand therefore still has significant potential to further increase the fuel efficiency of the vehicle as a whole. With the controlled pendulum-slider pump, Mahle has developed a highly efficient, patented technology.

In the Mahle pendulum-slider oil pump, pressure and volume flow are generated on demand, reducing the required power consumption to a minimum. The main advantages over other controlled oil pumps – such as external-gear and vane pumps [1] – derive from the combination of robustness with respect to contaminants (e.g., due to soot and other particles), its high overall efficiency over the entire service life, and its suitability for high engine speeds. Various control strategies with short adjustment and response times are possible.

Vacuum pumps are used to create the vacuum required to boost pneumatic brake performance. Generally, the vacuum pump is located on the camshaft. The speed of the camshaft is half the rotational speed of the crankshaft. Due to the low drive speed, the pump must have a large volume and the vacuum pump requires proportionate package space. Owing to the existing requirements for impact protection for people [2], this package is seldom available, particularly in the upper region of the engine in the direct vicinity of the hood. "Hard" components are removed from this area as much as possible, so as to avoid expensive active measures, such as a system for hood opening in the event of an accident [3]. Because the oil pump is driven at the speed of the crankshaft, positioning the component directly on the oil pump and actuating it with the same shaft increases the speed of the vacuum pump. With this higher speed, the vacuum pump can have a more compact design, with savings on components such as the housing and drive elements. This results in additional weight benefits in comparison with two separate components. Combined with consistent lightweight design, the weight requirements are undercut by about 450 g, although the individual elements must be designed to be more resistant to speed and wear due to the greater loads.

PENDULUM-SLIDER OIL PUMP

A pendulum-slider pump has a pendulum rotationally supported in the external rotor and guided by the internal rotor. In contrast to a vane in a vane pump, the pendulum does not create any friction; rather it rolls off in the groove of the internal rotor. The special design of the pendulum-slider pump provides several benefits. The use of an external rotor decisively improves the tribological conditions at the inner diameter of the slider. This prevents mixed friction under critical operating conditions. In addition to the controllability benefits and wear behaviour, the slider can now be made from a duroplastic material. This provides great potential weight savings, as the slider takes up a large volume in relation to the entire pump. In comparison with a vane pump, **FIGURE 1**, of the same size, the weight savings for the rotor set can be about 24 %.

An essential requirement for the controlled oil pump is good controllability, particularly for operating map control. Criteria include response time, hysteresis, and ability to reach the pressure requirements from the engine management system. This means ensuring the required minimum pressure even under hot, full-load conditions and the maximum permissible pressure under partial load. Especially for operating map control, the equilibrium of the force vectors is fragile, because the forces that can be used for adjustment – the spring preload on the one side and the oil pressure in the control pressure space on the other – are low, due to the minimum pressures that must be achieved. They are opposed by forces resulting from friction and pressures within the rotor set, which can have a disruptive effect on the control system. The goal is to minimise these in order to achieve high control accuracy. The disruptive forces in the pendulum-slider pump are low in comparison with a vane pump, **FIGURE 2**, leading to improved controllability and therefore to a greater usable pressure range. Due to the forces present in the vane pump, the achievable pressure is greatly dependent on temperature and speed.

Another essential aspect for evaluating pumps is the wear behaviour, such as the expected loss of efficiency over the service life. Because the pump is located upstream of the oil filter in the oil circuit, the associated contamination of the oil with particles and the design-dependent tight gaps between moving components

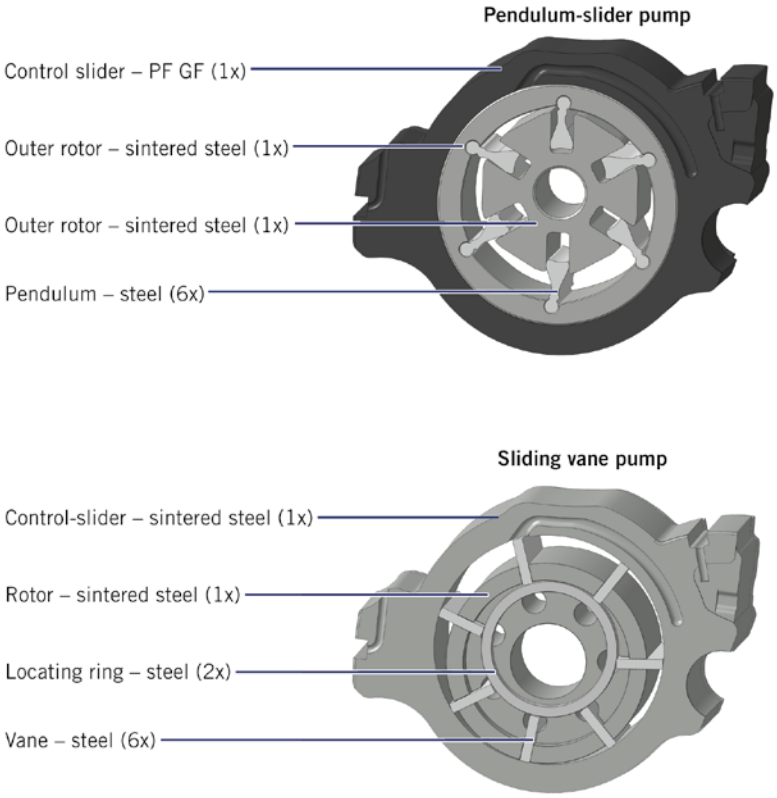

FIGURE 1 Design comparison of rotor sets for pendulum-slider and vane pumps

FIGURE 2 Rotor set with force vectors, vane versus pendulum slider

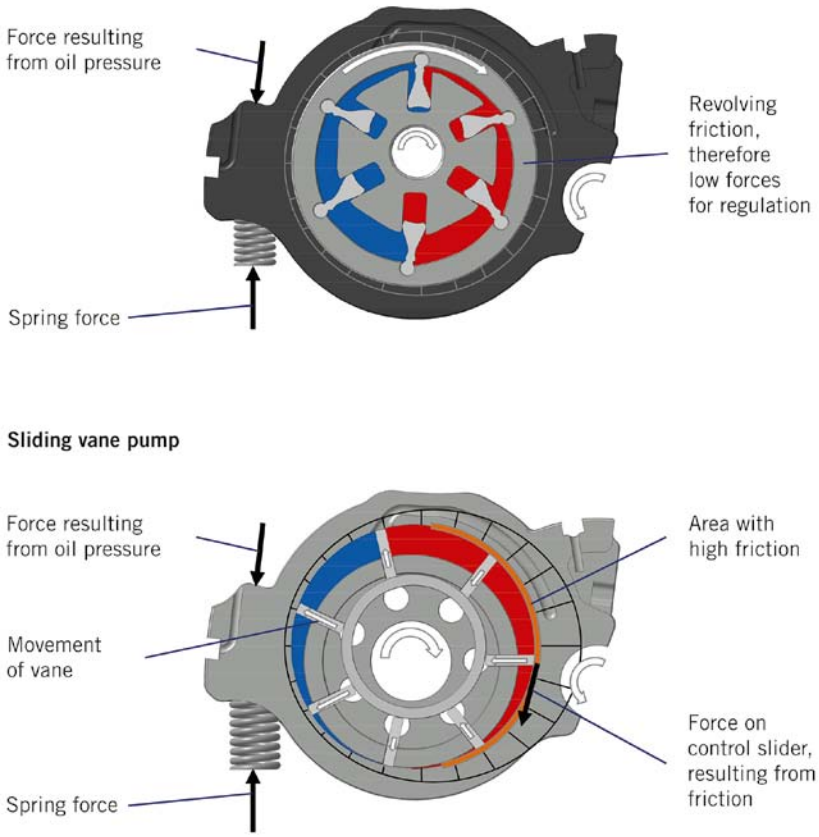

subject them to abrasive wear. In order to ensure sufficient lubricating oil supply to the engine even late in the service life, the reduction in hydraulic performance due to wear must be considered at the design stage by oversizing the component accordingly. The goal of development is thus primarily to reduce the occurring wear and its effect on pump performance. The self-sealing principle of the pendulum-slider pump provides very good preconditions for this goal.

FIGURE 3 compares the volume flow rates of a pendulum-slider pump and a vane pump as a function of the gallery pressure. The theoretical delivery volume and the relevant gaps are identical for both pumps. The pumps were measured in new condition and after an endurance test of 500 h under tough conditions.

Considering the volume flow at a gallery pressure of 3 bar and a pump speed of 1500 rpm for the different pump systems before and after the endurance test, for example, it is evident that the pendulum-slider pump produces higher volume flow rates under the same conditions, even when new. This is due to its superior internal sealing and associated volumetric efficiency. As the running time increases – and with it the resulting wear – the hydraulic performance levels diverge significantly. This proves the higher wear resistance of the pendulum-slider pump.

The comparison of the two pumps before and after the endurance test, **FIGURE 4**, also shows efficiency benefits for the pendulum-slider pump as pressure increases. As wear increases, efficiency drops overall; however, even after the endurance test, it is about 10 % higher for the pendulum-slider pump than for the vane pump as pressure increases. **FIGURE 4** illustrates this with a pump speed of 1500 rpm and an oil temperature of 120 °C. The blue curves show the overall efficiency of the pendulum-slider pump before and after the endurance test. The efficiency levels of the vane pump are shown in red. Both systems have lower efficiency after the endurance test. The distance and thus the advantage of the pendulum-slider pump over the vane pump, however, remains nearly constant.

FIGURE 5 shows the relationship between the control range and the temperature. The pendulum-slider pump and the vane pump are compared in

new condition. It becomes evident that the vane pump, due to its operating principle – changing tribological conditions between the vane and the inner diameter of the slider as temperature increases – can no longer produce the potential volume flow rates of the pendulum-slider pump even early on. The same applies at higher speeds as well. Especially at high temperatures and engine speeds, however, high oil volume flow rates are needed in order to ensure that the engine is lubricated and cooled.

VACUUM PUMP

The vacuum pump is designed as an uncontrolled rotary piston pump. The steel rotor is driven directly by the oil pump shaft. The oscillating vanes have wear caps. The enclosing cover is

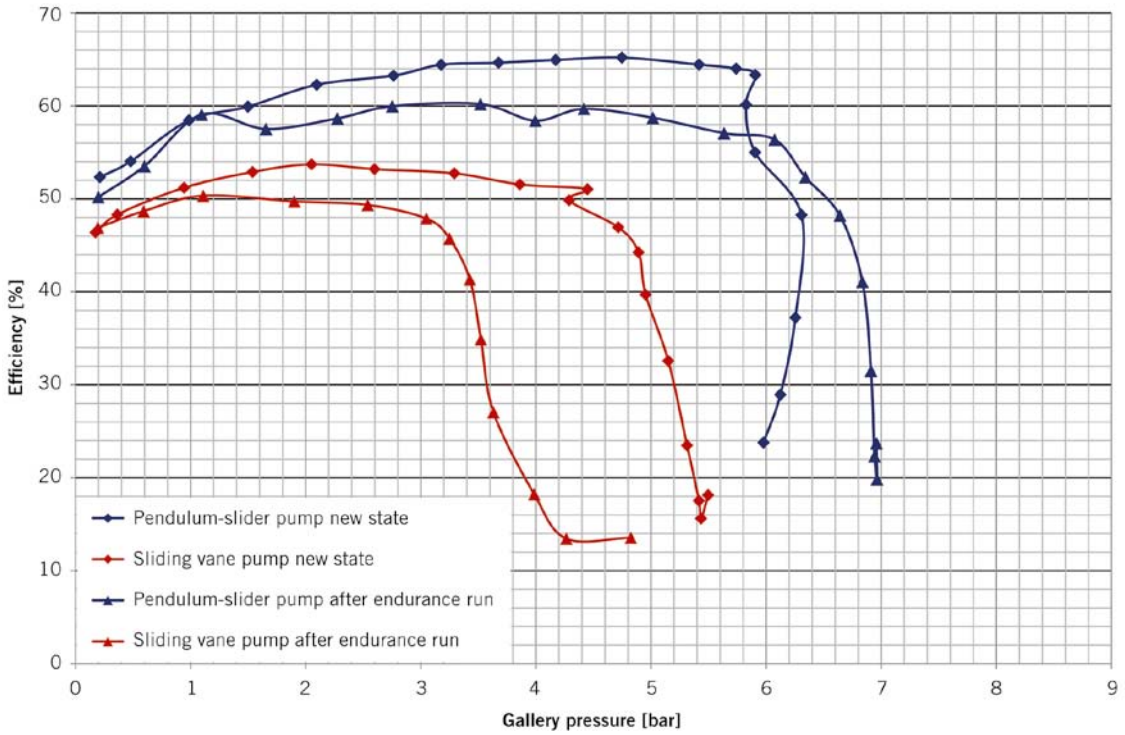

FIGURE 3 Comparison of volume flow rates of a pendulum-slider and a vane pump as a function of gallery pressure at 120 °C and 1500 rpm

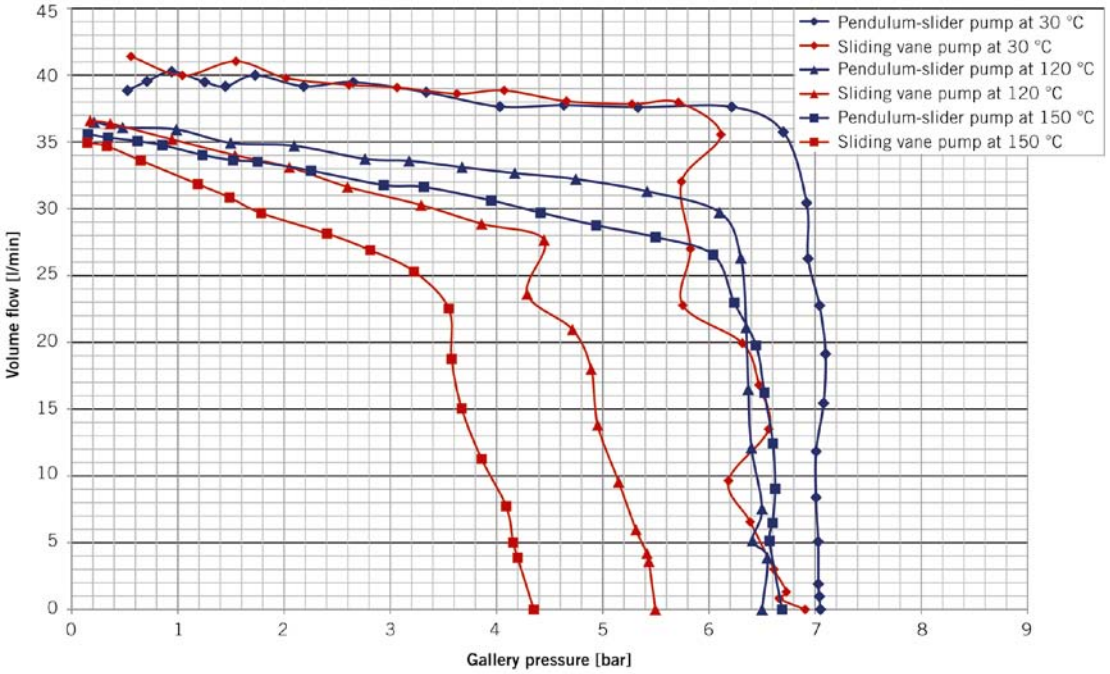

FIGURE 4 Efficiency comparison of pendulum-slider and vane pumps before and after endurance test at 120 °C and 1500 rpm

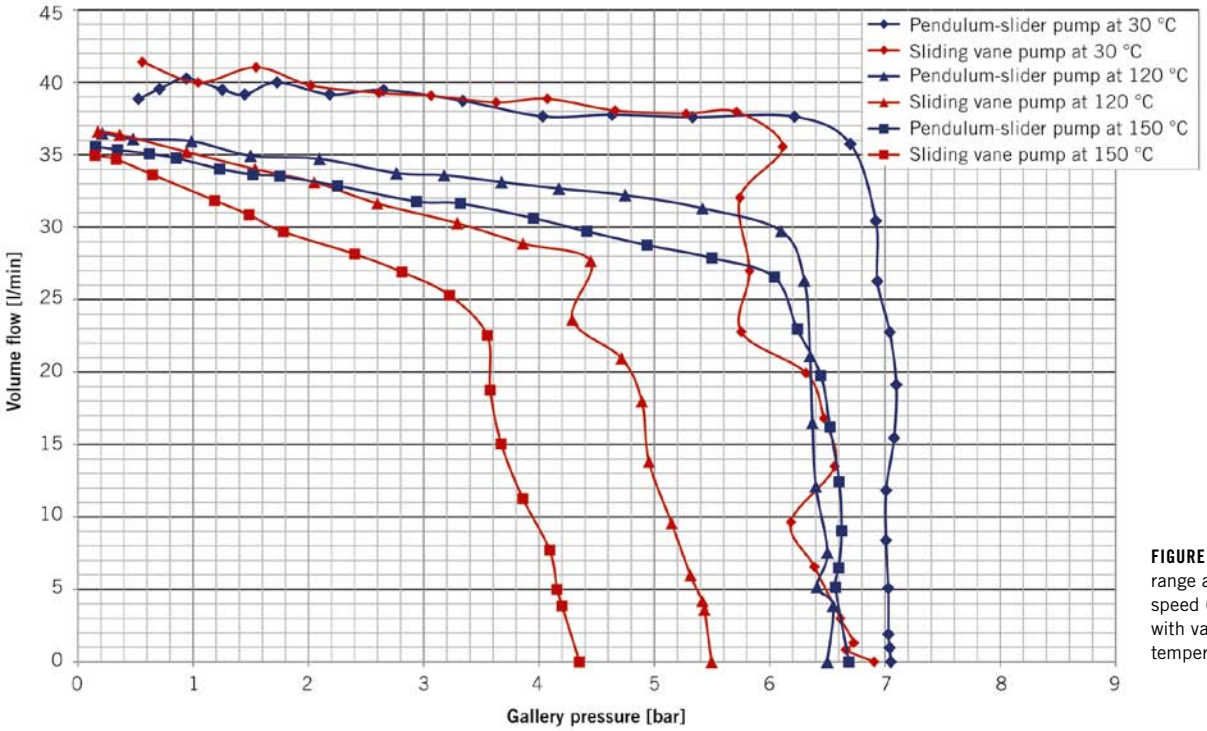

FIGURE 5 Control range at constant speed (1500 rpm) with various temperatures

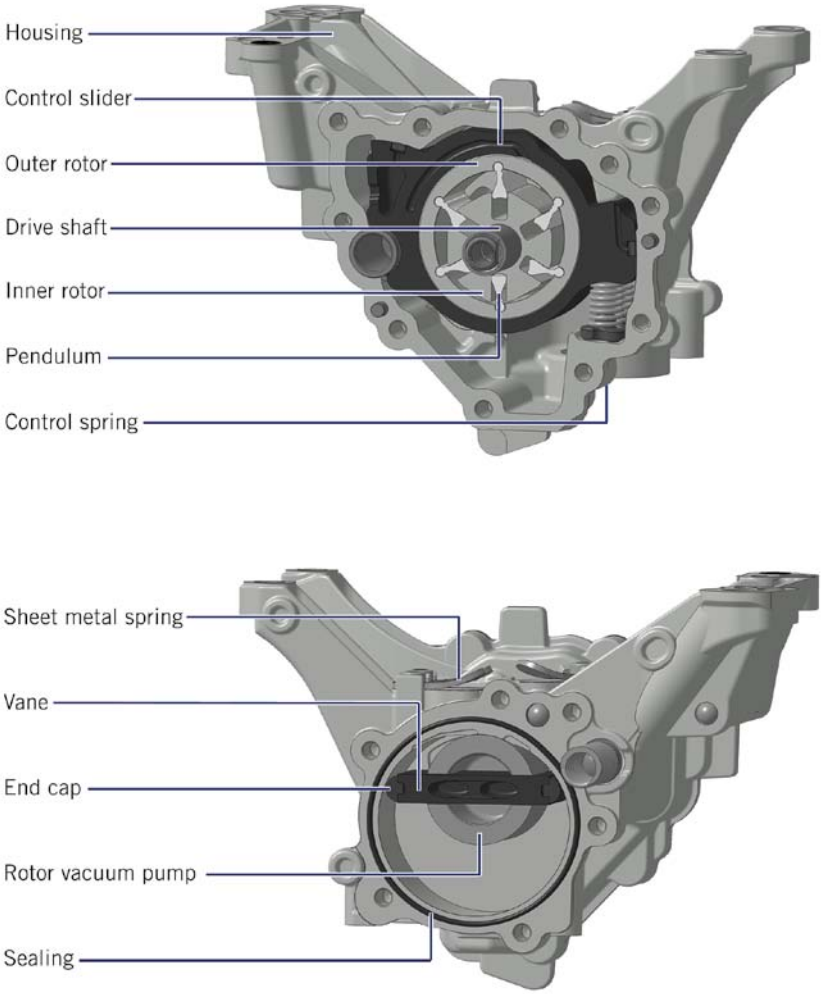

FIGURE 6 Design and components of the Mahle oil-vacuum pump (side view pendulum-slider oil pump (top) and vacuum pump side (bottom))

made of duroplastic material. The achieved weight savings amount to about 36 %.

COMBINED OIL-VACUUM PUMP

By operating the vacuum pump at the oil pump speed, the specific loads on the components are greater than for the variant driven at the camshaft speed. Especially the bending load that cycles with every rotation of the vane, and the wear resistance between the vane caps and the running surface in the housing, must be designed to meet the speed conditions. In addition to the speed profile, the load is primarily dependent on the mass of the oscillating and rotating components. The radial acceleration of the vane acts as a normal force on the friction pairing between the ends of vanes and the housing. A weight-optimised design is required in order to reduce the contact force. Considering the factors of density, tensile strength, and cost, a glass-fibre-reinforced polyamide is used for the vanes and a carbon-fibre-reinforced, high-performance thermoplastic material is used for the wear caps.

In addition to material selection, appropriate lubrication of the sliding contact is important. The optimal amount of lubricating oil is derived from the contrary requirements for reducing

contact frictional loss and wear on the one side, and the churning losses associated with too much oil on the other. Optimal dosing of the amount of oil is thus of great significance for the efficiency and service life of the vacuum pump.

The common drive shaft of the oil and vacuum pumps and the resulting sealing requirements also present a risk that the pumps will influence each other's function due to leakage flows. Even a slight change in the pressure level in the control pressure space of the oil pump due to the influence of the vacuum pump can lead to a large change in the oil pressure at the pump outlet. This must be prevented by design measures.

The vacuum pump can be lubricated from the pressure side, the suction side, or via the control lines of the oil pump. For supply on the pressure side, the high pressure differential, the high variance in the pump outlet pressure due to the operating map control, and thus the coupling between lubrication and operating map control must be seen as disadvantages. For lubricating oil supply on the suction side, the low variance in the pressure differential is an advantage, but the use of unfiltered oil for lubrication is a disadvantage. Supply via the control line would ensure that the oil supply is clean. In this case, however, there is an increased risk that control would be lost due to the varying influence at different vacuum pump suction pressures. The best compromise, therefore, is lubrication via the suction side of the oil pump.

CONCLUSION AND OUTLOOK

Tests demonstrate that the Mahle pendulum-slider oil pump offers very high efficiency and high control accuracy over the entire service life. It thus contributes to reducing CO_2 emissions. Combining the oil and vacuum pumps, **FIGURE 6**, yields significant additional benefits in terms of weight and package. In a further step, the vacuum pump can be driven via a special clutch, thus adapting its speed on demand, and enabling or disabling the vacuum pump. As the vacuum does not need to be generated constantly, this provides for a corresponding savings potential with regard to the pump's power input and thus fuel consumption. The control system for the vacuum pump does not influence the oil pump's control strategies.

REFERENCES

[1] Matthies, H. J.; Renius, K. T.: Einführung in die Ölhydraulik. 8th edition, Wiesbaden: Springer, 2014
[2] ECE/UN R127
[3] Aktive Motorhaube, Unfallschutz für Fußgänger. Hhttp://www.daimler.com/dccom/0-5-1210222-49-1210363-1-0-0-1210342-0-0-135-0-0-0-0-0-0-0-0.html, viewed on 03/18/2015

Euro 6 Engines for Volkswagen Commercial Vehicles

The new 2.0-l TDI engine developed based on the modular diesel engine kit MDB is celebrating its premiere with its launch in the Multivan and the Transporter. The four-cylinder predecessor engine will be successively superseded by a standardised basic engine adapted to meet the specific requirements of commercial vehicles, featuring a wider power range and lower fuel consumption. The top-of-the-range engine will feature a redesigned, regulated two-stage turbocharging system.

DEMANDING REQUIREMENTS

The requirements set for future drivetrains for light commercial vehicles are becoming ever more demanding. To make them highly economical and efficient, commercial vehicle engines must boast low fuel consumption combined with high power and torque figures. This is why modern diesel engines have for decades been the predominant drive source for light commercial vehicles, being superior to other drive layouts in terms of their all-round capabilities.

The engines from Volkswagen Commercial Vehicles already number among the best drivetrains in this segment [1]. In order to further improve competitiveness in the commercial vehicle segment, the following key aspects were addressed in the performance specification for the new engines:

AUTHORS

Dipl.-Ing. Friedrich Eichler
is Head of Engine Development at the Volkswagen AG in Wolfsburg (Germany).

Dipl.-Ing. Jörn Kahrstedt
is Head of Diesel Engine Development at the Volkswagen AG in Wolfsburg (Germany).

Dr.-Ing. Ekkehard Pott
is Head of Commercial Diesel Engine Development at the Volkswagen AG in Wolfsburg (Germany).

Dipl.-Ing. Carsten Thomfohrde
is Technical Project Manager Commercial Diesel Engine at the Volkswagen AG in Wolfsburg (Germany).

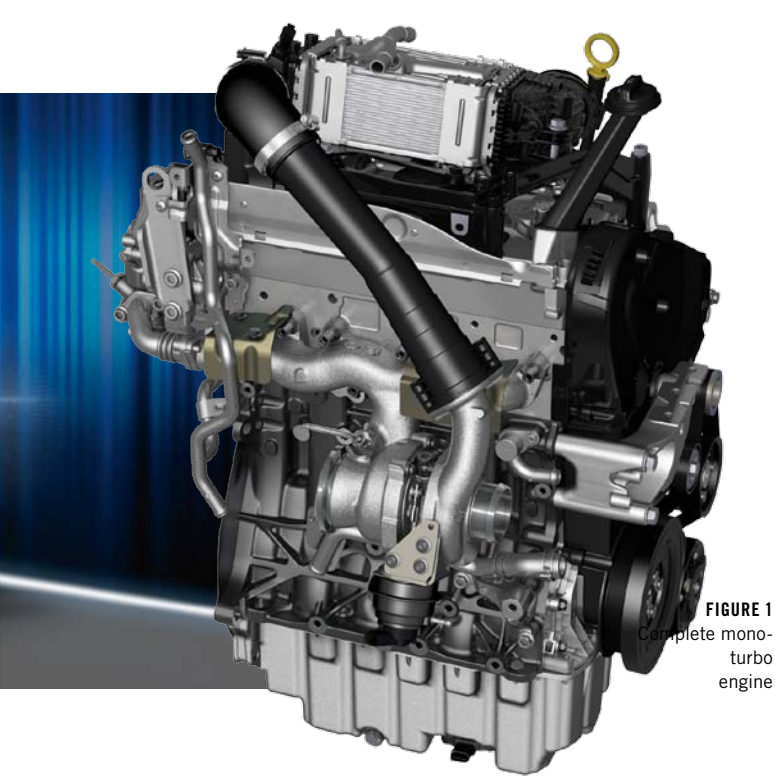

FIGURE 1 Complete mono-turbo engine

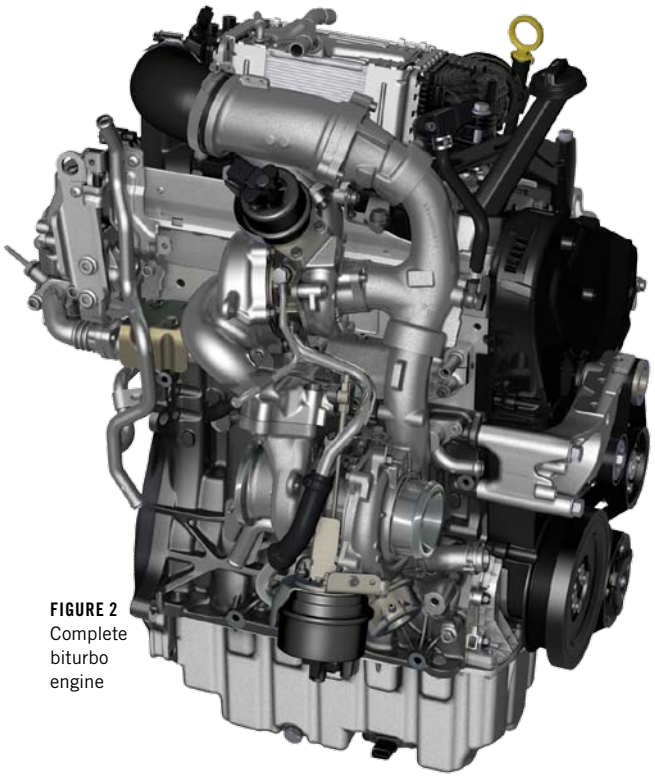

FIGURE 2 Complete biturbo engine

- reduction in complexity through use of the modular diesel engine kit
- consistent reduction of CO_2 emissions
- increase in specific power and torque figures
- optimisation of responsiveness and torque curve
- Euro 6 compliant exhaust emissions
- superior reliability and durability.

Volkswagen has enjoyed great success in passenger cars with its new modular diesel engine kit MDB with common rail technology since its introduction in 2012 [2, 3]. The commercial-vehicle-specific version of the MDB has been designed on this basis and will be first used in the new Volkswagen Transporter (T6) range. In markets subject to Euro 6 exhaust emission regulations, it will supersede all engines used so far.

Right from the conceptual phase, the new engine was designed for the more demanding operating conditions specific to commercial vehicles as well as for the specific installation situation, which differs from that of a passenger car. At the same time, given the high proportion of Transporter models with passenger car equipment ("Multivan"), the requirements for driving characteristics, acoustics, and vibration behaviour are on a passenger car level. Adequate power, a full-bodied torque curve, and superior starting behaviour throughout the rpm range are decisive here. This conflict of goals is further exacerbated by the high road resistance of light commercial vehicles. For this reason, turbochargers with variable turbine geometry (VTG) are used on engines with an output of up to 110 kW, **FIGURE 1**. For the top-of-the-range engine with 150 kW, **FIGURE 2**, the two-stage turbocharging system from the predecessor engine has been completely revised and likewise enhanced with variable turbine geometry in the high-pressure stage. This has provided a further significant improvement in spontaneity and torque characteristics.

MAIN COMPONENTS OF THE NEW COMMERCIAL VEHICLE ENGINE

In order to provide as large a usable space as possible for predefined exterior dimensions of a commercial vehicle, the installation length available for the engine is shorter than that in passenger cars with comparable engines (the Volkswagen standard here is the established modular transverse kit MQB). Moreover, the inclination of the engine also deviates from that of the MQB (8° to the front instead of 12° to the rear). As a result, several modules have had to be adapted specifically for the vehicle to make use of the higher available packaging space compared with the MQB, **FIGURE 3**.

The same base engine with a 2.0-l displacement is used for all output variants. The output-specific configuration is created only through adaptation of the turbocharging and injection system components. **TABLE 1** shows the key technical data of the new commercial vehicle engine in the Transporter model range.

CYLINDER BLOCK AND CRANKCASE, BALANCE SHAFT MODULE, DUO-PUMP

The cylinder block and crankcase is manufactured from GJL250 gray cast iron in the proven long-skirt design. The cylinder block and crankcase as well as the balance shaft module are both derived from the Volkswagen modular diesel engine kit MDB. Apart from the cylinder block and crankcase with balance shaft, there is also a weight-optimised, lower-cost variant without balance shaft for the engine variants with lower output and reduced torque.

The oil and vacuum pumps are designed as a duo-pump located in a common die-cast aluminium housing below the cylinder block and crankcase flange in the oil sump. Following adaptation of the suction line to suit the deeper and larger oil sump of the Transporter, it was possible to carry over the duo-pump from the passenger car variants of the MDB.

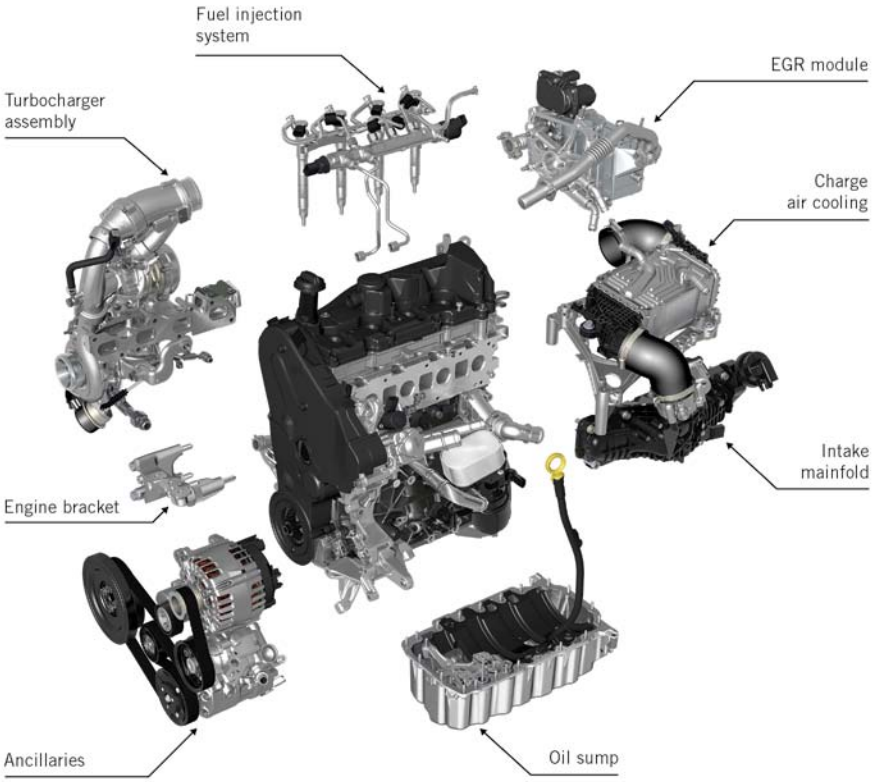

FIGURE 3 Modular structure of the new four-cylinder commercial vehicle engine

Displacement	1968 cm³			
Stroke/bore	95.5/81.0 mm			
Compression ratio	15.5			
Turbocharging	Monoturbo			Biturbo
Power outputs	62 kW	75 kW	110 kW	150 kW
Max. torque	220 Nm	250 Nm	340 Nm	450 Nm
Weight (DIN 70020-7)	155 kg	155 kg	172 kg	185 kg

TABLE 1 Key technical data of the new four-cylinder commercial vehicle engine in the Transporter model range

CYLINDER HEAD, INTEGRAL VALVETRAIN MODULE

The basis for developing the modified cylinder head on the commercial vehicle engine was the 176-kW biturbo passenger car engine [5]. Valves with a stem diameter of 5 mm are being used for the first time in diesel engines from Volkswagen. The lower valve mass has allowed valve spring forces to be reduced substantially, thereby making a significant decrease in friction possible.

As on the predecessor engine, the valves are arranged in a symmetrically straight layout, i.e., all intake and all exhaust valves are in line. This arrangement allows geometrically simple cooling ducts and high core robustness. Thanks to the parallel valves and port routing designed to minimise pressure losses, a high degree of cylinder charging is achieved. At the same time, the level of swirl required for good combustion is ensured by swirl chamfers on the valve seats and targeted adaptations of the port geometry. Carrying over the drilling and fastening solution allows the cylinder head to be manufactured particularly economically on the assembly lines for the modular diesel engine kit.

The valvetrain module of the new diesel engine for commercial vehicles has the same basic structure as that of the four-cylinder TDI MDB engine. However, the valve timing has been designed specifically for commercial vehicles to yield a particularly full-bodied torque curve.

CHARGE AIR COOLING AND INTAKE MANIFOLD

Like all MDB engines, the new diesel engine for commercial vehicles is also equipped with a water-cooled charge air cooler. Deviating from the four-cylinder engines used in passenger cars, the shorter engine compartment in the Transporter front end means that the charge air cooler must be positioned above the cylinder head.

The cooler core consists of a total of 22 cooling plates soldered in pairs, with air flowing through them in the counter-current principle. This ensures good heat transfer from the sheet aluminium to the coolant, while keeping pressure loss to a minimum. Baffles improve heat transfer from the charge air to the coolant. The plastic end tanks ensure uniform airflow to the cooling plates and are crimped to the cooler package. To minimise vibration load, the charge air cooler is decoupled from engine excitations by means of an elastic fastening mechanism.

The significantly larger bandwidth of customer driving profiles compared with passenger cars means that the combustion process must be designed to be particularly robust. Especially in low-speed delivery traffic, an operating-point-specific setting for swirl in the airflow entering the combustion chamber is required to minimise raw particulate emissions. Swirl is controlled using an intake manifold made from polyamide 6.6 that is equipped with pneumatically operated swirl flaps.

EXHAUST GAS RECIRCULATION

In order to meet the stricter requirements of the Euro 6 emission standard, and in particular to reduce emissions in the NEDC following a cold start, the effectiveness of the high-pressure exhaust gas recirculation (HP-EGR) system has been further improved significantly.

Based on experience gained with previous generations of EGR modules, a completely novel valve and cooling solution has been developed for use in the T6, which features a high level of robustness in all operating states. The focal points of development here were

FIGURE 4 High-pressure EGR module

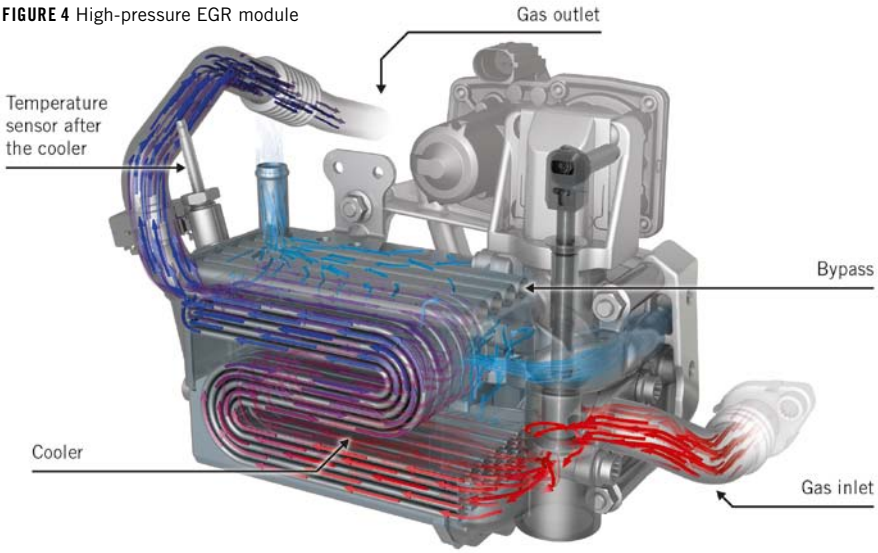

reliable switching of the cooler bypass function, avoidance of condensed combustion residues, and minimising wear around the valve guide through valve-rod operation with zero lateral forces.

A drive layout where both the cooler path and the bypass can be controlled steplessly with only a single actuator has been developed to make optimum use of the existing packaging space to the side of the engine, above the transmission. As a result, the vacuum supply for bypass flap actuation is no longer necessary. The EGR valve has two valve heads that are floating on the valve rod. These valve heads are pressed into their respective seat by a compression spring made of Inconel.

Due to the module's position in the gas path from the hot to the cold side of the engine, a conventional, U-flow cooler was out of the question. An I-flow cooler would be too inefficient within the same packaging space, so a new type of gas flow in S shaped pipes was used, **FIGURE 4**.

The valve has three different switching states:

- In the neutral position, both the cooler and the bypass path are closed.
- In the bypass position, the actuator pushes the valve rod down from the centre position, thereby opening the upper valve head and enabling the gas to flow through the cooler's bypass pipes.
- In the cooling position, the actuator pulls the valve rod up, thereby opening the lower valve head and freeing the path into the S-shaped cooling pipes.

INJECTION SYSTEM

The new diesel engine for commercial vehicles features a Delphi injection system with a system pressure of 2000 bar. Despite the stricter performance specification requirements compared with passenger cars, it was possible to use almost all DFS 1.20 components from the modular diesel engine kit in monoturbo engines with up to 110 kW [4]. The jet pattern of the eight-hole fuel injectors has been adapted to the new piston bowl geometry with compression reduced to 15.5.

In order to ensure the necessary injection quantities for the high torques that are already available at low engine speeds of the top-of-the-range biturbo engine, a DFP 7.20, two-piston, high-pressure fuel pump with a significantly higher delivery rate is used.

MONO-TURBOCHARGER SYSTEM

An updated version of the VTG turbocharger familiar from the 2.0-l TDI engine is used on the 62, 75 and 110 kW output variants. The turbocharging system has been adapted for this vehicle class to comply with Euro 6 emission limits, to reduce fuel consumption and CO_2 emissions, and to provide torque characteristics that optimise tractive power.

In order to achieve the optimum for each output level, new turbochargers have been developed for the engines with up to 75 kW and for the 110 kW variant respectively. Furthermore, the compressor and turbine wheels from the predecessor engine have been redesigned to improve efficiency levels throughout the operating range.

BI-TURBOCHARGER SYSTEM FOR THE 150 KW VARIANT

Since 2009, when two-stage turbocharging was successfully introduced in the Transporter, Volkswagen has been setting the benchmark for commercial vehicle engines with optimised tractive power. The aim with the new 2.0-l biturbo engine was to increase power and torque perceptibly compared with the predecessor engine in order to safeguard and improve the competitive advantage.

As with the lower-output variants, use in commercial vehicles with a high load spectrum and demanding requirements in terms of starting behaviour, even at a maximum laden weight of 5.5 t, has also been taken into account in this top-of-the-range engine. Due to positive experiences with the predecessor engine, the choice was once again for a regulated two-stage turbocharging system with the turbine and compressor including bypass connected in series. To further improve the performance when puling away, variable turbine geometry (VTG) is used on the high-pressure charger. The low-pressure turbine is still controlled using a waste gate.

Apart from a passive compressor bypass, there is also an active turbine bypass valve as well as the familiar waste gate. The latter two are equipped with vacuum-operated actuators, **FIGURE 5**. The variable turbine geometry is also vacuum-adjusted.

OUTPUT AND TORQUE

The 2.0-l four-cylinder common rail engines for the new Transporter now provide a broader output bandwidth of 62 to 150 kW compared with the predecessor model (62 to 132 kW). Despite the increase in output, the most powerful monoturbo variant with 110 kW (predecessor: 103 kW) now makes its rated torque available at as low as 1500 rpm (predecessor: 1750 rpm). In addition, the maximum torque of 340 Nm is maintained up to 3000 rpm. The increased output of 110 kW is available over a wide rpm range from 3200 to 3800 rpm, **FIGURE 6**.

The top-of-the-range model of the new Volkswagen commercial vehicle engine is

a 2.0-l four cylinder biturbo engine with a rated output of 150 kW at 4000 rpm, **FIGURE 7**. With over 76 kW/l, the engine therefore sets the benchmark in the commercial vehicle segment. Its maximum torque of 450 Nm is based on the drivetrains mechanical transmission limits and is available from as low as 1400 rpm. This allowed the usable torque to be increased by more than 12 % over the whole rpm range compared with the previous top-of-the-range engine.

PERFORMANCE, EMISSIONS AND FUEL CONSUMPTION

The focus when designing the new Transporter engines was on achieving a significant reduction in both fuel consumption and CO_2 emissions across all output variants, while also improving their performance. The objective of meeting the Euro 6 exhaust emission limits across all output variants follows from the legal requirements.

Intensive detail work and the turbocharging system designed specifically for commercial vehicles have provided a more full-bodied torque curve for all engine variants. This, in turn, has lead to improvements compared to the predecessor vehicle both in terms of standard acceleration from 0 to 100 km/h and in terms of elasticity, which is more important during driving operation. For the top-of-the-range engine, the substantial increase in output compared with its predecessor made a new transmission ratio necessary, resulting in a particularly pronounced performance improvement, **TABLE 2**.

At the same time, the reduction in emission limits called for a significant reduction in untreated emissions by optimising charge, charge movement, and injection system, but also for the use of a selective catalytic reduction (SCR) system for exhaust gas treatment.

The exhaust gas treatment system comprises an improved oxidation catalyst and a particle filter with a special coating for reducing nitrogen oxide levels. AdBlue is fed in upstream of the particle filter. A slip catalyst integrated in the particle filter housing prevents NH_3 slip. Together with the actions taken on the engine itself, this has helped to reduce emissions – particularly in NO_x emissions – significantly throughout the operating range of the engine.

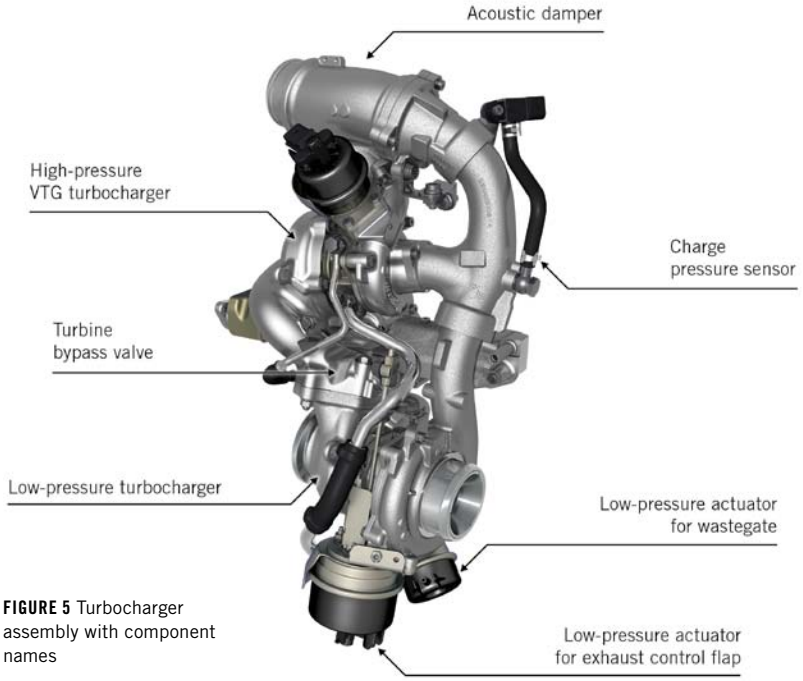

FIGURE 5 Turbocharger assembly with component names

FIGURE 6 Output and torque curves of the new engine versus predecessor (103 versus 110 kW monoturbo)

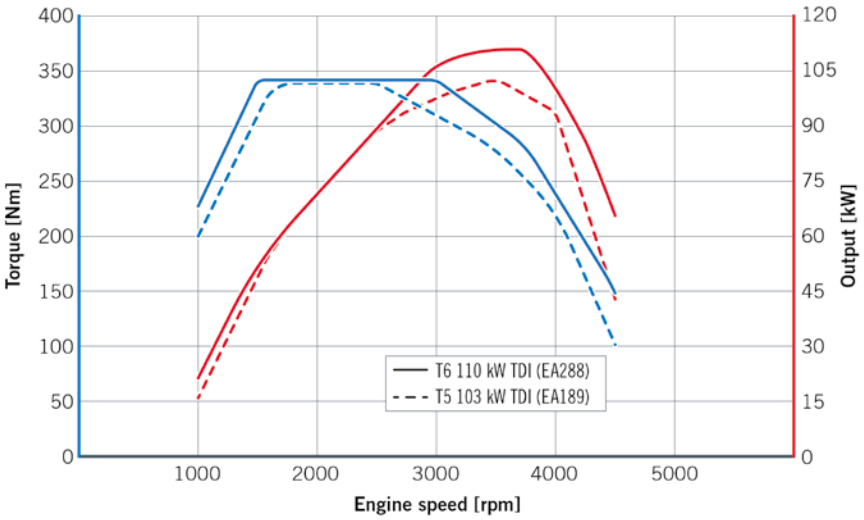

FIGURE 7 Output and torque curves of the new engine versus predecessor (132 versus 150 kW biturbo)

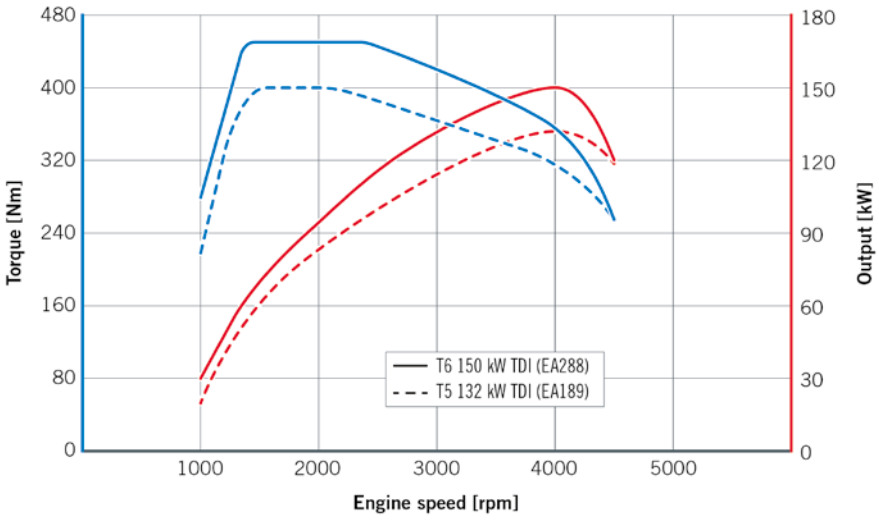

Power [kW] at [rpm]	62 3500	62 2700-3750	75 3500	75 3000-3750	103 3500	110 3250-3750	132 4000	150 4000
Torque [Nm] at [rpm]	220 1250-2500	220 1250-2500	250 1500-2500	250 1500-2750	340 1750-2500	340 1500-2500	400 1500-2500	450 1400-2250
v_{max} [km/h]	146	146	157	157	173	182	191	203
Acceleration 0-100 km/h [s]	22.2	21.1	17.9	16.4	14.7	11.9	11.8	9.0
Elasticity 80-120 km/h (5th gear) [s]	28.3	25.5	21.6	19.0	16.0	14.0	11.3	8.5
Emission standard	Euro 5	Euro 6	Euro 5	Euro 6	Euro 5	Euro 6	Euro 5	Euro 6

TABLE 2 Performance data for the new Transporter (grey) compared with the predecessor model (white), (manual version, front-wheel drive)

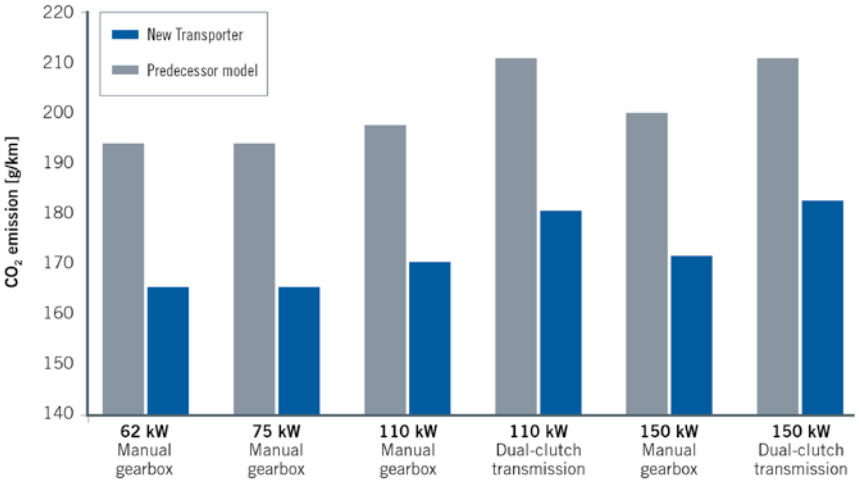

FIGURE 8 CO_2 emissions of the new Transporter compared with the predecessor model (provisional values, front-wheel drive variants only)

Consequently, despite substantial reductions in pollutant emissions and improvements in performance, it was still possible to significantly reduce CO_2 emissions for all variants. A decisive contribution has also been made by further refining the manual and dual clutch (DSG) transmissions. On vehicle variants equipped with DSG, the use of a dual-mass flywheel with centrifugal pendulum-type absorber has perceptibly reduced the shifting speeds, thereby reducing fuel consumption and increasing driving comfort. In conjunction with other steps taken in the vehicle, CO_2 emission have been improved by up to 30 g/km compared with the predecessor model, **FIGURE 8**.

SUMMARY AND OUTLOOK

With the new 2.0-l four-cylinder four-valve TDI engine, Volkswagen has created a universal and future-proof basis for its light commercial vehicles. Using the modular diesel engine kit MDB as the starting point for deriving the commercial-vehicle specific variants allows for cost-effective realisation of the engine and economical production through utilisation of existing MDB production systems.

Currently, the engine covers an output range from 62 to 150 kW and a torque range from 220 to 450 Nm. With over 76 kW/dm³ and more than 225 Nm/dm³, the Transporter engines set the benchmark in their segment in terms of specific engine characteristics and outperform the predecessor engines by approximately 13 % in terms of specific output and specific torque. The increase in starting torque has been disproportionate, with full advantage being taken of the VTG high-pressure stage in the biturbocharger unit.

One of the focal points of development activities was the reduction of fuel consumption and CO_2 emissions. By optimising the combustion process, minimising friction, and reducing charge cycle losses, a decrease in fuel consumption of approximately 14 % has been achieved on average compared with the predecessor vehicles. At the same time, all Transporter variants meet the requirements of the Euro 6 emission standard, while the predecessor engines were designed to comply with the Euro 5 standard.

Each engine variant on offer is superior to its respective predecessor in all customer-relevant properties, such as performance, fuel consumption, and emissions. Given the achieved increase in both power and torque, the extremely compact construction of the engine, and in view of the use of existing modules from passenger car versions of the modular diesel engine kit, further applications in the commercial vehicle segment can be conceived and implemented as required at short notice.

REFERENCES

[1] Rudolph, F.; Thomfohrde, C.; Ziesenis, J.; Pott, E.: The New Diesel Engines for the Volkswagen Transporter Range. Aachen Colloquium Automobile and Engine Technology, 2009

[2] Neußer, H.-J.; Kahrstedt, J.; Jelden, H.; Engler, H.-J.; Dorenkamp, R.; Jauns-Seyfried, S.; Krause, A.: The New Modular TDI Generation from Volkswagen. 33rd International Vienna Motor Symposium, 2012

[3] Neußer, H.-J.; Kahrstedt, J.; Jelden, H.; Engler, H.-J.; Dorenkamp, R.; Düsterdiek, T.: The EU6 Engines of the Modular Diesel Engine Kit from Volkswagen – Innovative Close-Coupled Exhaust Emission Control for Further Reductions in NO_x and CO_2. 34th International Vienna Motor Symposium, 2013

[4] Eichler, F.; Kahrstedt, J.; Pott, E.; Beddies, H.: The New 3-Cylinder TDI Engine from Volkswagen. 35th International Vienna Motor Symposium, 2014

[5] Eichler, F.; Kahrstedt, J.; Köhne, M.; Krause, A.; de Graaff, M.: The New 4-Cylinder Biturbo TDI Engine from Volkswagen. Aachen Colloquium Automobile and Engine Technology, 2014

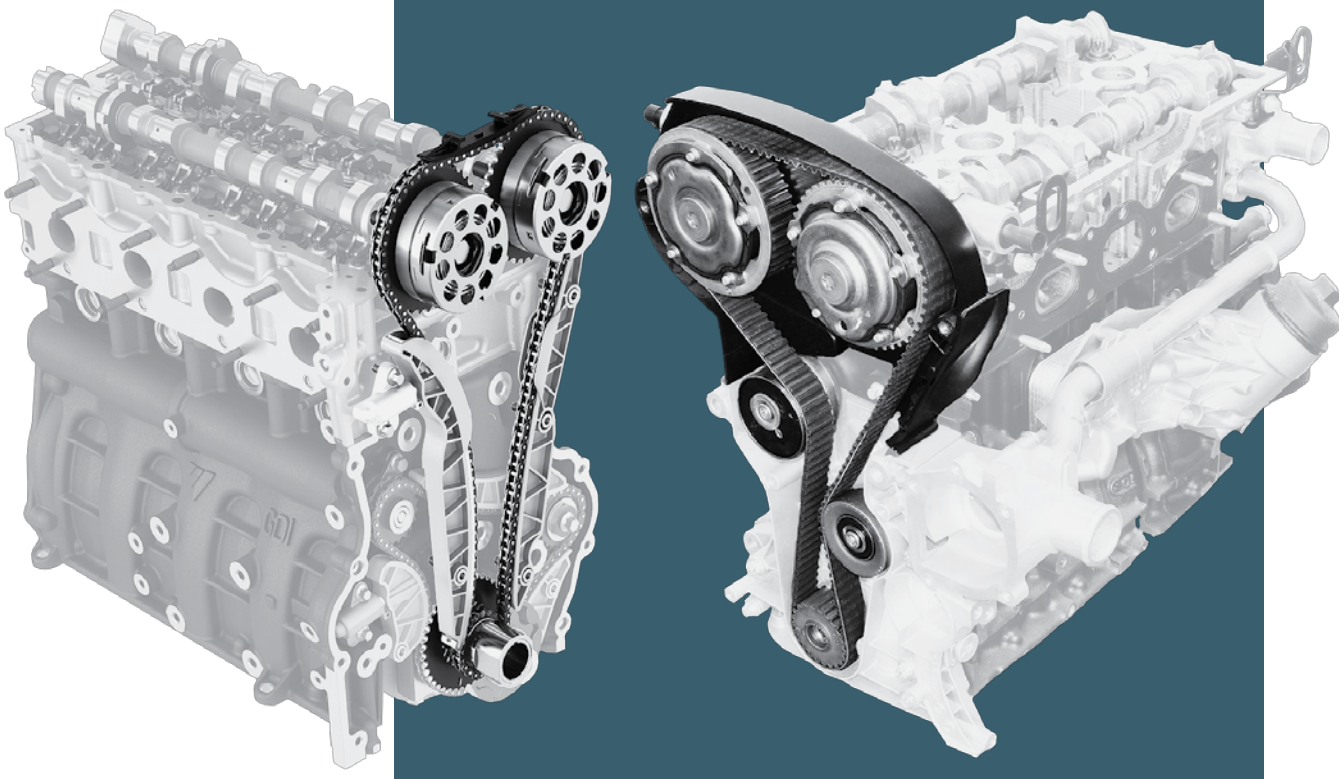

Future Timing Drives
Chain and Belt in Competition

Modern gasoline and diesel engines for cars generally have timing chains or timing belts. AVL has investigated the advantages and disadvantages of the two different systems and presents the results in this article.

OBJECTIVE CRITERIA TO DETERMINE SYSTEM SELECTION

The choice of technology for the timing drive system is one of the key decisions that determines the overall characteristics of new engine designs with far reaching implications on the remaining architecture. For passenger car engines the mainstream technologies are toothed belts and chains. Each of these offers several sub-variants, such as dry versus wet belt, or toothed versus roller chain. Over the last decade there has been a continuing trend towards chain systems for new engines. The main markets for belt driven engines are Europe and South America; in Asia the split remains close to 50 %. Belt in oil technology has been introduced in volume production in Europe and will be localised in Asia. Based on currently ongoing development programmes, the global share for this relatively new technology is projected to grow to between 3 and 10 %.

The selection of the appropriate system for a particular application must be made based on an evaluation of the performance in relation to the key attributes at engine system level including frictional losses, durability and maintenance, timing accuracy over lifetime, dynamic behaviour, NVH, weight, packaging and production cost.

FRICTION

The timing drive influences fuel consumption directly through its contribution to the engine friction. Therefore, the layout of timing drives for low friction is of increasing importance. Recent measurements [1, 2] performed on state-of-the-art engines show no consistent pattern of differences between belt drives and chain

AUTHORS

Dr. Wolfgang Schöffmann
is Head of Design Passenger Car Powertrain at the AVL List GmbH in Graz (Austria).

Mike Howlett, B. Sc.
is Lead Engineer Passenger Car Engine Design at the AVL List GmbH in Graz (Austria).

Caroline Truffinet, M. Sc.
is Development Engineer Vehicle & Powertrain Acoustics at the AVL List GmbH in Graz (Austria).

Dipl.-Ing. Norbert Ausserhofer
is Lead Engineer Valve Train & Timing Drive Simulation at the AVL List GmbH in Graz (Austria).

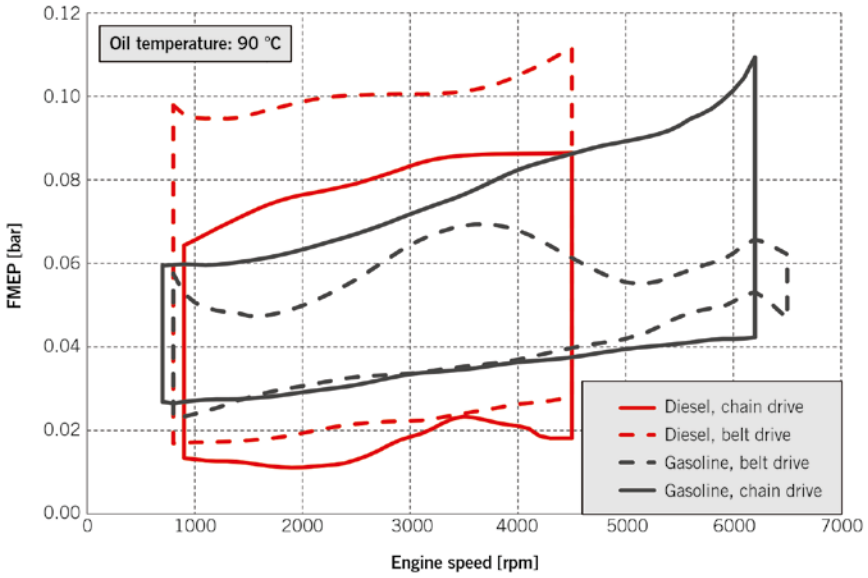

FIGURE 1 Measured friction of the timing drive and camshafts (FMEP) by strip-down method for chain and belt

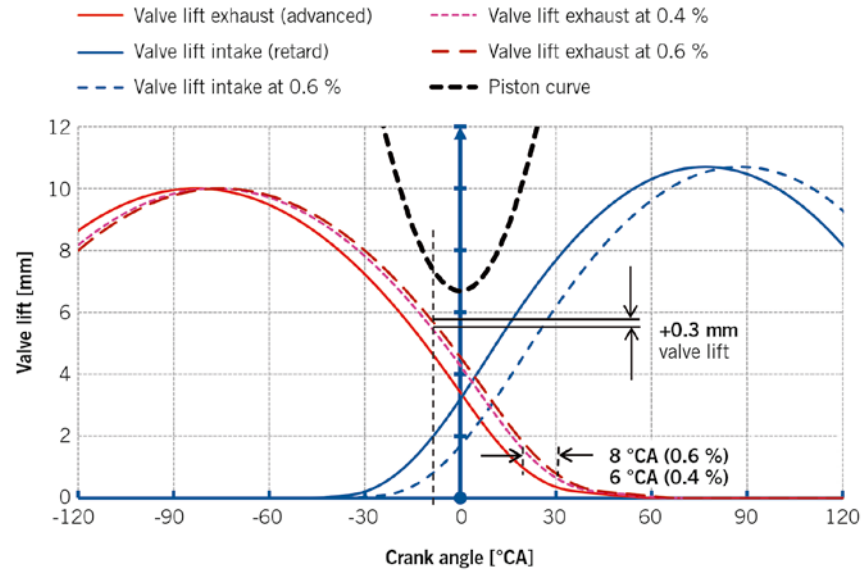

FIGURE 2 Effect of elongation on valve timing and clearance

drives. The lower end of scatter band for gasoline engines is on a very similar level for chain- and belt drive systems as summarised in **FIGURE 1** based on measurements at twelve gasoline and eight diesel passenger car engines.

Inverted tooth chains have a higher friction disadvantage to bush and roller chains, based on AVL measurements. Development efforts at chain suppliers regarding new inverted tooth and roller/bush chains as well as at belt suppliers working on new compounds and coatings show the potential for further friction optimisation.

TIMING ACCURACY

Changes in the length of the belt or chain over time lead to an angular timing error between camshaft and crankshaft. **FIGURE 2** illustrates the effect on valve timing and piston to valve clearance of maximum 0.6 % elongation. A timing drift of 8 °CA (crank angle) over lifetime is currently considered acceptable. Combustion systems with high compression ratio and extreme cam phasing ranges, for example for Miller Cycle combustion [3] will require more stringent limits.

A chain elongation of 0.2 to 0.6 % is typically considered as layout criterion, based on the selected chain type and the oil condition. The belt elongation over lifetime varies depending on the belt technology used with different belt suppliers specifying values between 0.1 and 0.25 %. The development trend is towards the lower end of this range.

DYNAMIC BEHAVIOUR

The timing drive system transmits torque from the crankshaft to the camshafts whereas the engine crankshaft speed

varies over the cycle. Also the camshaft drive torque demand varies over the cycle due to the cam profiles, and may reverse due to the reaction torque from the valve springs. The relative phases of these loads may be varied by VVT devices dependent on engine load and speed. The whole system is thus a highly dynamic one and the layout of the geometry and the tensioning system has to be designed accordingly. Evaluation criteria are the maximum belt or chain tension which must remain below the design limit for the chosen technology, and the dynamic timing error due to relative torsional vibration at the camshaft.

Typically, mechanical or hydraulic tensioner systems have comparable performance characteristics. Mechanical systems typically used on dry belts have the advantage of being independent from engine lube oil condition and oil pressure. The location of the timing drive (at the engine front or engine flywheel side) does not have a significant influence onto the overall dynamic behaviour. Typical timing drive systems have at least one resonance in the engine speed range as shown in **FIGURE 3** (top).

Due to their low stiffness, belt drive systems frequently exhibit two separate resonance areas appearing within the engine operating speed range as shown in **FIGURE 3** (bottom). However, this is of itself not an issue provided the force peaks are within the design limits.

The high pressure fuel injection pump torque is one of the main loads to the timing drive. Future gasoline fuel injection pump driving torques are expected to further increase to reach the level of today's diesel injection pumps, while diesel injection pressures and torques also increase further. Very high torque peaks are directly converted to high tensions in a stiff chain, whereas a belt may be better able to compensate peaks through its flexibility.

Cancelling effects of the cam torque fluctuations can be utilised, if an optimum shift angle between the cam lobes and the fuel injection pump cam lobe is achievable. An optimised phasing of the high pressure fuel injection pump is a requirement in diesel engines in order to avoid excessive forces in the drive.

The cam angular vibration as well as crank angular vibration amplitudes can vary in a wide range depending on factors such as cylinder pressure, crankshaft

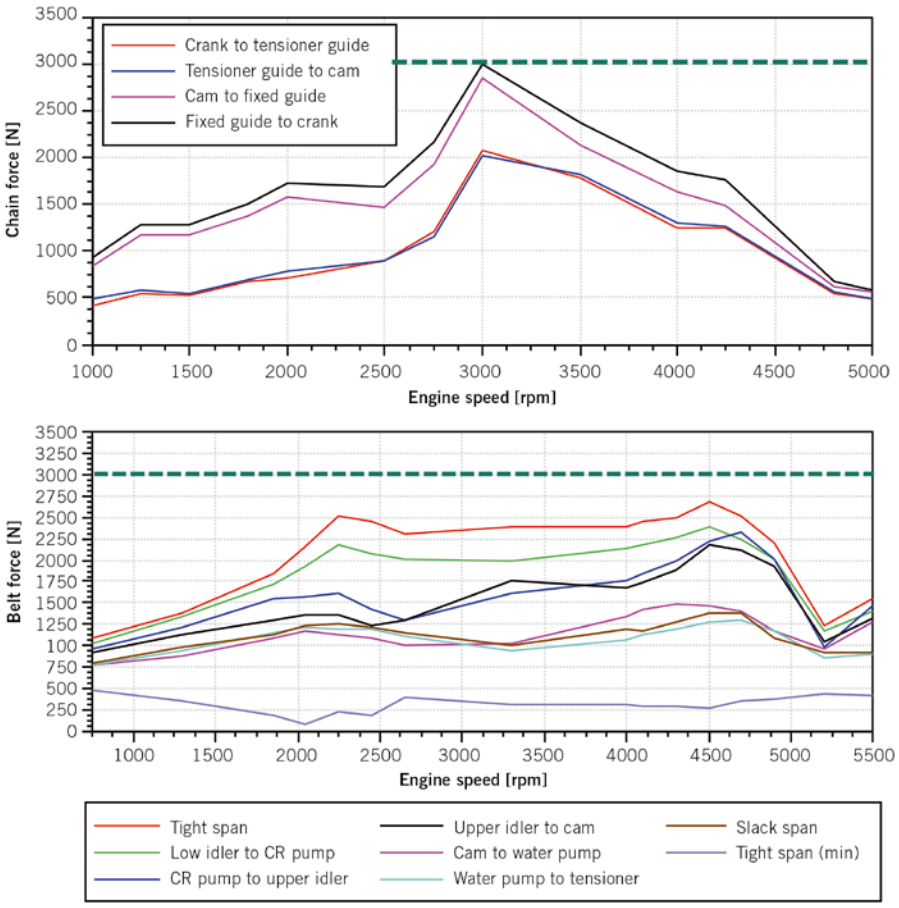

FIGURE 3 Chain and belt timing drive – dynamic forces

stiffness and flywheel inertia. Reference examples of chain drives as well as belt drive systems show values in a similar range. The timing error is not constant over the entire engine cycle; a maximum dynamic deviation of 3 to 4 °CA is considered normal and does not lead to an emission or performance penalty.

NVH BEHAVIOUR

Meshing noise is the major noise phenomenon of timing drives, and is inherent to the meshing process of the belt or chain with the sprocket. This process creates whine noise with a discrete frequency (and its multiples) which is related to the speed and the number of teeth of the sprocket. This noise can be reduced by concept choice and detail design work (e.g. influence of tension, type of chain, sprocket teeth geometry) but cannot be eliminated. Other noise phenomena can be strongly reduced or even avoided by applying design rules. Particularly, the common noise amplification by the timing drive cover, due to structural resonances of the cover, can be suppressed with a careful design.

Generally, the risk of audible meshing noise is low with well-developed timing drive systems, for both chain and belt drives. However, due to less masking effects from the engine noise, this risk is higher at low load conditions than at full load. If meshing noise becomes audible, chain noise is usually more annoying than belt noise because of the sharper noise character associated with the metal-to-metal contact between chain and sprocket.

Regarding overall engine noise, **FIGURE 4** shows the situation for the noise levels measured on gasoline engines in an acoustic engine test cell at 1 m in front of the timing drive cover, under no load conditions. The thick line in **FIGURE 4** represents the average (mean) level, the box represents the scattering between best and worst engines. The average levels are represented with respect to the belt drives average (green mean = 0 dB). The mean noise level of silent chain drives

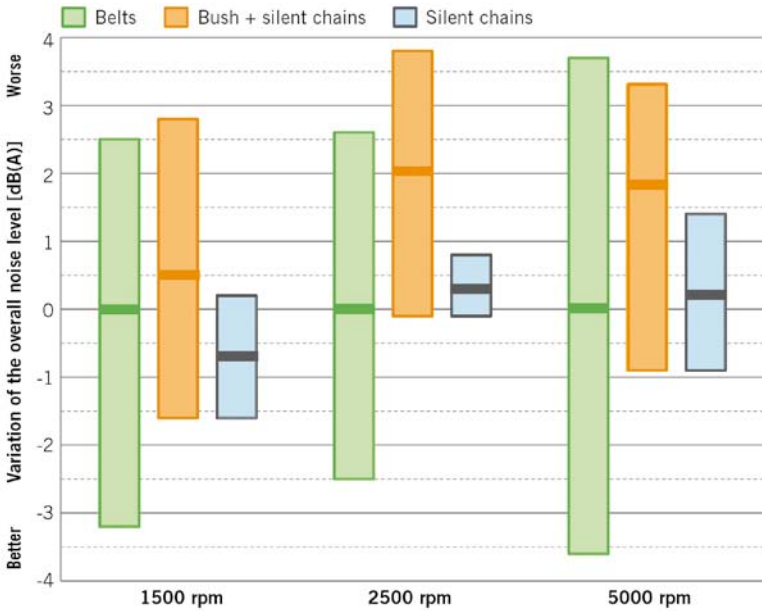

FIGURE 4 Scatter ranges of noise measured at engine front side

is lower than with bush chain drives and is very similar to that of belt drives, sometimes even lower.

However, the variation of the overall noise level within one type of timing drive is much higher than the typical mean differences between chain and belt drives. The strong influence of the engine structural dynamics on the radiation of the timing drive noise contributes significantly to this big variation. This effect may be further enhanced by the dynamic behaviour of the engine installation in the vehicle and the dynamics of the vehicle body. Both chain and belt drives can enable good vehicle acoustics, if the timing drive system and the engine and vehicle NVH are well developed.

Belt drives generally have very good NVH behaviour. For wet belts, the good NVH behaviour of the belt in combination with the stiff structure of the oil-tight cover results in superior overall NVH.

All chain drive concepts can reach good engine NVH characteristics if the major engine conception rules are considered. Non-optimised chain drive layouts may lead to noticeable whine noise with a sharp and annoying noise character. Inverted tooth chains achieve comparable NVH performance with belt drives.

SYSTEM WEIGHT AND PACKAGING

The weight analysis reflect current inline diesel engine configurations (so far not including a wet belt reference), **FIGURE 5**: A dry timing belt system driving the water pump and fuel pump, a two-step chain drive driving the fuel pump at the intermediate position and a simple chain drive with camshaft driven fuel pump are compared.

Integrating the high pressure fuel pump into belt timing drive systems requires additional idlers, resulting in higher system weight than at chain drives, even considering the guides, tensioners and double sprockets of a stepped drive. The lightest system overall is the simple chain drive with cam driven fuel pump.

Engine length and height are the critical dimensions in terms of engine packaging. The timing drive directly influences both dimensions. After the cylinder spacing, the length of the timing and oil pump drive is a decisive factor for the overall engine length. The additional length of the belt drive compared to the single chain drive comes from the belt width itself, which is dependent on loading and lifetime requirements.

SUMMARY AND CONCLUSIONS

The timing drive is one of the key engine systems and its layout is a significant part of any new engine layout; for passenger cars the choice is usually made between chain and belt. Future engine development will be focussed on CO_2 reduction and extension of the emission relevant operating range resulting in an increase of the dynamic loading on the timing drive while also demanding more consistent accuracy of timing. At the same time global engine production increases the range of environmental influences.

The performance of the competing drive systems is very similar and conti-

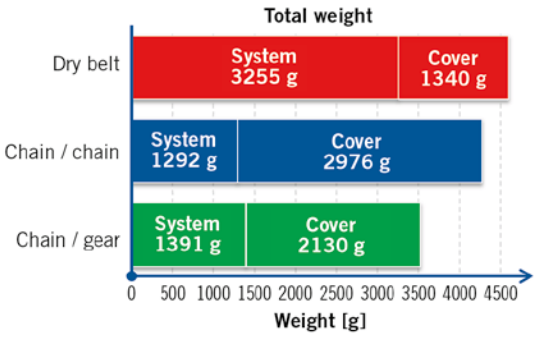

FIGURE 5 Diesel engine timing drive weight comparison

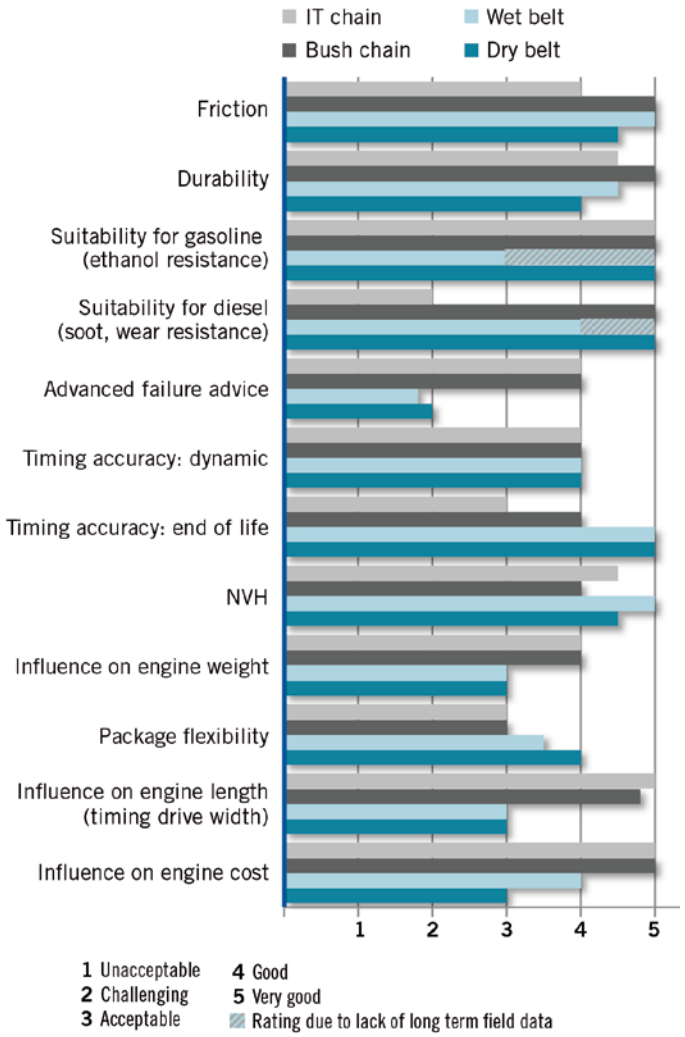

FIGURE 6 Summary of relative ratings of four main drive technologies

nuous technological development at all suppliers means that the ratings must be subject to frequent critical revision. Based on the evidence presented, it is not possible to select a "best technology" that suits all engine applications as summarised in **FIGURE 6** [5].

The current state of the art from the engine design point of view can be summarised as:

- Chain drives have an advantage over belt drives when absolute minimum engine length is required by vehicle package.
- Chain as well as wet belt drives are a lower cost solution for engines with hydraulic VVT, which in future will be a clear majority of gasoline engines and possibly some diesel engines.
- Belt drives achieve higher timing accuracy at end of life. The importance is increasing for future emissions and fuel consumption targets.
- The loads from the fuel injection pump due to increasing injection pressures are crucial for the durability of belt or chain.

Irrespective of the chosen drive type, a careful design layout and optimisation loops are required in order to achieve the best results in NVH, friction, and dynamic behaviour. The intense competition between belt and chain concepts is expected to continue in future.

THANKS

Special gratitude by the authors is owed to Dr. Helfried Sorger, Ing. Andreas Zurk and Dipl.-Ing. (FH) Jürgen Gelter, all AVL, for the realisation of essential parts of the study, the valuable contribution to the ratings as well as the discussions with belt and chain developers and suppliers.

REFERENCES

[1] Howlett, M.; Enzi, B.; von Falck, G.; Schoeffmann, W. et al.: CO_2 Reduction Potential through Improved Mechanical Efficiency of the Internal Combustion Engine: Technology Survey and Cost-Benefit Analysis. In: SAE International Journal of Engines, Technical Paper No. 2013-01-1740

[2] Schöffmann, W.; Sorger, H. et al.: Lightweight design, function integration and friction reduction – the base engine in the challenge between cost and CO_2 optimization". 34th International Vienna Motor Symposium, 2013

[3] Kapus, P.; Prevedel, K.; Wolkerstorfer, J.; Neubauer, M.: 200 g/kWh – Can The Stoichiometric Gasoline Engine Beat The Diesel? 22nd Aachen Colloquium Automobile and Engine Technology, 2013

[4] Krehl, D. : Riementrieb versus Kettentrieb. In: MTZ 74 (2013), No. 12

[5] Howlett, M.; Schoeffmann, W.; Ausserhofer, N.; Zurk, A.; Truffinet, C.: Demands on future timing drives – chain and belt in competition. In: SAE International Journal of Engines, Technical Paper No. 2015-01-1275

2g less CO_2 per km

FTE automotive

Lightweight and more efficient:
Developed by FTE automotive

FTE automotive – Innovation drives

While working with a customer on an innovative gearbox we achieved significantly reduced CO_2 emissions with this electrically powered oil pump made of high-performance plastic.

We could be taking the next step with you.

www.fte.de

Variable Compression Ratio in Diesel Engines

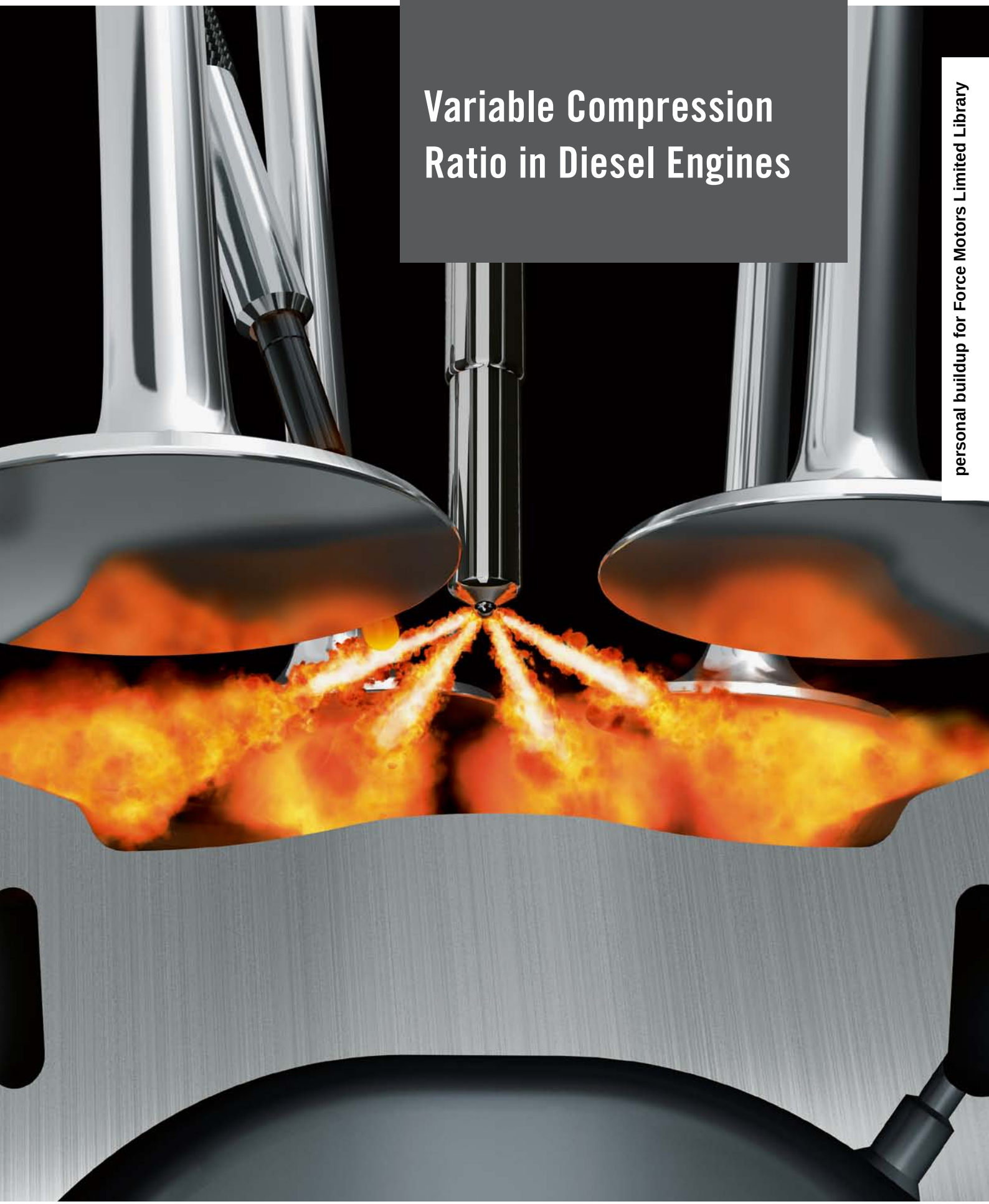

In diesel engines, downsizing is a well-established method of reducing fuel consumption and exhaust emissions. However, downsizing seems to be reaching its limits, because a further increase in the power output of engines will put their durability at risk. The solution could be a variable compression ratio, as a study by IAV shows.

DOWNSIZING IS REACHING LIMITS

The prediction that zero-emission vehicles would make a major contribution to achieving the necessary reduction in CO_2 levels to 95 g CO_2/km by 2020 currently appears to be highly unlikely. As a result, nearly the whole burden of fulfillment lies on vehicles driven by internal combustion engines. Plug-in hybrid electric vehicles (PHEVs) are one possibility for reaching the CO_2 target. Another possibility is to continue improving the engine processes of combustion engines.

The diesel engine is particularly relevant in this context. It serves as a good starting point with its low CO_2 emission per useful energy unit, while its popularity in both passenger cars and commercial vehicles in Europe means it can make a considerable contribution to achieving the objective. In the past, evolutionary development of the diesel engine has shown that the greatest progress can usually be achieved by new variabilities in engine components. Downsizing is currently one of the key technologies. However, downsizing would appear to have reached its limits, as any further increase in specific output jeopardises engine durability. Cylinder peak pressures of 220 bar and more do not appear feasible in cost efficiency terms for passenger car engines. Furthermore, every increase in cylinder peak pressure increases piston friction, with a negative impact on fuel consumption particularly in urban traffic. A variable compression ratio (VCR) of the engine is one possible remedy. It makes it possible to reduce the compression ratio for a high specific output, thus complying with the permissible maximum cylinder peak pressure.

In the conventional diesel engine, the geometric compression ratio is defined as a compromise between engine output requirements (ε = low) on the one hand and cold start/part load behaviour (ε = high) on the other.

The variable geometric compression ratio now permits construction of an efficient engine that combines the advantages of the high thermodynamic efficiency of combustion with high ε, and the ultra-downsizing of engine rating with low ε. In addition, cold start behaviour can be improved with minimised HC and CO emissions during low-temperature operation. **FIGURE 1** shows the possible uses and associated advantages of VCR in diesel engines.

FIGURE 1 Possible uses and potential for VCR in diesel engines

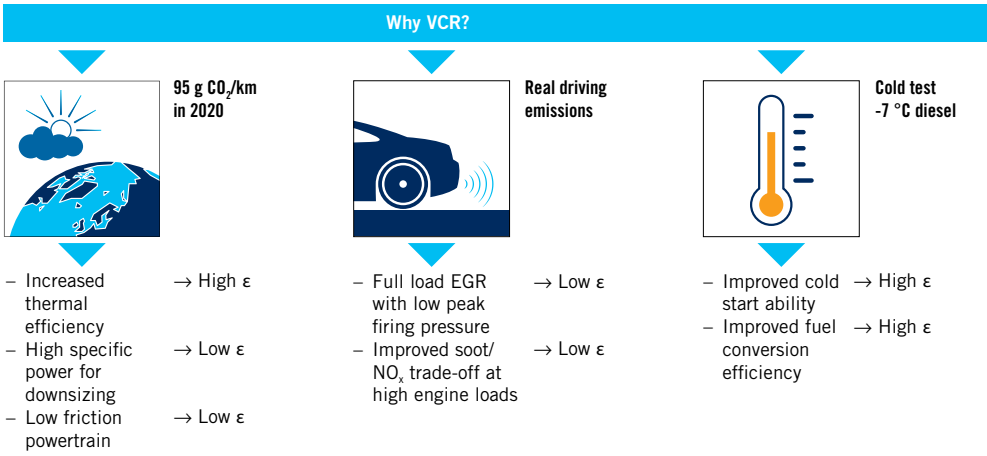

AUTHORS

Dipl.-Ing. Matthias Diezemann is Senior Technical Consultant for Technology Scouting in the Business Area Powertrain Mechatronics Diesel at the IAV GmbH in Berlin (Germany).

Dipl.-Ing. Christian Schramm is CFD Simulation Engineer in the Business Area Powertrain Development at the IAV GmbH in Chemnitz (Germany).

Dr.-Ing. Maximilian Brauer is Head of the Diesel Engine Concepts Department in the Business Area Powertrain Mechatronics Diesel at the IAV GmbH in Berlin (Germany).

Dr.-Ing. Christopher Severin is Head of the System Development and Combustion Concepts Department in the Business Area Powertrain Mechatronics Systems at the IAV GmbH in Gifhorn (Germany).

STATE OF THE ART

VCR systems are already being tested in gasoline engines. In recent years, the advantages of VCR in diesel engines have been discussed in various publications, with differing statements being made about the necessary spread of variability, mechanical design and fuel economy potential [1, 2, 3]. But the extensive activities pursued by engineering service providers in this field indicate that attention is focusing on the last unused variability of the diesel engine.

TEST SETUP AND METHOD

The studies are based on an inline four-cylinder 2.2-l diesel engine with common rail direct injection and two-stage exhaust turbocharging. The main engine parameters are:

- bore: 83 mm
- stroke: 99 mm
- geometric compression ratio: 16.2
- number of valves: 4
- maximum injection pressure: 2000 bar
- nominal power at n = 4000 rpm: 163 kW; BMEP = 25 bar
- specific output at n = 4000 rpm: 76 kW/l
- maximum cylinder pressure: 190 bar
- maximum exhaust temperature upstream of turbine: 835 °C
- exhaust emission standard: Euro 6.

The following method is used to assess potential: In a first step, the used combustion method is designed in terms of the necessary spread in compression ratio ε, taking account of the variable quench gap based on 3-D CFD simulation. Then the design is validated at the single-cylinder test bench under given restrictions for air efficiency, peak pressure and exhaust gas temperature. After that, the power potential of a decrease in ε is analysed for the goal P_S = 110 kW/l by expanding the boundary conditions based on 1-D simulation. In a last step fuel economy is evaluated in comparison to a six-cylinder engine.

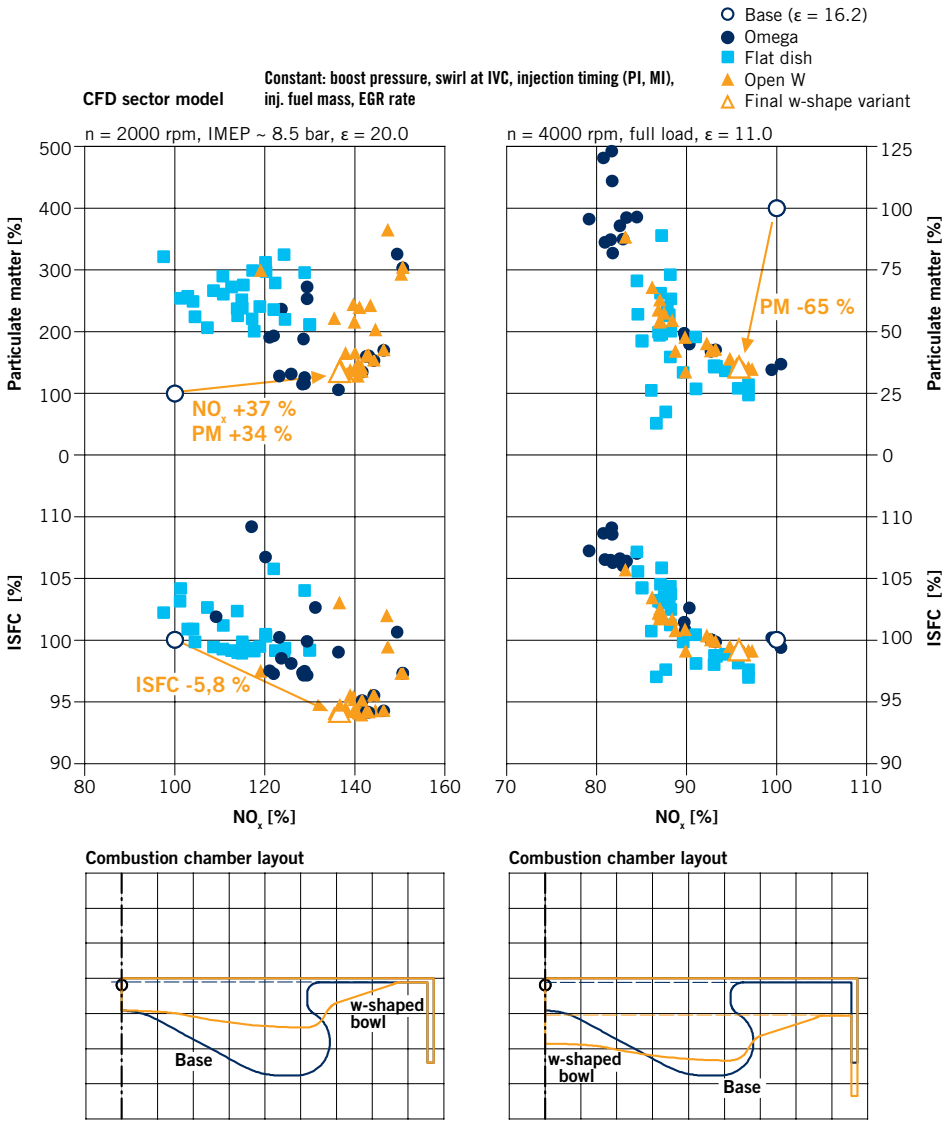

FIGURE 2 Results of bowl optimisation with 3-D CFD simulation at the operating points n = 2000 rpm, IMEP = 8.5 bar and n = 4000 rpm, full load

DESIGNING THE COMBUSTION PROCESS

Suitable solutions for the diesel engine consist in mechanical VCR concepts that do not change the cubic capacity. Usually these solutions change the TDC position and thus the quench gap height between piston and cylinder head. 3-D CFD simulation was used to examine the influence of the variable quench gap on combustion. Optimisation of the piston bowl took account of parameters such as part-load consumption, trade-off of soot and NO_x as well as the conversion rate in the near full-load map range between two operating points:

- operating point 1: part load with ε = 20 (n = 2000 rpm, BMEP = 7 bar)
- operating point 2: part load with ε = 11 (n = 4000 rpm, BMEP = 23 bar).

FIGURE 2 (top) shows a 5.8 % consumption improvement for the part-load operating point for the selected w-shaped bowl with ε = 20.0, compared to the basic bowl with ε = 16.2. Enhanced, thermodynamically more efficient combustion comes at the cost of a slight increase in NO_x and particulate matter emissions. The full-load operating point shows a slight improvement in the indicated fuel consumption for the chosen w-shaped bowl with ε = 11 compared to the basic bowl with ε = 16.2. The clear reduction in particulate matter emissions at the nominal power point indicates improved conversion of the fuel quantity injected. **FIGURE 2** (bottom) shows the basic recess and the current status of the w-shaped bowl, used for subsequent engine tests.

TEST RESULTS FOR INCREASING COMPRESSION RATIO

To assess the potential of increasing ε, engine test were carried out at part-load

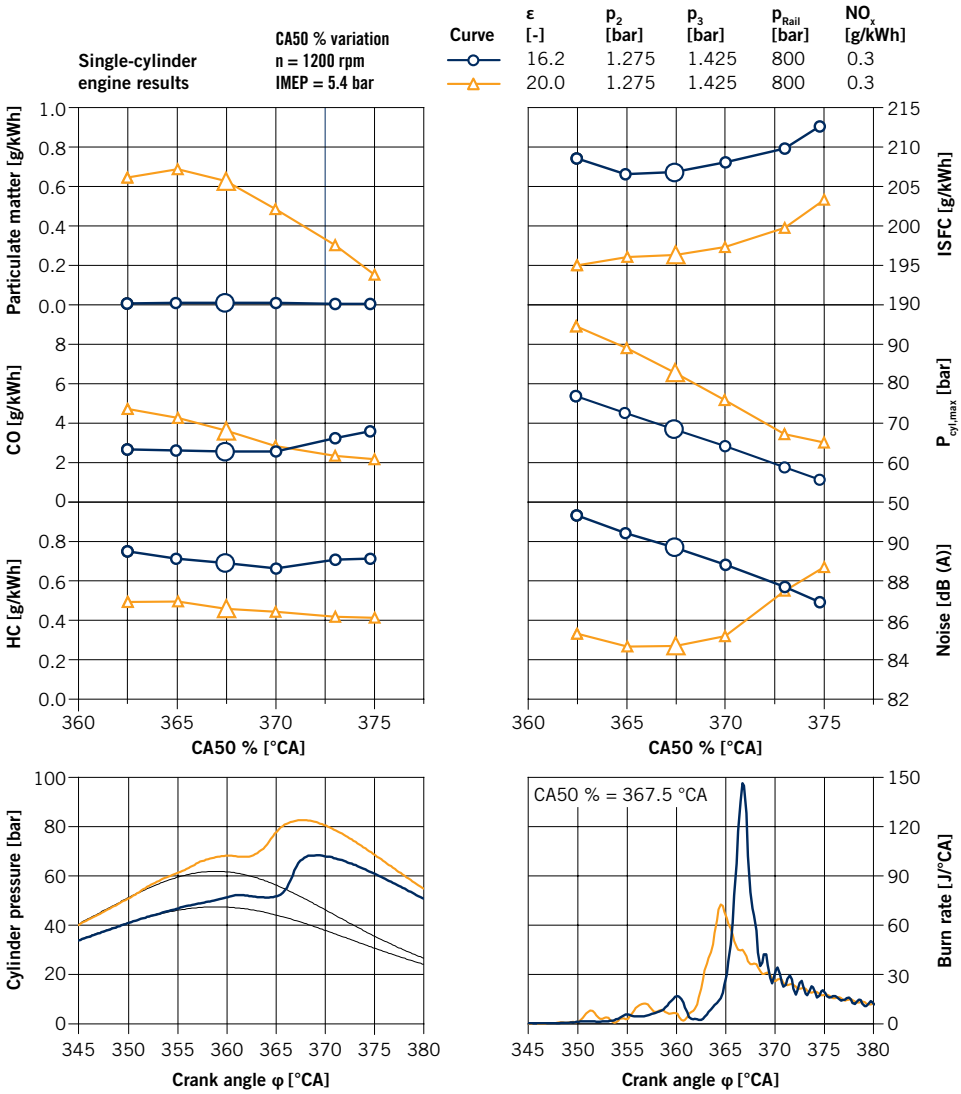

FIGURE 3 Fuel consumption potential by varying the VCR COHR at operating point n = 1200 rpm, IMEP= 5.4 bar (single-cylinder engine test)

operating points on the single-cylinder engine. **FIGURE 3** shows an example with operating point n = 1200 rpm, IMEP = 5.4 bar. The main centre of heat release (COHR) was varied for a NO_x emission value of 0.3 g/kWh. Optimum consumption was obtained for ε = 20 at COHR = 367.5 °CA. This calibration also brought about clear reductions in combustion noise and HC emissions, and is a result of a distinctly more diffusive combustion process, as shown in the combustion curve in **FIGURE 3** (bottom right). The increase in particulate matter and CO emissions remains acceptable at this very low-load operating point so that recalibration could be dispensed with for the most part. The optimum COHR revealed an indicated fuel economy of 5 % for ε = 20.0, compared to the basic bowl with ε = 16.2.

VALIDATING THE POTENTIAL OF DECREASING COMPRESSION RATIO

Validating the potential of decreasing ε again consisted in carrying out engine tests on the single-cylinder engine. **FIGURE 4** shows an example with operating point n = 4000 rpm at full load. For ε = 11 tests, the piston was fitted with the ε = 20 bowl and a quench gap of 4.7 mm was adjusted. In the tests, the cylinder peak pressure was limited to 190 bar and the maximum exhaust gas temperature T_3 to 835 °C. The ratio of exhaust gas pressure to intake manifold pressure was kept constant at 1.4. The injection nozzle of the base engine can be used to achieve a maximum indicated mean pressure of 28 bar with the basic rate of ε = 16.2 at COHR = 377.5 °CA. This already requires 3.1 bar boost pressure. For ε = 11, the basic injection nozzle makes it possible to increase the IMEP by 19 % to 33.3 bar. The necessary boost pressures show that the cylinder head has to be adjusted for the high specific performance requirements in terms of flow rate.

ANALYSING THE POWER POTENTIAL OF DECREASING COMPRESSION RATIO

On account of the inadequate flow rate of the single-cylinder test engine, the limit analysis for a specific power output of 110 kW/l was performed using 1-D simulation. The maximum admissible cylinder peak pressure was increased to 200 bar and the maximum admissible exhaust gas temperature (T_3) to 850 °C. Furthermore, a turbocharging group was used with high-pressure, medium-pressure and low-pres-

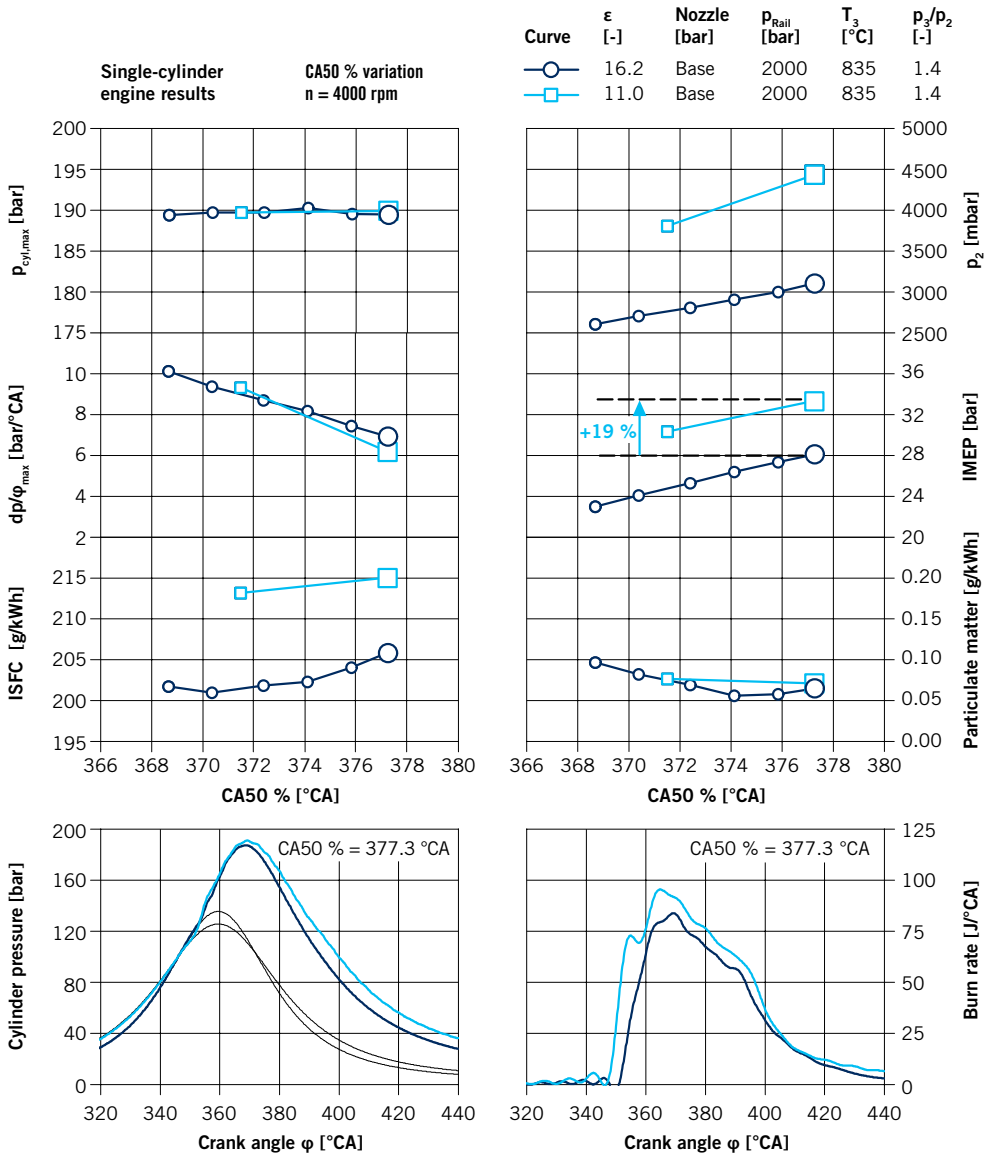

FIGURE 4 Power potential of VCR – CA50 % variation at = 4000 rpm (single-cylinder engine test)

sure stage (so-called Ser-Tri-Turbo) and injection nozzles with higher flow rates were fitted. **FIGURE 5** shows the VCR four-cylinder inline engine with variable compression in green and the basic four-cylinder inline engine without VCR in blue. The specific power curve shows that 110 kW/l was achieved at the rated engine speed of 3800 rpm. It is quite clear that a full ε decrease to ε = 11 is only required from n = 3200 rpm. But the 44 % increase in power to P_s = 110 kW/l is not owed solely to the VCR system: rather VCR permits higher turbocharging rates without exceeding cylinder peak pressure ($p_{cyl, max}$ = 200 bar). The orange curve shows the potential for a two-stage VCR system (ε = 20 / ε = 11). The full-load curve can also be achieved although this entails a slight deterioration in consumption and somewhat higher exhaust gas temperatures.

FIGURE 6 shows the theoretical consumption advantage in the map for the four-cylinder inline VCR Ser-Tri-Turbo diesel engine (validated 1-D simulation) compared to a conventional six-cylinder, single-stage TC VTG diesel engine with current emission level (test bench measurement). The dark green markings are the scatter diagram for the NEDC, with pale green markings for the WLTC of a current D-segment vehicle. The consumption-relevant map area reveals an advantage of about 12 % for the VCR engine compared to the six-cylinder engine. Below the black curve the engine can be operated with ε = 20. A great consumption advantage is thus also feasible for a two-stage VCR system. The small TC high-pressure stage of the Ser-Tri-Turbo makes the torque in the lower engine speed range comparable with the 3.0-l six-cylinder engine. Thanks to the far better conversion rate with ε = 20 in the cold start and warming-up phase, further consumption advantages are expected for cold-start cycles.

SUMMARY AND OUTLOOK

The paper describes the positive influences of variable compression ratio (VCR) on diesel engine combustion. The following potential is indicated by the results from 1-D and 3-D simulation with engine test validation:

– At the part-load operating point illustrated here (n = 1200 rpm, IMEP = 5.4 bar), the flat, open w-shaped piston bowl optimised for VCR application shows potential for reducing fuel consumption from Δb_i = 5 % through the transition from ε = 16.2 to 20.0. It is presumed

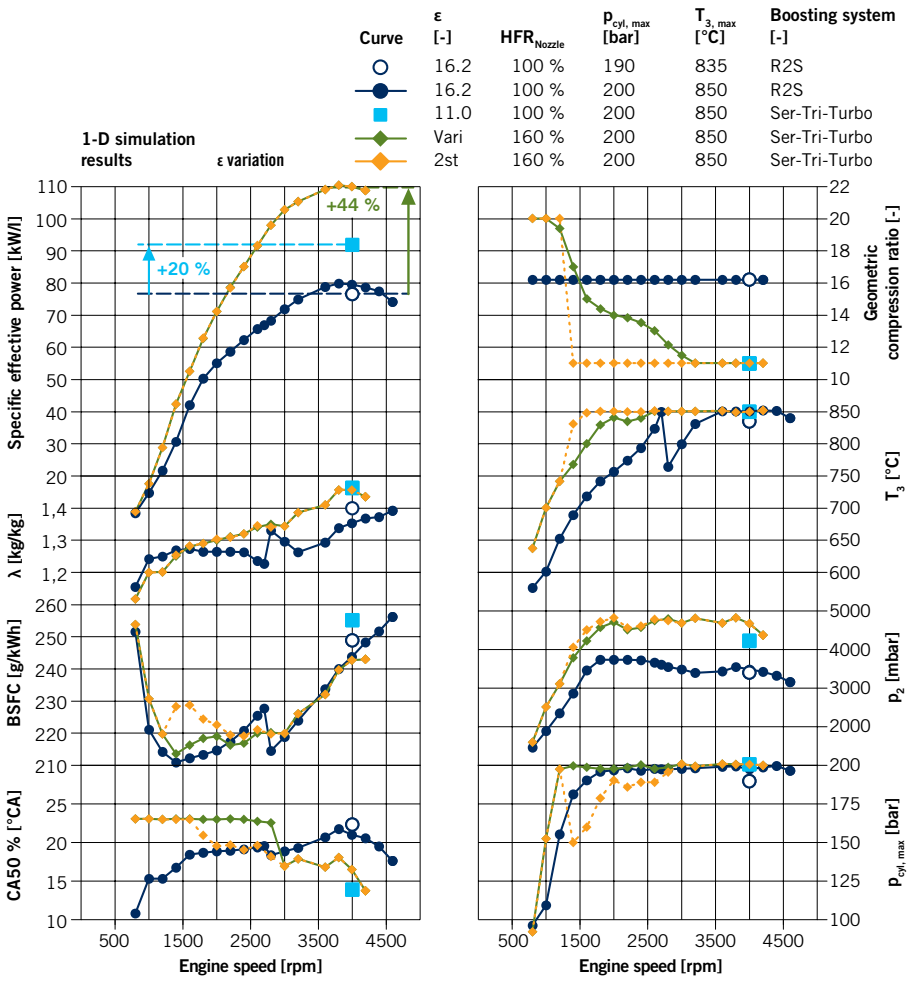

FIGURE 5 Power potential by varying the compression ratio at full load (1-D simulation)

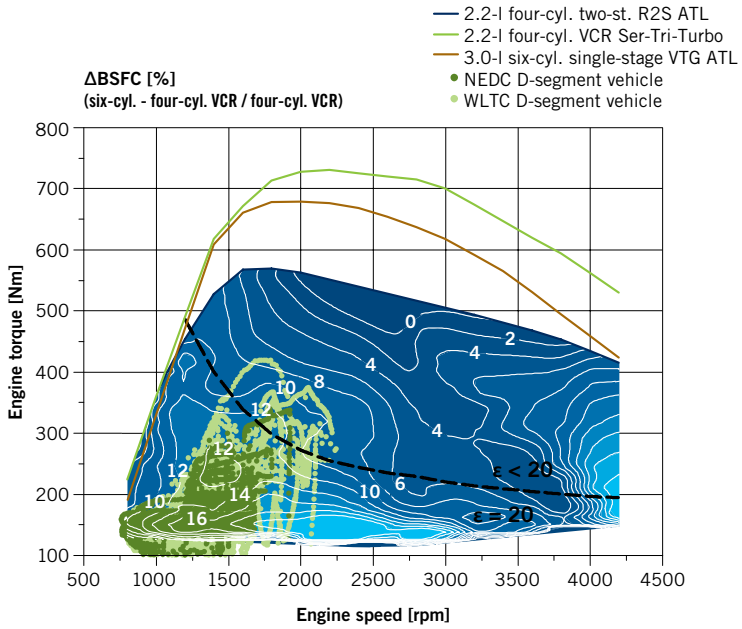

FIGURE 6 Consumption advantage of the four-cylinder VCR diesel engine compared to a six-cylinder diesel engine

that an effective fuel consumption advantage of approximately 4 % out of this indicated fuel consumption advantage will be feasible in reality. About 1 % of the theoretical improvement will be lost on account of recalibration measures and an increase in friction losses at the VCR engine.

- Reducing the compression ratio from ε = 16.2 to 11.0 with the reference injection nozzle results in gains of 19 % in indicated mean pressure to IMEP = 33.3 bar.
- An innovative turbocharging system with three exhaust turbochargers in a multi-stage arrangement (Ser-Tri-Turbo) with a maximum pressure ratio of 4.8, an engine with a maximum admissible cylinder peak pressure of 200 bar and a slightly increased exhaust gas temperature limit (T_3 = 850 °C) with an enlarged injection nozzle (+60 % flow) and higher injection pressure (p_{Rail} = 2500 bar) is capable of achieving an increase in power of 44 % to P_s = 110 kW/l with ε = 11.0, compared to the base engine (1-D simulation).
- The comparison with a current six-cylinder diesel engine shows the consumption benefit achieved with a combination of downsizing and increasing ε at part load. An effective consumption advantage of about 12 % can be expected in the cycle-relevant map area.

The presented studies show that VCR can be used to resolve the trade-off between high power density and thermodynamic efficiency in the part load range. However, the degree of downsizing in particular is not defined by VCR alone. The increased air demand needs a more efficient turbocharging concept with an increase in the nozzle flow rate.

REFERENCES

[1] Brauer, M.; Pohlke, R.; Beier, H.; Severin, C.; Oetjens, H.; Schramm, C.; Diezemann, M.; Hielscher, K.: Variable Verdichtung am Dieselmotor – Anwendungspotenziale und Herausforderungen. 7th Emission Control Symposium, Dresden, 2014

[2] Heuser, B.; Holderbaum, B.; Rohs, H.; Körfer, T.: Potential of a variable compression ratio for modern Diesel applications to balance future demands. FEV Diesel Powertrain 3.0 Symposium, Montabaur, 2014

[3] Weissbaeck, M.; Dreisbach, R.; Beichtbuchner, A.; Buergler, L.: Future HSDI Diesel – Dynamic, Clean and Efficient. 26th International Conference "Motor und Umwelt", Graz, 2014

THANKS

The conceptual studies using 1-D simulation and the tests at the single-cylinder test bench were conducted by René Pohlke and Christopher Hellwig, both IAV, to whom the authors extend their special thanks for their valuable contribution to this publication.

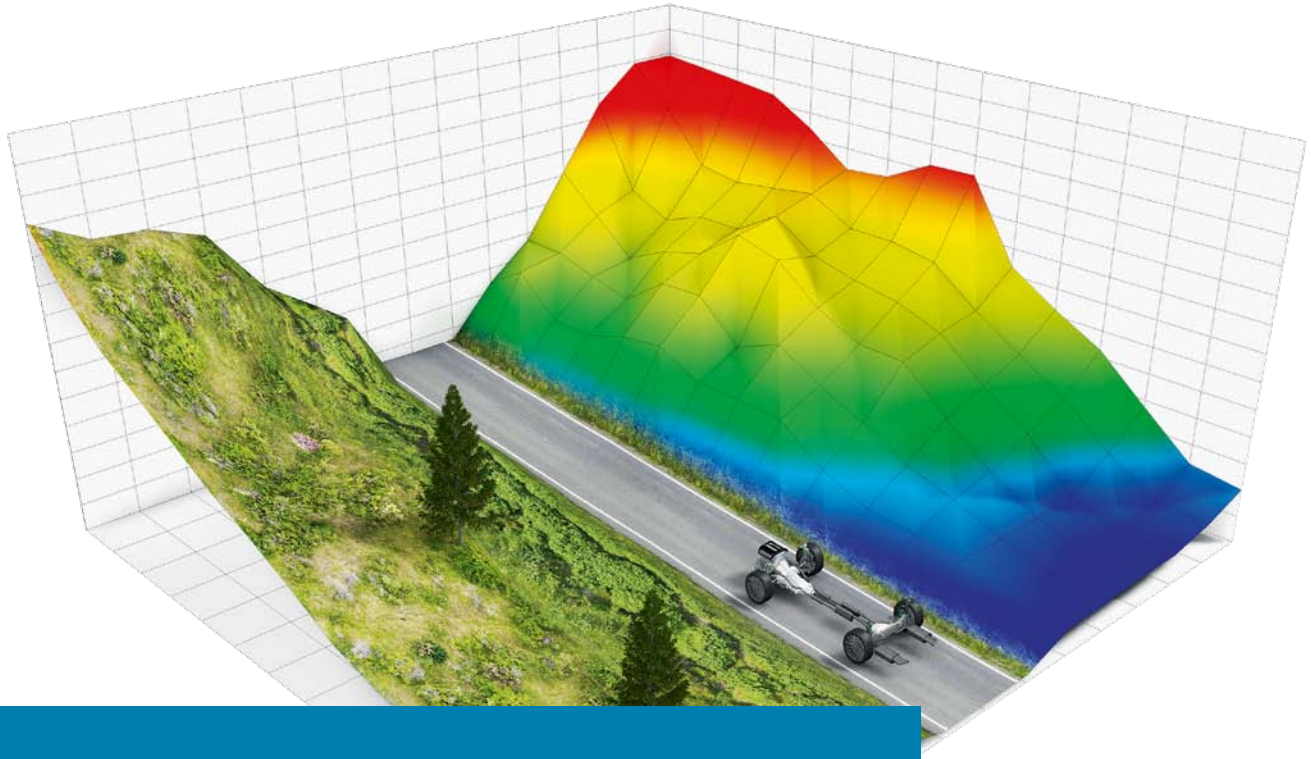

Methods for the Development of a RDE-capable Powertrain

On the background of the continuously changing statutory regulations, increasing customer requirements for efficiency and dynamic, as well as competition for market shares, the complexity in automotive engineering, with at the same time shorter development cycles, has dramatically increased. Near future emission regulations like the limitation of particle number for direct injection gasoline engines or the RDE legislation are going to increase the necessary effort for development, validation and compliance considerably over the current level, as the APL Group shows.

INTRODUCTION

The desire for individual mobility is a substantial driver for the development in the automotive industry. Besides the energy efficiency the reduction of all the limited emissions is in focus and should lead to a "zero-impact-emission vehicle" [1]. This goal can only be reached through the combination of a variety of different measures, **FIGURE 1** (right). Among other the optimisation of the spray targets and the injection rate profile in combination with variable air inlet control, improved means of charging as well as alternative

AUTHORS

Prof. Dr.-Ing. Jens Hadler
is Managing Director of the APL GmbH in Landau (Germany).

Dipl.-Ing. Christian Lensch-Franzen
is Head of Engineering at the APL GmbH in Landau (Germany).

Dr.-Ing. Marcus Gohl
is Team Leader Mechanical Development in the Engineering Sector of the APL GmbH in Landau (Germany).

Dr.-Ing. Carsten Guhr
is Project Engineer in the Engineering Sector of the APL GmbH in Landau (Germany).

ignition methods present considerable potential. An important factor in the process optimisation is the implementation of alternative fuels. The reduction of friction loss, not only in the base engine, but also in the whole powertrain will contribute significantly to the lowering of the fuel consumption and thereby in most cases also of the regulated emissions.
The assessment of emissions is done in test cycles. In the future this procedure is going to be replaced with assessment under real driving conditions [2].

The comparison of the different driving profiles in regards to the map utilisation and the actual power and torque gradients, **FIGURE 1** (left), displays important differences. The extension of the load field and the occurrence of higher gradients from NEDC (blue), WLTC (red) and an example of a real driving cycle (green) have a significant influence on the emission behaviour. In addition the system robustness and the emission compliance over lifetime must be warranted. The aspects described, yield far-reaching requirements for the development of a RDE capable powertrain, which will be closely examined in the following.

LOAD SHIFT AND INCREASED DYNAMIC

When plotting the frequency of each of the load bands used by the powertrain in the driving cycles NEDC and WLTC as well as for a real driving cycle against the distribution of for example the HC and particle exhaust emissions from a direct injection (DI) gasoline engine, it shows a strongly non-linear behaviour, **FIGURE 2**. Despite the relative low frequency of the dynamic in the high load areas under real driving conditions these contribute considerably to the emission behaviour. For this example the limit value for particle number is even with inclusion of the not yet clearly defined „not-to-exceed"-limit probably exceeded.

SYSTEM ROBUSTNESS AND LIFETIME

A challenge not to be ignored is the minimisation of the spread of the emission values due to the applied hardware and similar, i.e. the system robustness. For this the validation of the total system must be done in regards to lifetime. This doesn't limit itself to the consideration of mechanical components of the powertrain, but also of fuel and lubricants as well as the consideration of aging, deposit

FIGURE 1 Requirements and measures

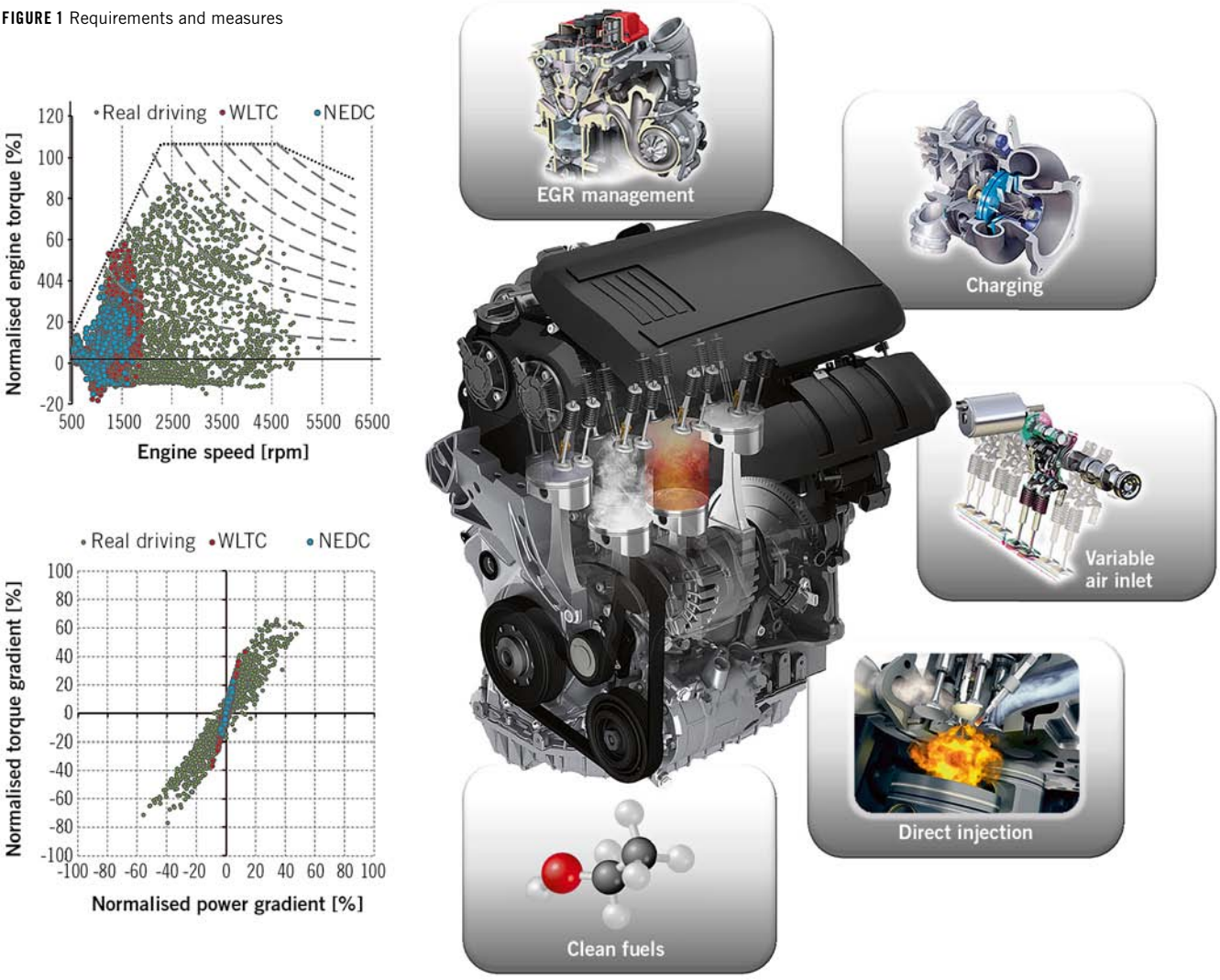

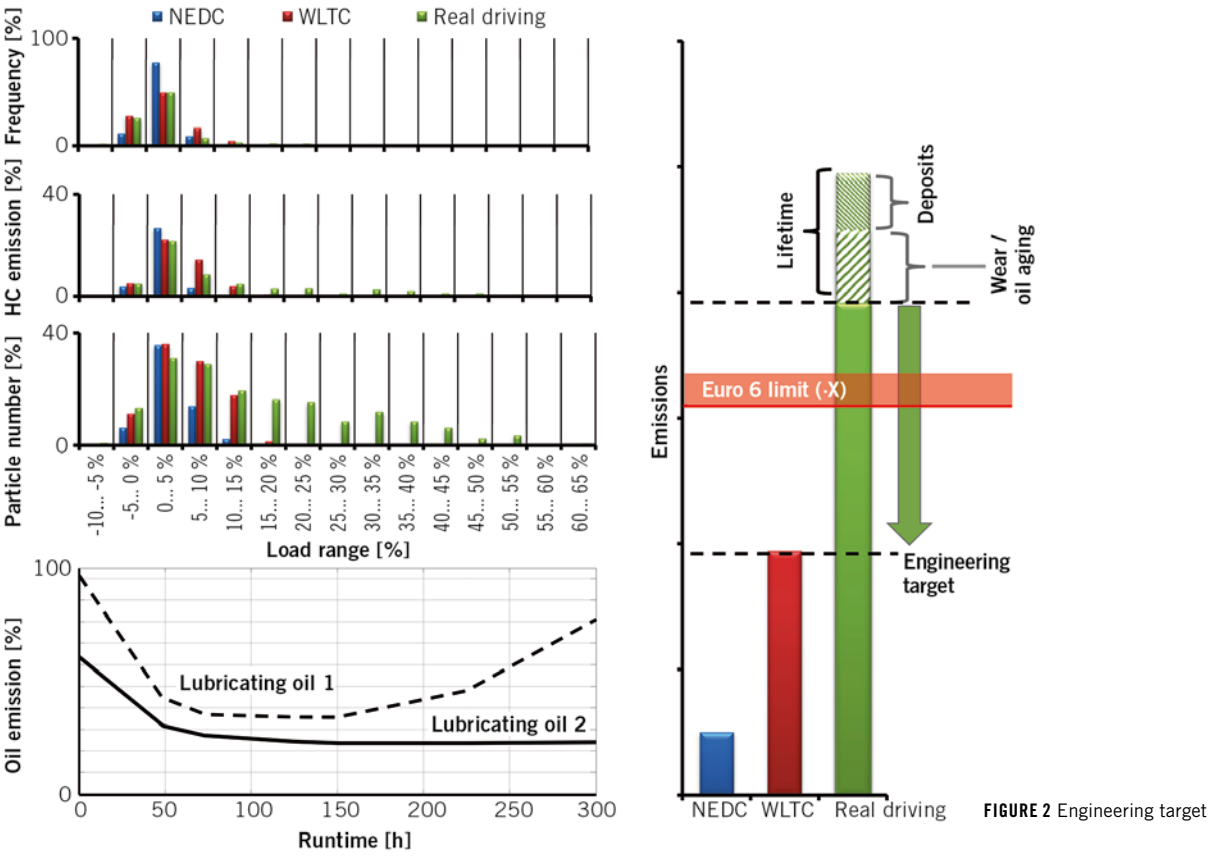

FIGURE 2 Engineering target

and drift effects in the function structure and the calibration.

Already in the early phases of the development process the wear behaviour of different variants is investigated. Besides, for instance the evaluation of contact pressure distribution with elastohydrodynamic (EHD) simulation, the extreme high resolution radionuclide-technique (RNT) measurement technique for wear analysis and the mass spectrome-

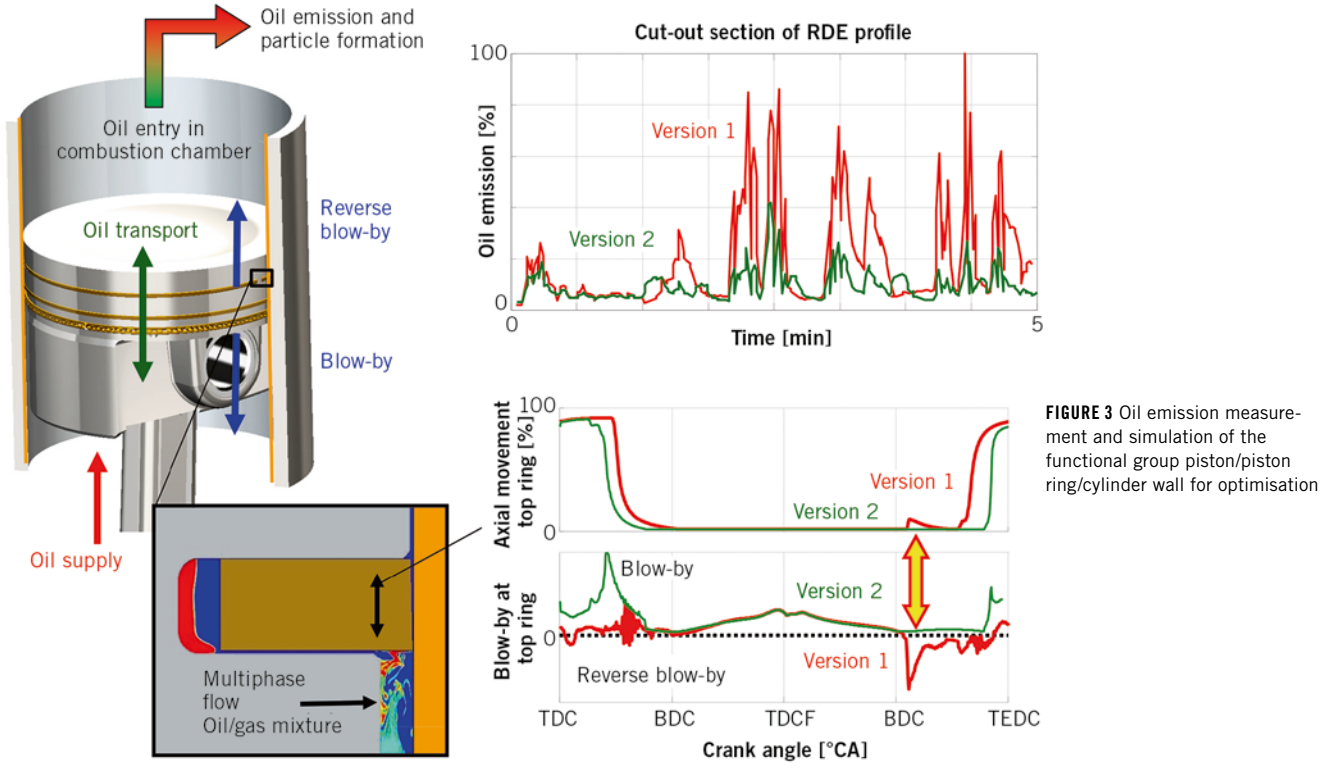

FIGURE 3 Oil emission measurement and simulation of the functional group piston/piston ring/cylinder wall for optimisation

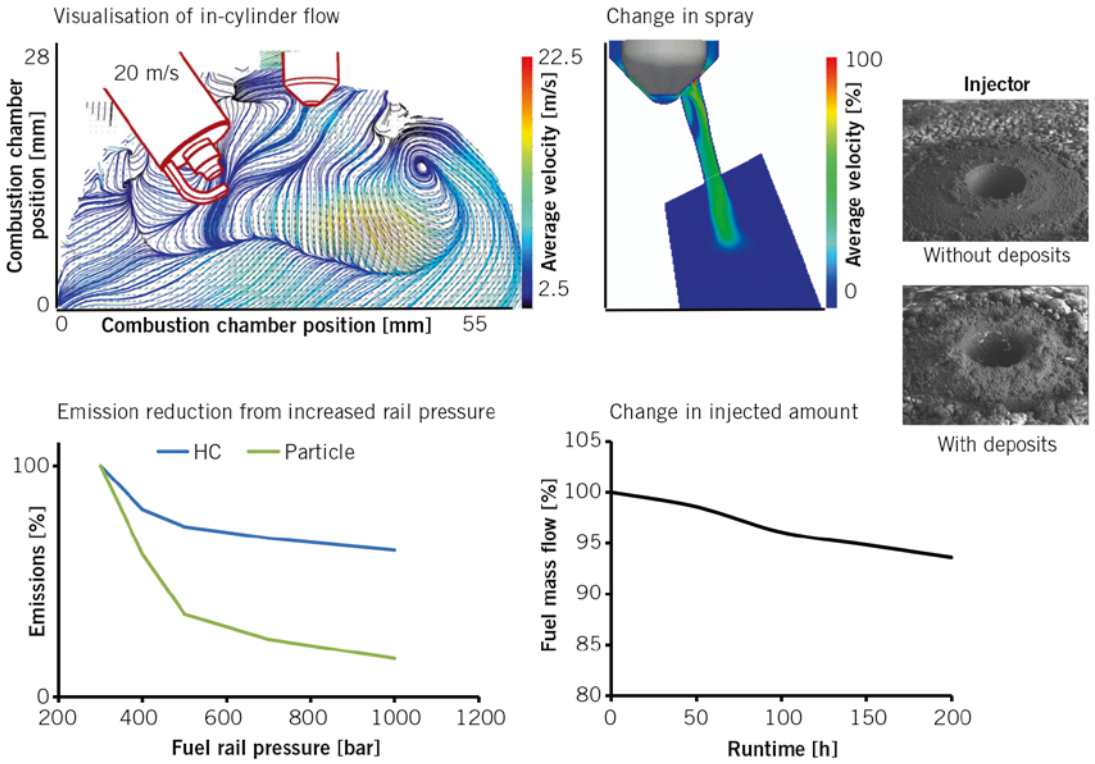

FIGURE 4 Fuel injection and mixture formation

try are applied on test beds. In this combination and under consideration of the influencing parameters mentioned, an optimal layout with reduced friction loss and moderate oil emission, by maximal lifetime, can be made.
A further aspect that has a strong influence on the lifetime of the total system is different aging effects of the engine oil. They have a significant influence on parameters like friction power and wear as well as deposit phenomena and oil related malfunctions. Depending on the lubricating oil condition and composition, the wear and emission behaviour can be significantly influenced over lifetime for the same hardware design, **FIGURE 2** [3].

Relevant for lifetime and emissions are also deposits, for instance in the injector. Besides a change in the relation between activation duration and injected amount of fuel, also the spray is negatively affected.

APPLICATION OF THE APL DEVELOPMENT CONCEPT

For detailed consideration of dynamic, load shift and reproducibility by simultaneous separation of the influencing parameters, the system behaviour can be deducted from representative load requirements under knowledge of the statistical probability of the occurrence of the speed-load-combinations. The result is individual synthetic speed-load profiles which are representative for the driving behaviour in NEDC, WLTC and RDE. With the help of these synthetic, but to the real driving conditions aligned, cycles solution proposals can be tested for their effectiveness and evaluated against each other. With targeted optimisation through a combination of different measures in the areas lubricant oil formulation, tribological systems, combustion process and calibration a significant reduction of the emissions can be achieved.

The engineering target for the actual case is mainly to reduce the particle number and the HC emissions at load shift and increased dynamic by concurrently warranting the system robustness and the validation for lifetime under consideration of lubricant aging and wear as well as emissions relevant deposits, **FIGURE 2**.

OIL CAUSED EMISSIONS

A detailed comprehension of the tribological processes and the different mechanisms is a prerequisite for the application of selective measures for optimisation. The application of online measurement techniques in connection with test bed investigations allows for an early evaluation of hardware layout as well as the validation of critical component design and tolerances. Integration of simulation tools on EHD and CFD basis lead to methodical advantages and allows for the reduction of time and cost intensive engine tests [4].

The oil emissions from the piston group could increase through a non-optimal piston ring or gas dynamic [5]. Investigations in a RDE-representative drive cycle, **FIGURE 3**, show in particularly that the transient phases result in increased oil emissions, which could be optimised for the second version through mechanical changes and changes to the calibration. The reverse blow-by and the oil transfer to the combustion chamber can be significantly reduced by affecting the piston ring and

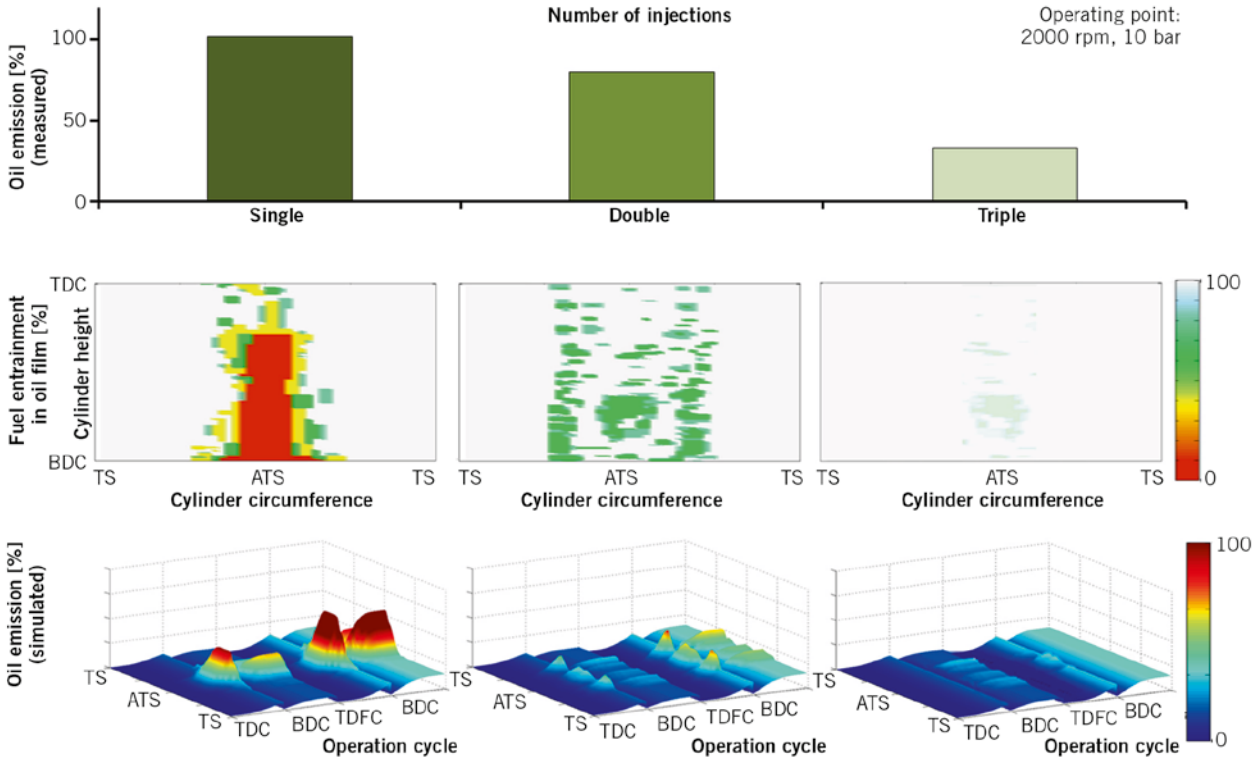

FIGURE 5 Fuel entrainment in the oil wall film

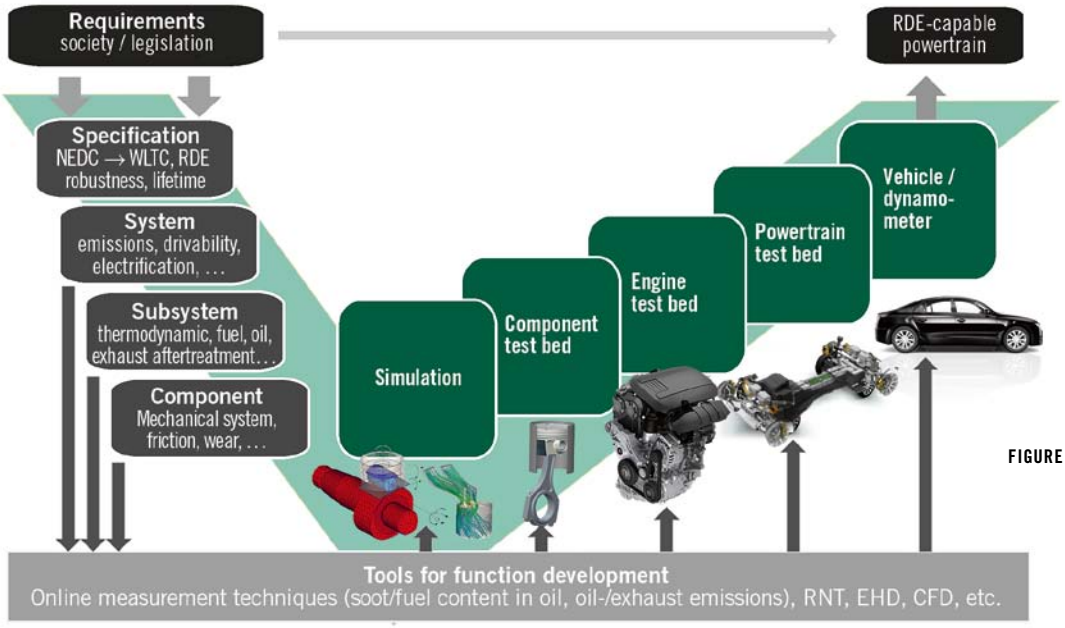

FIGURE 6 APL development method

gas dynamic as well as by an improved sealing within the piston group.

FUEL AND MIXTURE FORMATION CAUSED EMISSIONS

Another influence on the HC and particle emissions comes from the calibration of the fuel injection [6]. With an increase in rail pressure and a corresponding adjustment of the calibration a significant reduction in HC and particle emissions can be achieved for a turbocharged DI gasoline engine, **FIGURE 4**. A targeted adjustment of the interaction between the spray and the in-cylinder flow is here essential. For the optimisation of injector position and spray targeting optical measurement methods (high-speed particle image velocimetry, PIV) in combination with CFD simulation (large eddy simulation, LES) serve along others as development tool for detailed investigation of the individual phenomena occurring [7]. The determination of parameters is derived for a stable mixture formation. This is particularly

important in relation to improving the system robustness. However, by the optimisation of the mixture formation interactions with other mechanisms should not be neglected, which means a continuous monitoring has to take place. An important factor is the deposit behaviour on the injector body and in particular in the spray orifice. The layout of geometry and surfaces as well as the evaluation of the influence of developing deposits and their dependency of the operating fluids used is done in a comprehensive optimisation process with chemical analysis, CFD simulation and, on the engine, optical analysis of the spray formation.

INTERACTION BETWEEN OIL AND FUEL CAUSED EMISSIONS

Through the injection strategy, the local air/fuel ratio and the charge motion the mixture formation can have a significant influence on the lubricant oil emission. **FIGURE 5** shows the influence of the injection strategy on the interaction of the fuel with the oil film. By multiple injections the CFD simulation shows a significant reduction of the local fuel entrainment in the oil film around the injector target. The resulting reduced oil emission could in this connection be validated with measurements as well as with simulation of the evaporation.

Besides the fuel entrainment in the oil wall film directly by the injection, there is also a permanent addition of fuel to the oil that doesn't completely evaporate. The resulting changed lubricant formulations and mixed viscosities have an effect on the evaporation behaviour as well as on the oil wall film heights and the oil transport behaviour around the piston rings. Next to these influences the fuel entrainment also leads to an aging of the engine oil and affects hereby the lifetime robustness negatively.

RESULT OF THE OPTIMISATION

The optimisation in the actual case incorporated an oil composition whereto the tribological system of the functional group of piston/piston rings/cylinder wall was matched and thereby lowering the HC and particle emissions caused by oil. In addition an increase in the rail pressure with the corresponding adjustment of the calibration was made. By applying these measures as a whole, the as engineering target defined lowering of HC and particle emissions, **FIGURE 2**, can be achieved. A suitable margin to the Euro 6 limit value, to warrant the lifetime robustness, is achieved.

CONCLUSION

The legislator has decided for all vehicle types in the future to evaluate the emission behaviour under real driving conditions. To this comes the requirement to warrant the compliance of the RDE over a defined lifetime. This means new challenges for the development process of the powertrain. Besides the focus on load shift and increased dynamic the implemented optimisation measures also have to be validated for system and lifetime robustness.

The APL Group has, based on a comprehensive portfolio of development methods and tools developed a complex chain of methods to specify and develop the mechanical properties and emission behaviour of powertrain systems in regards to RDE, **FIGURE 6**. The basis for the development method is the reproducible reproduction of real driving conditions on powertrain and engine test beds, the analysis of these to the level of representative operative parameter gradients and the derivation of functional relations. The development depth stretches from the complete system over individual components to the point of the physical phenomenon [8].

Using the example of a turbocharged DI gasoline engine the chain of methods involves analysis by synthetic cycles, an extensive simulation framework and the implementation of the measures presented. In the shown example the focus is on reducing the HC and particle emissions caused by oil and fuel.

A detailed understanding of the tribological processes and the different mechanisms is the prerequisite for targeted measures for the improvement of the emission behaviour and the system robustness. The application of online measurement methods combined with chemical and metallographic laboratory analysis allow for an early evaluation and validation of critical component design. The combination with CFD and EHD simulation tools leads to further methodological advantages and allows for the reduction of time and cost intensive engine tests.

In regards to reducing the emissions caused by the fuel, an increase in rail pressure for a direct injection gasoline engine with the corresponding adjustment of the calibration prove to be an effective measure. For assessment and optimisation of the system robustness a detailed knowledge of the mixture formation and the charge motion is essential. Detailed insight in the proceeding phenomena comes from optical measurement methods in combination with CFD tools. The validation for lifetime requires a deep understanding of the proceeding wear mechanisms, as well as the detection and evaluation of the build-up of deposits and other lifetime phenomena, as this is in the end crucial for the definition of the engineering targets. It was shown that with the implemented optimisation measures in total the RDE capability of the DI gasoline engine powertrain, here used as an example, was achieved. With the method developed and the results achieved the APL Group contributes to the vision of the „Zero-Impact-Emission Vehicle".

REFERENCES

[1] Hadler, J.; Lensch-Franzen, C.; Kirsten, K.; Faubel, L.; Kehrwald, B.; Spicher, U.: Die objektive Notwendigkeit eines Zero Impact Emission Powertrains. 35th International Vienna Motor Symposium, 2014

[2] Weiss, M.; Bonnel, P.; Hummel, R.; Steininger, N.: A complementary emissions test for light-duty vehicles: Assessing the technical feasibility of candidate procedures. Joint Research Centre (JRE) Scientific and Policy Reports, EUR 25572 EN, 2013

[3] Müller, G.; Stern, D.; Berlet, P.; Pöhlmann, K.: Praxisnahe Alterung von Motorenölen und Auswirkung auf tribologisch relevante Eigenschaften. 54. Tribologische Fachtagung der Gesellschaft für Tribologie, Göttingen, 2013

[4] Hadler, J.; Gohl, M.; Knoll, G.; Backhaus, K.: Entwicklungswerkzeuge für die reibungsoptimierte Auslegung des Grundtriebwerks. In: MTZ 75 (2014), No. 3, pp. 56-61

[5] Hadler, J.; Lensch-Franzen, C.; Gohl, M.; Mink, T.: Ganzheitliches Konzept zur Optimierung der Ölemission. In: MTZ 75 (2014), No. 2, pp. 44-49

[6] Buri, S.; Dahnz, C.; Kubach, H.; Spicher, U.: Reduzierung von Rußemissionen durch Steigerung des Einspritzdruckes bis 1000 bar in einem Ottomotor mit strahlgeführtem Brennverfahren. 9. Internationales Symposium für Verbrennungsdiagnostik, Baden-Baden, 2010

[7] Disch, C.; Kubach, H.; Spicher, U.; Pfeil, J.; Altenschmidt, F.; Schaupp, U.: Investigations of Spray-Induced Vortex Structures during Multiple Injections of a DISI Engine in Stratified Operation Using High-Speed-PIV. SAE Technical Paper 2013-01-0563, 2013

[8] Hadler, J.; Lensch-Franzen, C.; Kehrwald, B.; Spicher, U.; Kirsten, K.; Gohl, M.; Guhr, C.: Methoden für die Entwicklung eines RDE-fähigen Antriebs. 36th International Vienna Motor Symposium, 2015

IMPRINT

MTZ

WORLDWIDE

www.MTZonline.com

Founded 1939 by Prof. Dr.-Ing. E. h. Heinrich Buschmann and
Dr.-Ing. E. h. Prosper L'Orange

Organ of the Fachverband Motoren und Systeme im VDMA, Verband Deutscher Maschinen- und Anlagenbau e.V., Frankfurt/Main, for the areas combustion engines and gas turbines
Organ of the Forschungsvereinigung Verbrennungskraftmaschinen e.V. (FVV)
Organ of the Wissenschaftliche Gesellschaft für Kraftfahrzeug- und Motorentechnik e.V. (WKM)
Organ of the Österreichischer Verein für Kraftfahrzeugtechnik (ÖVK)
Cooperation with the STG, Schiffbautechnische Gesellschaft e.V., Hamburg, in the area of ship drives by combustion engine

07-08I2015 _ Volume 76
Springer Vieweg I Springer Fachmedien Wiesbaden GmbH
P. O. Box 15 46 · 65173 Wiesbaden · Germany I Abraham-Lincoln-Straße 46 · 65189 Wiesbaden · Germany

Amtsgericht Wiesbaden, HRB 9754, USt-IdNr. DE811148419
Managing Directors Armin Gross, Joachim Krieger, Dr. Niels Peter Thomas

Managing Director Marketing & Sales Armin Gross I **Director Magazines** Stefanie Burgmaier I **Director Production** Dr. Olga Chiarcos

EDITORS IN CHARGE
Dr. Johannes Liebl, Wolfgang Siebenpfeiffer

EDITOR IN CHIEF
Dr. Alexander Heintzel
phone +49 611 7878-342 · fax +49 611 7878-462
alexander.heintzel@springer.com

VICE EDITOR IN CHIEF
Dipl.-Ing. (FH) Richard Backhaus
phone +49 611 5045-982 · fax +49 611 5045-983
richard.backhaus@rb-communications.de

MANAGING EDITOR
Kirsten Beckmann M. A.
phone +49 611 7878-343 · fax +49 611 7878-462
kirsten.beckmann@springer.com

EDITORIAL STAFF
Dipl.-Ing. (FH) Andreas Fuchs
phone +49 6146 837-056 · fax +49 6146 837-058
fuchs@fachjournalist-fuchs.de
Angelina Hofacker
phone +49 611 7878-121 · fax +49 611 7878-462
angelina.hofacker@springer.com
Dipl.-Ing. Michael Reichenbach
phone +49 611 7878-341 · fax +49 611 7878-462
michael.reichenbach@springer.com
Stefan Schlott
phone +49 8726 9675-972
redaktion_schlott@gmx.net
Markus Schöttle
phone +49 611 7878-257 · fax +49 611 7878-462
markus.schoettle@springer.com
Martina Schraad
phone +49 611 7878-276 · fax +49 611 7878-462
martina.schraad@springer.com

PERMANENT CONTRIBUTORS
Andreas Burkert, Prof. Dr.-Ing. Stefan Breuer, Hartmut Hammer, Detlef Krehl, Dipl.-Ing. Ulrich Knorra, Roland Schedel

ENGLISH LANGUAGE CONSULTANT
Paul Willin

ONLINE I ELECTRONIC MEDIA
Portal Manager Automotive
Christiane Brünglinghaus
phone +49 611 7878-136 · fax +49 611 7878-462
christiane.bruenglinghaus@springer.com
Editorial Staff
Katrin Pudenz M. A.
phone +49 6172 301-288 · fax +49 6172 301-299
redaktion@kpz-publishing.com

SPECIAL PROJECTS
Managing Editorial Journalist
Markus Bereszewski
phone +49 611 7878-122 · fax +49 611 7878-462
markus.bereszewski@springer.com
Editorial Staff I Coordination
Dipl.-Reg.-Wiss. Caroline Behle
phone +49 611 7878-393 · fax +49 611 7878-462
caroline.behle@springer.com
Christiane Imhof M. A.
phone +49 611 7878-154 · fax +49 611 7878-462
christiane.imhof@springer.com

PROJECT MANAGEMENT I ASSISTANCE
Yeliz Konar
phone +49 611 7878-180 · fax +49 611 7878-462
yeliz.konar@springer.com

ADDRESS
Abraham-Lincoln-Straße 46 · 65189 Wiesbaden
P. O. Box 1546 · 65173 Wiesbaden, Germany
redaktion@ATZonline.de

ADVERTISING

SALES MANAGEMENT
Volker Hesedenz
phone +49 611 7878-269 · fax +49 611 7878-78269
volker.hesedenz@best-ad-media.de

MEDIA SALES
Frank Nagel
phone +49 611 7878-395 · fax +49 611 7878-78395
frank.nagel@best-ad-media.de

KEY ACCOUNT MANAGEMENT
Rouwen Bastian
phone +49 611 7878-399 · fax +49 611 7878-78399
rouwen.bastian@best-ad-media.de

DISPLAY AD MANAGER
Nicole Brzank
tel +49 611 7878-616 · fax +49 611 7878-78164
nicole.brzank@best-ad-media.de

AD PRICES
Advertising ratecard from October 2014.

MARKETING I OFFPRINTS

HEAD OF MARKETING MAGAZINES + EVENTS
Jens Fischer

PRODUCT MANAGEMENT AUTOMOTIVE MEDIA
Jens Fischer
phone +49 611 7878-340 · fax +49 611 7878-407
jens.fischer@springer.com

OFFPRINTS
Martin Leopold
phone +49 2642 907-596 · fax +49 2642 907-597
leopold@medien-kontor.de

PRODUCTION I LAYOUT
Heiko Köllner
phone +49 611 7878-177 · fax +49 611 7878-78177
heiko.koellner@springer.com

SUBSCRIPTIONS
Springer Customer Service Center GmbH
Haberstraße 7 · 69126 Heidelberg · Germany
phone +49 6221 3454-303 · fax +49 6221 3454-229
Monday to Friday, 8 a.m. to 6 p.m.
springervieweg-service@springer.com
www.my-specialized-knowledge.com/automotive

SUBSCRIPTION CONDITIONS
The eMagazine appears 11 times a year at an annual subscription rate 199 € for private persons and 333 € for companies. Special rate for students on proof of status in the form of current registration certificate 98 €. Special rate for VDI/ÖVK members on proof of status in the form of current member certificate 172 €. Special rate for studying VDI members on proof of status in the form of current registration and member certificate 71 €. Annual subscription rate for combination MTZworldwide (eMagazine) and MTZ (print) 399 €. All prices include VAT at 7%. Every subscription comes with access to the online archive. However, access is only available for the individual subscription holder. To obtain access for your entire company/library/organisation, please contact sales@springerprofessionals.de or phone +49 611 7878-686. The subscription can be cancelled in written form at any time with effect from the next available issue.

HINTS FOR AUTHORS
All manuscripts should be sent directly to the editors. By submitting photographs and drawings the sender releases the publishers from claims by third parties. Only works not yet published in Germany or abroad can generally be accepted for publication. The manuscripts must not be offered for publication to other journals simultaneously. In accepting the manuscript the publisher acquires the right to produce royalty-free offprints. The journal and all articles and figures are protected by copyright. Any utilisation beyond the strict limits of the copyright law without permission of the publisher is illegal. This applies particularly to duplications, translations, microfilming and storage and processing in electronic systems.

Springer Vieweg is part of Springer Science+Business Media.

Springer Vieweg

PEER REVIEW

Peer Review Process for Research Articles in ATZ, MTZ and ATZelektronik

Scientific articles of universities in ATZ Automobiltechnische Zeitschrift, MTZ Motortechnische Zeitschrift and ATZelektronik are subject to a proofing method, the so-called peer review process. Articles accepted by the editors are reviewed by experts from research and industry before publication. For the reader, the peer review process further enhances the quality of the magazines' content on a national and international level. For authors in the institutes, it provides a scientifically recognised publication platform.

In the Peer Review Process, once the editors has received an article, it is reviewed by two experts from the Advisory Board. If these experts do not reach a unanimous agreement, a member of the Steering Committee acts as an arbitrator. Following the experts' recommended corrections and subsequent editing by the author, the article is accepted.

In 2008, the peer review process utilised by ATZ and MTZ was presented by the WKM (Wissenschaftliche Gesellschaft für Kraftfahrzeug- und Motorentechnik e. V./German Professional Association for Automotive and Motor Engineering) to the DFG (Deutsche Forschungsgemeinschaft/German Research Foundation) for official recognition. ATZelektronik participates in the Peer Review since 2011.

3-D CFD Simulation of the Lubrication Film in a Journal Bearing

Current journal bearing calculation programmes are based on a two-dimensional calculation approach which makes them fast and efficient in terms of the design process of journal bearings. But there are great uncertainties regarding the results in the proximity of lubrication grooves, pockets, and oil supply bores. Modern CFD methods can help reducing these uncertainties or even dispel them. In a FVV research project under the direction of the BTU Cottbus it was investigated together with the HAWK University of Applied Science and Arts and the University of Kassel how modern CFD methods can be used to significantly expand the validity of current journal bearing calculation programmes.

AUTHORS

Prof. Dr.-Ing. Christoph Egbers is Head of the Chair Aerodynamics and Flow Mechanics of the Brandenburg University of Technology Cottbus-Senftenberg (Germany).

Dipl.-Ing. Paul Gorenz is Ph. D. Student at the Chair of Aerodynamics and Flow Mechanics of the Brandenburg University of Technology Cottbus-Senftenberg (Germany).

Dipl.-Ing. (FH) Marcus Schmidt, M. Sc. is Research Associate at the Faculty of Natural Sciences and Technology at the HAWK University of Applied Sciences and Arts Hildesheim/Holzminden/Göttingen (Germany).

Dipl.-Ing. Carsten Wolf is Research Associate at the Institute for Powertrain and Automotive Engineering (iaf) at the University of Kassel (Germany).

THE SEAL OF APPROVAL FOR SCIENTIFIC ARTICLES IN MTZ.
MTZ PEER REVIEW
RECEIVED 2014-12-05
REVIEWED 2015-01-12
ACCEPTED 2015-04-07
REVIEWED BY EXPERTS FROM RESEARCH AND INDUSTRY.

1 MOTIVATION

Today the design of journal bearings is done by calculation programmes that are based on the Reynolds differential equation (RPDE). This equation is two-dimensional and was stated by Osbourne Reynolds in 1886 [1]. In general, it is applicable to any flow mechanical problem with thin lubrication films. Mostly, Finite Difference methods (FD) or Finite Elements methods (FE) are used to iteratively solve this partial differential equation. The solution delivers a two-dimensional pressure distribution of the lubrication film. The RPDE is based on the assumption that the film thickness is negligible compared to the other lubrication film dimensions (axial and circumferential direction). Therefore, the film thickness is not a solution variable of the equation, that is to say, the calculated pressure always represents an average value across the gap width. But this assumption loses its validity when the journal bearing shell is not a plain surface which means the bearing contains deep oil supply feedings and/or oil grooves. In these cases the gap width increases discontinuously and is then not negligible compared to the axial and circumferential direction.

These geometrical discontinuities induce three-dimensional flow effects into the journal bearing which can not be resolved or reproduced by the original RPDE. Over the years different Reynolds solvers were developed which expand the area of validity of the original RPDE due to smart modelling techniques. These software tools are well spread, work very efficiently, and represent the current industrial standard.

Within a research project the abilities of modern Computational Fluid Dynamics (CFD) methods were investigated to capture their capabilities of calculating complex, unsteady loaded, hydrodynamic journal bearings. Especially the prediction of cavitation effects were in the focus as well as finding indications for the limits on the scope of the 2-D calculations and deriving guidelines for a safe usage of these fast and efficient 2-D tools. Therefore, different CFD models with variable depth of detail of a journal bearing were developed and an experiment for validation was built up.

2 OVERVIEW OF THE DEVELOPED CFD MODELS

The CFD models of the research project base upon a real journal bearing geometry according to [2]. The experimental results of this bearing are very well documented and reproducible cavitation is generated. An overview of 3-D models is shown in **FIGURE 1**. For the 3-D simulations the programme OpenFoam is used. The three-dimensional equations of motion are treated with the method of the finite volume (FVM). The spatial as well as the temporal discretisation is done using methods from a second order accuracy. The simulation of multiple phases is modelled with the approach of continuum method. The flow of the different phases are calculated separately and connected via a variable phase interface. For the calculation of the phase transition between the liquid and vapour phase, the mass transfer model according to [3] is used. This model is based on a bubble dynamic approach to calculate bubble growth and implosion in a separate equation of motion for the volume fraction. Every 3-D CFD model uses a computational grid with a minimum cell count of 14 cells in the radial direction over the gap. Only in this way the necessary resolution is achieved, which must be expended for a correct simulation of the real, experimentally validated flow structures.

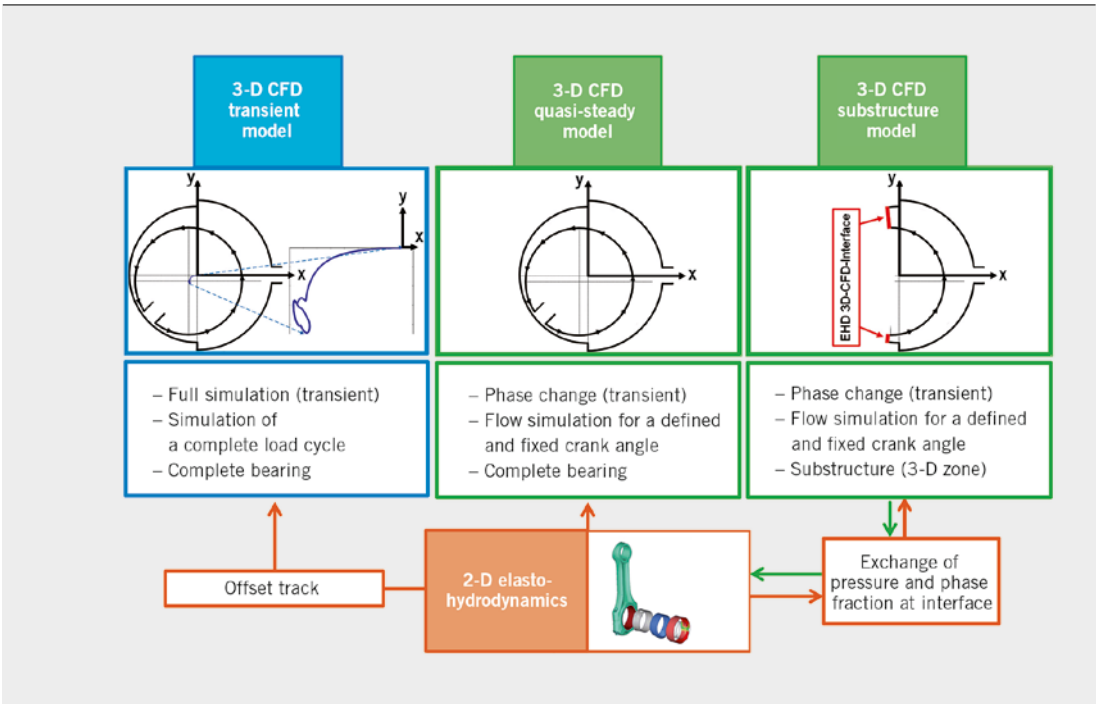

FIGURE 1 Overview of the 3-D CFD models

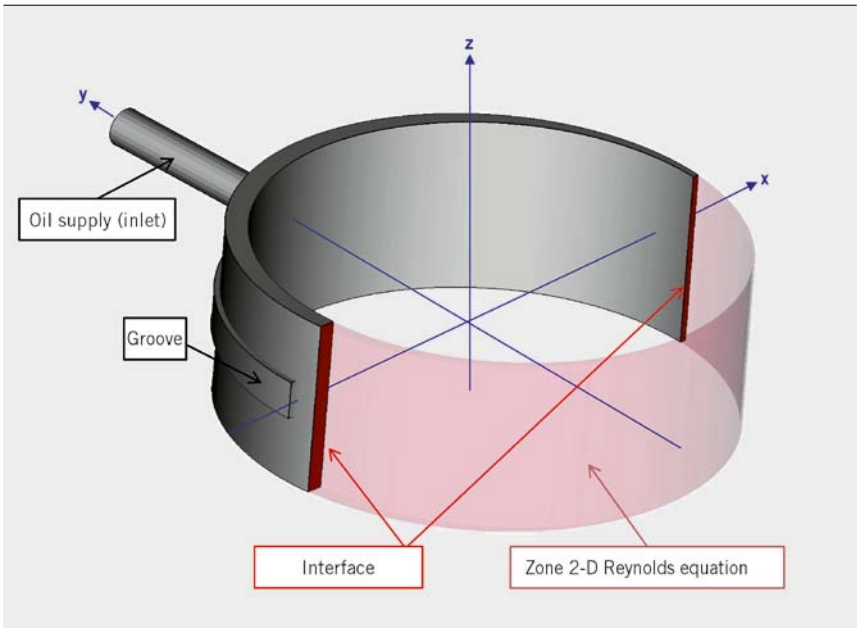

FIGURE 2 Schematic 3-D substructure model

2.1 SUBSTRUCTURE MODEL AND QUASI-STEADY MODEL

Methods have been developed for the investigation of local, three-dimensional flow structures and their influence on cavitation effects regarding to minimal computational effort. Calculation data from efficient 2-D EHD methods are used and coupled with the 3-D simulation. The goal is to study the flow at critical angular positions with a local 3-D simulation, where the 2-D EHD simulation indicates a risk of cavitation.

The quasi-steady model includes the calculation of the flow lubricating film of the complete bearing at a fixed time or crank angle in three dimensions and in the required resolution to resolve the local structures accurately. Boundary conditions as the oil flow, pressure data and the current bearing geometry (eccentricity, orientation of the outlet feedhole in the shaft) are transferred from the 2-D EHD simulation.

In **FIGURE 2** the substructure model is shown. In opposite of the quasi-steady model only the part of the lubricating gap is modelled where three-dimensional flow structures are expected due to the bearing geometry. In general, the flow in the region of the narrowest gap is two-dimensional and can therefore be calculated with 2-D methods. In addition to the quasi-steady model the pressure profile and the gap filling ratios along the interface transferred between 2-D and 3-D zones.

2.2 UNSTEADY CFD MODEL

To be able to analyse three-dimensional effects induced by the dynamics of the journal bearing a very complex CFD model was developed. The rotational movement of an oil outlet bore in the journal was included as well as the offset track of the journal itself and the cavitation model from [3]. The unsteady simulation of three-dimensional effects in the lubrication film requires dynamic meshes. The shaft rotation is realised by splitting the mesh into a resting (outer) and rotating (inner) mesh part. Both are connected via a so called Arbitary Mesh Interface (AMI) which allows an interpolated data exchange. A second dynamic mesh is required to cover the offset track of the journal. This one is implemented into the resting mesh part. By changing the size of the cells it is possible to move the rotating part and, hence, the journal itself along a realistic offset track. But this offset track cannot be calculated by the unsteady model. Thus, it has to be provided from another source. Therefore, an interface was implemented to allow coupling with a RPDE solver.

3 VALIDATION OF THE 3-D CFD MODELS

A thorough validation of numerically calculated data flow can only be made with experimental data that have been measured inside the flow field. Only a simple contemplation of the pressure distribution on the walls is not sufficient to analyse the whole structure of the flow. Therefore, a flow model in scale 3 : 1 was constructed, which maintains the geometric similarity of the real referenced bearing and allows optical access to the flow for laser doppler anemometry (LDA) and flow visualisation. The main components of the flow model experiment were made of in acrylic glass, **FIGURE 3**. By appropriate choice of speed and viscosity of the fluid the experiment can operate in typical Reynolds number ranges in terms of bearings. In order to achieve sufficient spatial resolution in the lubricating film, a relative clearance in the experiment of $\psi = 2.5$ % has been used. The outer cylinder is adjustable for an eccentric position with respect to the inner cylinder. For the depiction of the flow conditions of an engine journal bearing, the fluid introduces the system at the outer cylinder, and can flow out at both axial ends of the inner cylinder, as also through a radial feedhole in the inner cylinder.

The numerical simulation is in perfect agreement with the experimental measurement. **FIGURE 4** shows a comparison of selected experimental and numerical velocity profiles at a measurement position of $\psi = 8.9°$ downstream of the supply inlet. At an angular position of the outlet feedhole of 40°, the normalised velocity U1 is exactly one at the surface of the inner cylinder (y/h = 0). The incoming oil is accelerated near the inner cylinder in rotating direction towards the convergent gap. A typical area of reversed flow is found adjacent to the outer cylinder and inside the groove (y/h = 0.5). The

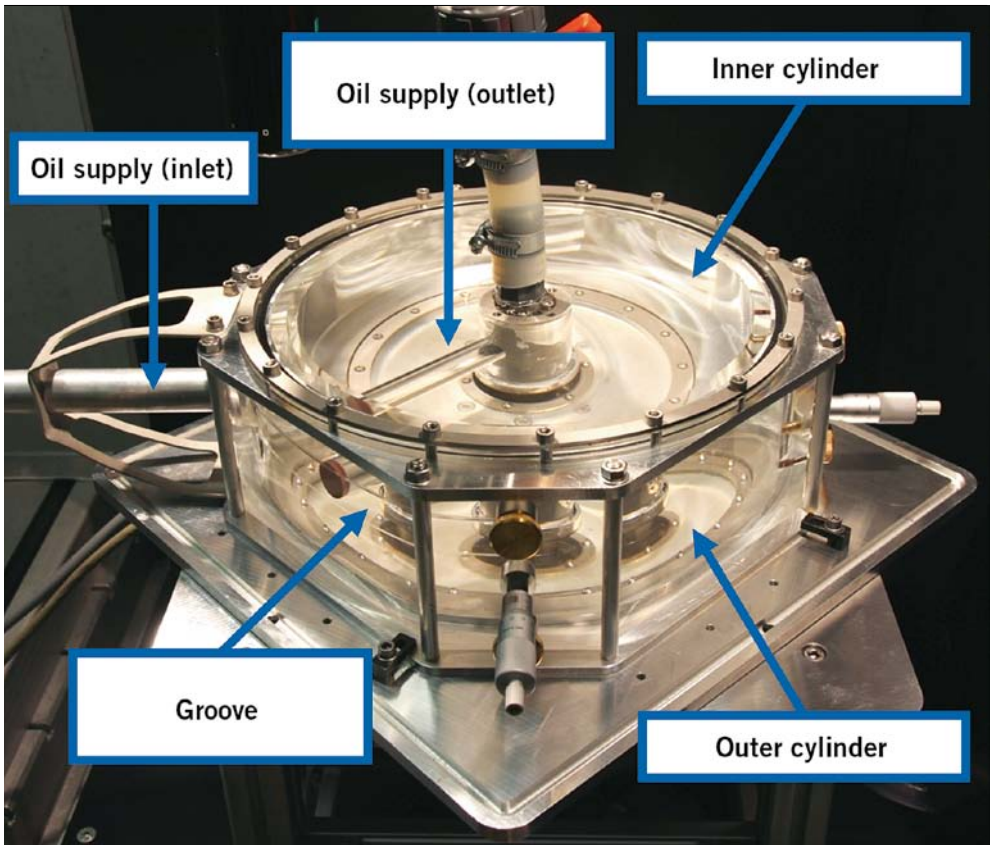

FIGURE 3 Experimental test rig

influence of oil suction is clearly visible, when the outlet feedhole is in the vicinity of the measuring position at 9°. The oil is drawn from both sides of the gap region. Therefore, the velocity in the direction of rotation near the shaft surface reduces and a backflow region over the entire gap is formed.

The two-phase flow and the phase change model were validated with results by [4]. The Jakobsson and Floberg experiment consists of a simple eccentric arrangement of a fixed outer bushing and rotating shaft similar to a bearing system without any supply flow. The gap between both cylinders is filled with lubricant. The pressure distribution was measured experimentally along a circumferential line of 10 % of the bearing width.

FIGURE 5 presents the comparison of the pressure distribution over the circumference from CFD (blue line) to the experimental data. The simulation fits the experimental points regarding to the maximum pressure peak upstream of the minimum gap and the vapour region in the divergent gap. The vapour region is characterised by an isobaric pressure profile at φ = 200 to 300°. In addition, the comparison to the commercial calculation programme [5] shows no significant differences in the calculation of the phase change.

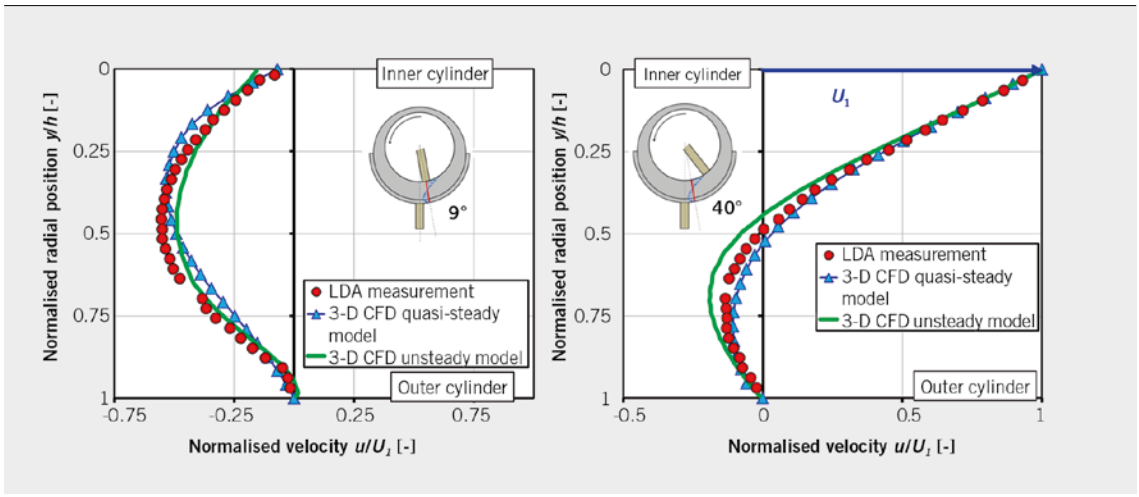

FIGURE 4 Comparison of velocity profiles of a LDV measurement and 3-D CFD simulation

4 SIMULATION OF CAVITATION IN JOURNAL BEARINGS

Current RPDE solvers calculate the gap filling on basis of the algorithm according to [6, 7]. In journal bearings the gap filling ρ and the gap filling change $d\rho/dt$ are suitable as an indicator of cavitation. From the literature it is known that cavitation occurs on component surfaces where the gap is not completely filled with oil and suddenly the filling raises quickly (implosion of cavitation bubble), which means a large positive change in gap filling $d\rho/dt$. 2-D hydrodynamic simulation models have been developed and simulated with the boundary conditions of the PhD thesis of Wollfarth [2].

FIGURE 6 compares the cavitation damage in the journal bearings from experimental investigations and the regions where cavitation damage can be detected in the 2-D simulation. In the experiment the damage by flow cavitation is caused by a backflow into the pin hole when it passes the ending of the groove. As a result of this, bubbles can produce damage in the convergent gap. This is a three dimensional flow that cannot be solved by the Reynolds equation. The damage caused by impact cavitation in the divergent gap and cavitation erosion near the oil supply can be proved with the cavitation indicators. To correlate the 2-D and 3-D simulation techniques a substructure model was built. The area of the oil supply and the upper half of the bearing is simulated with 3-D CFD, while the area of the bearing with the minimum gap is simulated with the Reynolds equation. At the interface nodes the pressure and the gap filling from the Reynolds equation is a boundary condition of the 3-D CFD model. **FIGURE 7** shows the gap filling based on Reynolds equation and the vapour fraction of the 3-D CFD simulation. The results of the Reynolds equation detect an area where a cavitation damage can occur but is not found in the experiments. The 3-D CFD model shows in this area bubbles on the shaft side and not on the journal bearing surface. That is the reason why no damage occurs in the experiments. To proof the possibility of cavitation damage, the vapour fraction in gap height can be investigated by 3-D CFD. These details cannot be analysed by the Reynolds equation. The results suggest that gap filling and gap filling change are useful indicators of cavitation, but they are not suitable as indicators of surface damage.

The prediction of the critical cavitation region upstream of the inlet feedhole by the 2-D simulation and the corresponding experimental damages is confirmed by the 3-D simulation. The upper part of **FIGURE 8** shows the distribution of vapour on the bearing

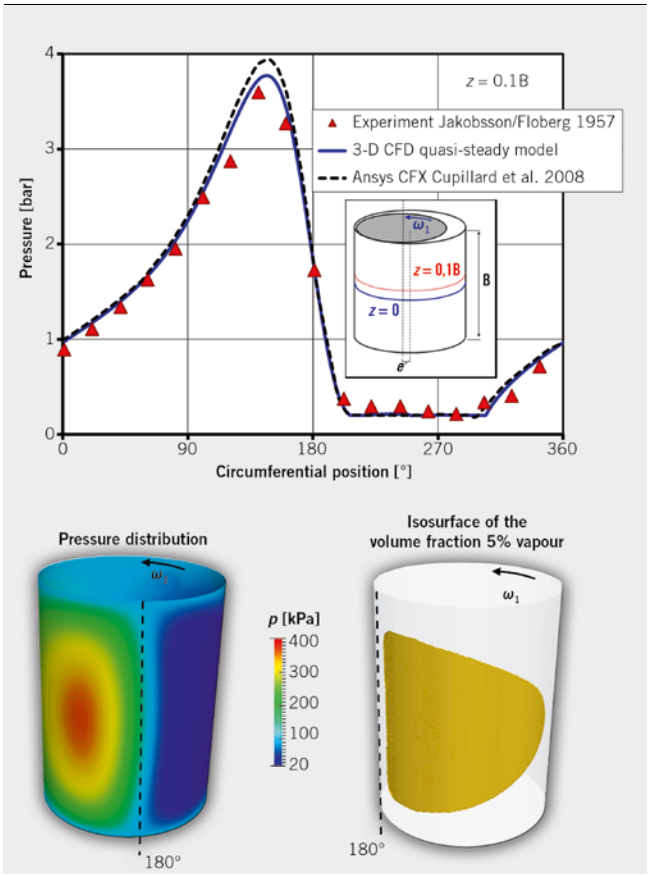

FIGURE 5 Validation of phase change model with experimental data

bushing when the outlet feedhole is approaching the inlet feedhole. The amount of incoming oil flows directly to the outlet. The static pressure in the vicinity of the feedhole reduces by high velocity flow around the feedhole edges and leads to vapour production.

The comparison of the numerical results with the experimental data at the end of the groove is presented in the lower part of **FIGURE 8**. The vapour fraction distribution at the end of the groove from 3-D simulation is similar size and in the same local position to the experimental erosion pattern. The nature of the damage caused

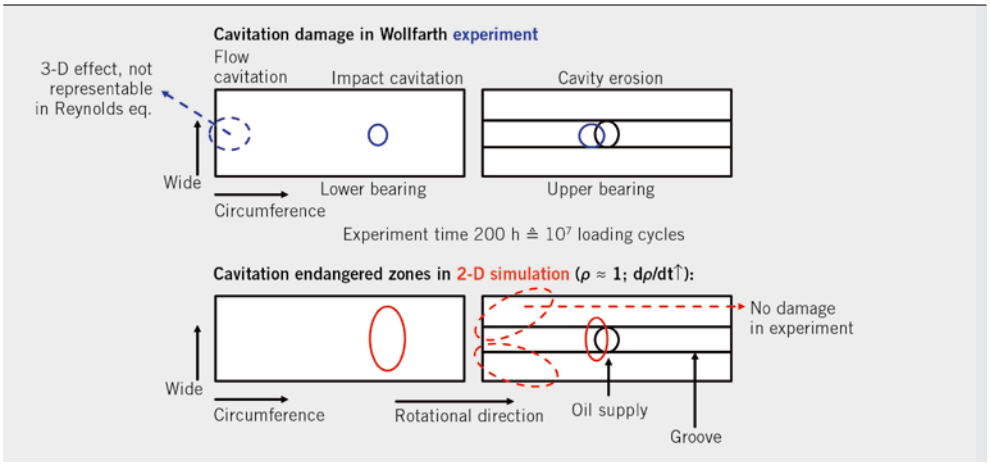

FIGURE 6 Comparison of cavitation damage between PhD thesis Wollfarth and Reynolds equation

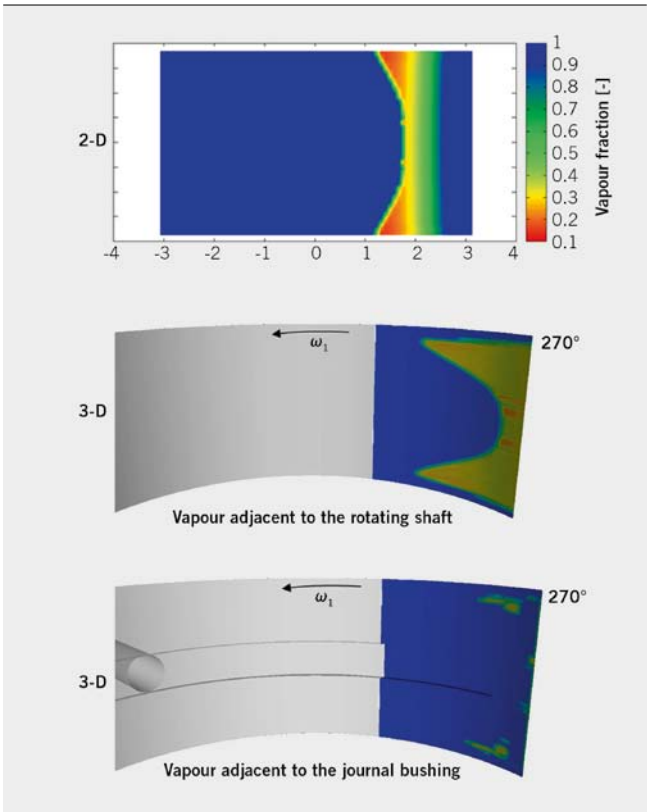

FIGURE 7 2-D EHD and 3-D CFD vapour fraction in real journal bearing in the divergent gap

by flow cavitation, when the oil overflowing the end of the groove in the convergent gap region and forms local three-dimensional flow structures, which is not predicted by the 2-D EHD simulation.

Furthermore, due the high flow velocities in the outlet feedhole there are regions were the static pressure drops below the vapour pressure and the formation of vapour bubbles begins. **FIGURE 9** presents the calculated 3-D vapour region in the outlet feedhole and the photo of the damage from [2]. Formed vapour bubbles remain inside the rotating feedhole and transported in rotational direction towards the region with the minimum gap, where the shaft is close to the bushing wall. In this case, when the bubbles implode adjacent to the bushing a typical impact cavitation damage is produced. Main feature is that the damage is in the size of the feedhole diameter. In order to investigate the influence of the supply pressure to the vapour distribution in the outlet feedhole, the supply pressure was gradually increased from 4 bar to 15 bar in the numerical calculations.

FIGURE 10 shows the normalised vapour fraction in the outlet feedhole above the oil supply pressure. With increasing pressure, the vapour fraction rises squarely up to four times of the initial value. Furthermore, it is illustrated that the distance of the vapour region to the bearing bushing decreases significantly. Due the higher supply pressure, the flow rate and thus the flow velocity is increased in the cross section of the feedhole. The high velocity results in a lowering of the local pressure. Furthermore, complex three-dimensional flow structures formed in the outlet feedhole. Both mechanisms, the increased vapour fraction and the smaller distance in the direction of the bearing bushing increase the potential risk of impact cavitation.

5 SUMMARY

This research project confirmed the validity of the Reynolds equation in regions narrow gap widths and some of the cavitation indicators with the help of the 3-D substructure model. In other regions the value of the 2-D results could be expanded by the use of the CFD models. These allow detailed analyses of flow patterns and cavitation danger which cannot be resolved by the Reynolds equation due to its two-dimensional nature. All three-dimensional CFD models were vali-

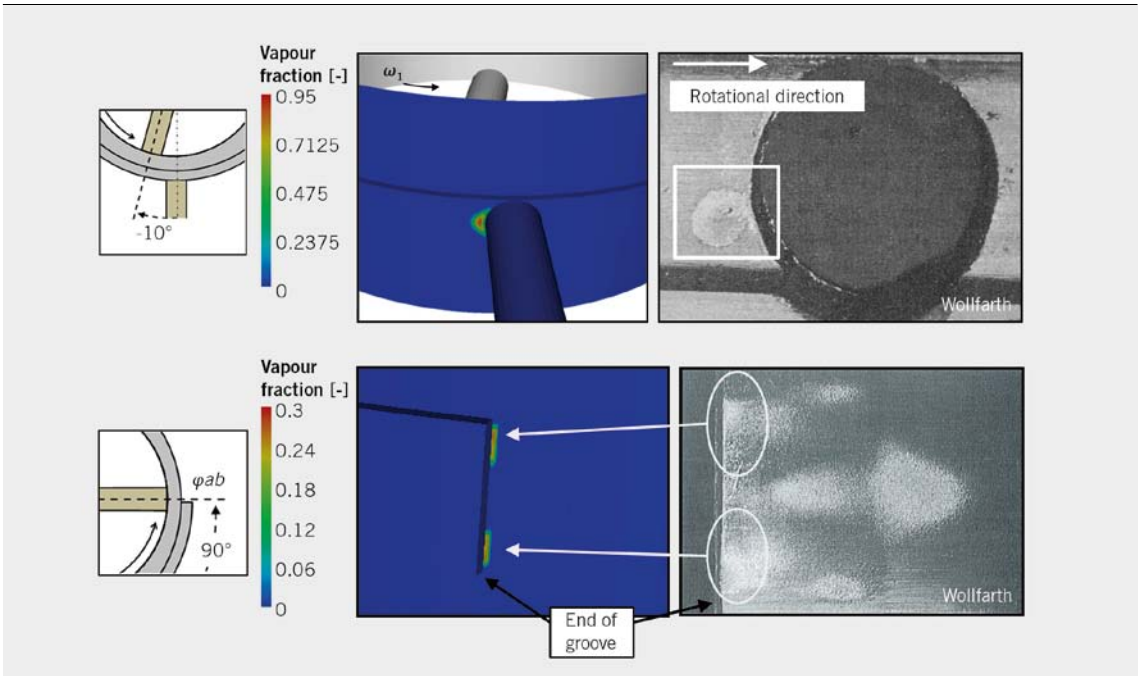

FIGURE 8 Effects of flow cavitation at the oil supply inlet and at the end of groove

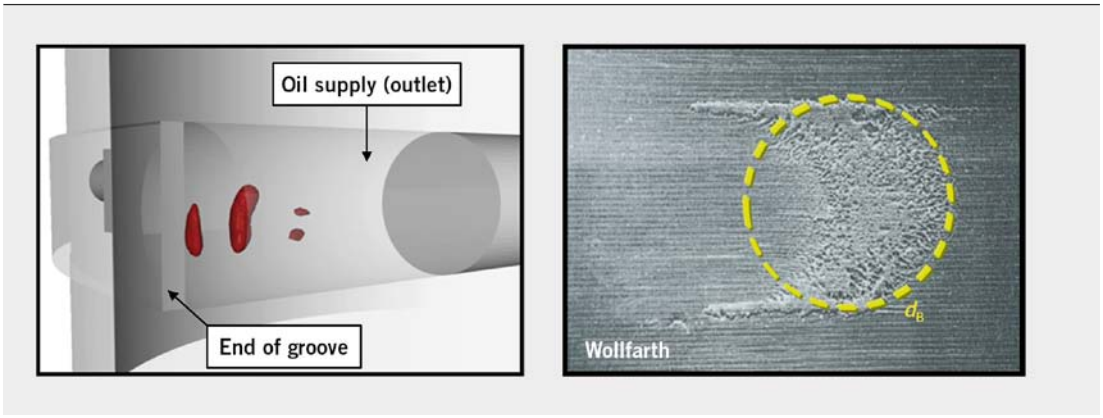

FIGURE 9 3-D CFD vapour fraction in real journal bearing in the outlet feedhole

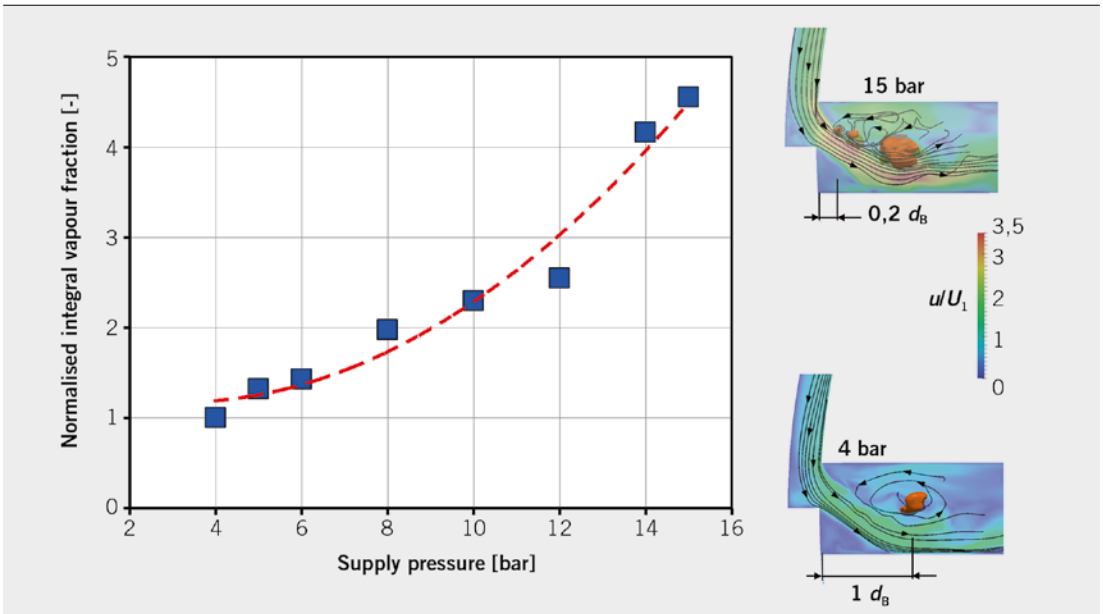

FIGURE 10 Vapour fraction in the outlet feedhole by variation of the supply pressure

dated against the experimental rig that was built up in this project. The performance of the CFD calculations could be demonstrated, too.

REFERENCES

[1] Reynolds, O.: On the Theory of Lubrication and Its Application to Mr. Beauchamp Tower's Experiments, Including an Experimental Determination of the Viscosity of Olive Oil. Philosophical Trans. of the Royal Society of London, Vol. 177, pp. 157-234, 1886

[2] Wollfarth, M.: Experimentelle Untersuchungen der Kavitationserosion im Gleitlager. Universität Karlsruhe, Dissertation, 1995

[3] Schnerr, G. H.; Sauer, J.: Physical and Numerical Modeling of Unsteady Cavitation Dynamics. Proc. 4th International Conference on Multiphase Flow, New Orleans, U.S.A., 2001

[4] Jakobsson, B.; Floberg, L.: The finite journal bearing considering vaporization. Transactions of Chalmers University of Technology, 1957

[5] Cupillard, S.; Glavatskih, S., Cervantes, M. J.: Computational fluid dynamics analysis of a journal bearing with surface texturing. Proceedings of the Institution of Mechanical Engineers, Part J, Journal of Engineering Tribology, 2008

[6] Knoll, G.; Longo, C.; Schlerege, F.; Brandt, S.; Lang, J.: Software-Entwicklungswerkzeuge zur reibungsoptimierten Auslegung von Kurbeltriebskomponenten. ATZ/MTZ conference "Reibungsminimierung", 2009

[7] Kumar, A.; Booker, J. F.: A Finite Element Cavitation Algorithm. ASME J. Tribol., 113 (2), pp. 276-286, 1991

THANKS

This research project (Nr. 16805 BG/2) was funded by the Federal Ministry for Economic Affairs and Technology (BMWi) on the basis of a decision by the German Bundestag over the German Federation of Industrial Research Associations Otto von Guericke e. V. (AiF) and the Research Association for Combustion Engines e. V. (FVV). The authors want to acknowledge the financial support and the support by the industrial commodity team directed by Frank Schmidt (MTU Friedrichshafen). Furthermore, the authors gratefully thank Prof. Dr.-Ing. Peter Reinke (Faculty of Natural Sciences and Technology, HAWK University Hildesheim/Holzminden/Göttingen) and Prof. Dr.-Ing. Adrian Rienäcker (Institute for Powertrain and Automotive Engineering, University of Kassel) for the support as heads of their research centres, as well as Andreas Christl (Ph.D. student at BTU Cottbus), Matthias Neben (Ph.D. student at BTU Cottbus), Dr. rer. nat. Nicoleta Herzog (ZHAW Zürich), Matthias Nobis (WHZ Zwickau), Marco Riedel (WHZ Zwickau), Prof. Dr.-Ing. habil. Gunther Knoll (iST GmbH, Aachen) and Dr.-Ing. Katja Backhaus (iST GmbH, Aachen), who all were involved in this project and brought it to success.

Heavy-Duty, On- and Off-Highway Engines

Sustainable concepts put to the test

10th International MTZ Conference
24 and 25 November 2015
Speyer | Germany

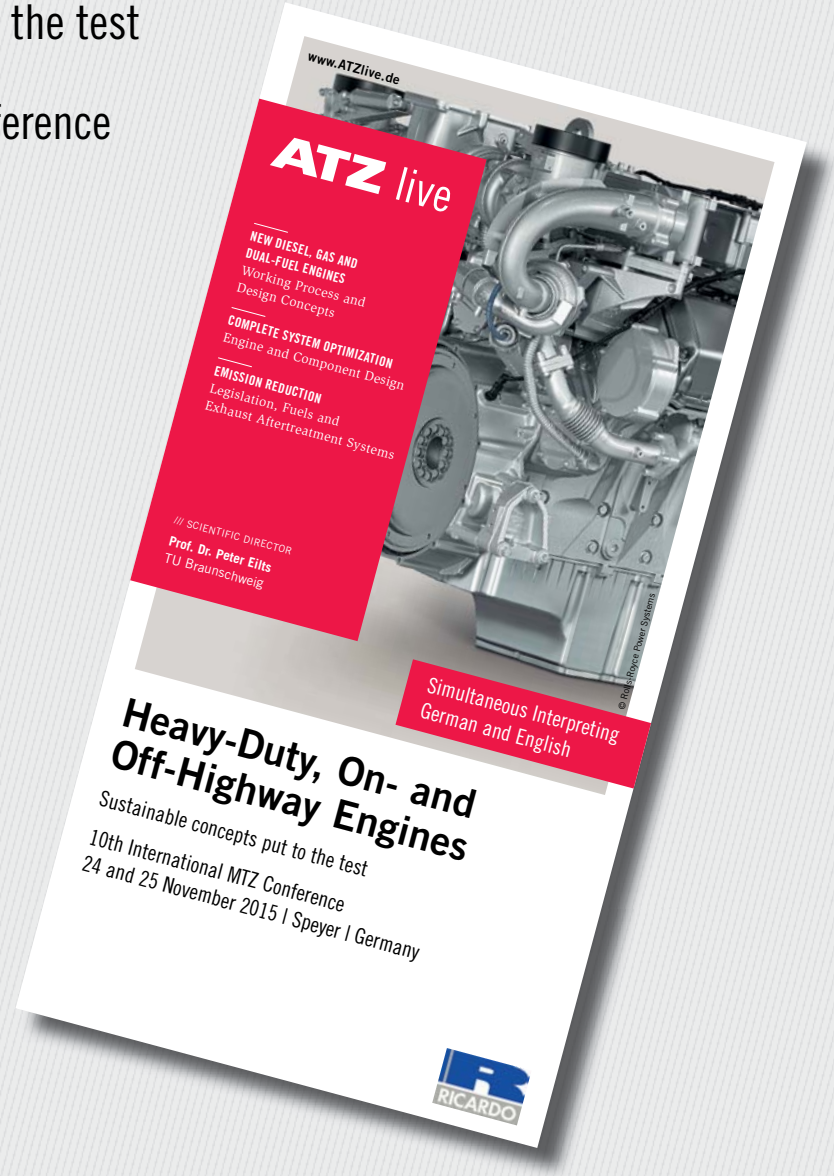

NEW DIESEL, GAS AND DUAL-FUEL ENGINES
Working Process and Design Concepts

COMPLETE SYSTEM OPTIMIZATION
Engine and Component Design

EMISSION REDUCTION
Legislation, Fuels and Exhaust Aftertreatment Systems

/// SCIENTIFIC DIRECTOR
Prof. Dr. Peter Eilts
TU Braunschweig

/// KINDLY SUPPORTED BY

RICARDO

ATZ live
Abraham-Lincoln-Straße 46
65189 Wiesbaden | Germany

Phone +49 611 7878-131
Fax +49 611 7878-452
ATZlive@springer.com

PROGRAM AND REGISTRATION
www.ATZlive.com

Twin-jet Sprays to Improve High-pressure Diesel Injection Systems

Single-hole diesel fuel injectors are considered with respect to their average drop size and onset time of their spray formation. To obtain better spray quality and higher dynamics for multiple fuel injections, for single-hole spray injectors a continuous injection pressure increase is required for diesel injection systems. This tendency of present developments imposes high demands on developments of high-pressure pumps and causes increases of the entire costs of the fuel injection system. The present investigations of FMP Technology GmbH point out that a different spray mechanism can be employed to yield an improved spray quality with a reduced injection pressure. This recommends itself as an alternative direction of development for diesel combustion engines for a reduction of the injection pressure to satisfy more stringent legal emission laws. This is theoretically considered in the paper and shown by experiments.

THE SEAL OF APPROVAL FOR SCIENTIFIC ARTICLES IN MTZ.
MTZ
PEER REVIEW
RECEIVED 2014-08-15
REVIEWED 2014-10-13
ACCEPTED 2015-03-12
REVIEWED BY EXPERTS FROM RESEARCH AND INDUSTRY.

AUTHORS

Prof. Dr. Dr. h.c. Franz Durst
is CEO and Shareholder of the FMP Technology GmbH in Erlangen (Germany).

Yu Han, M.Sc.
is Project Engineer at the FMP Technology GmbH in Erlangen (Germany).

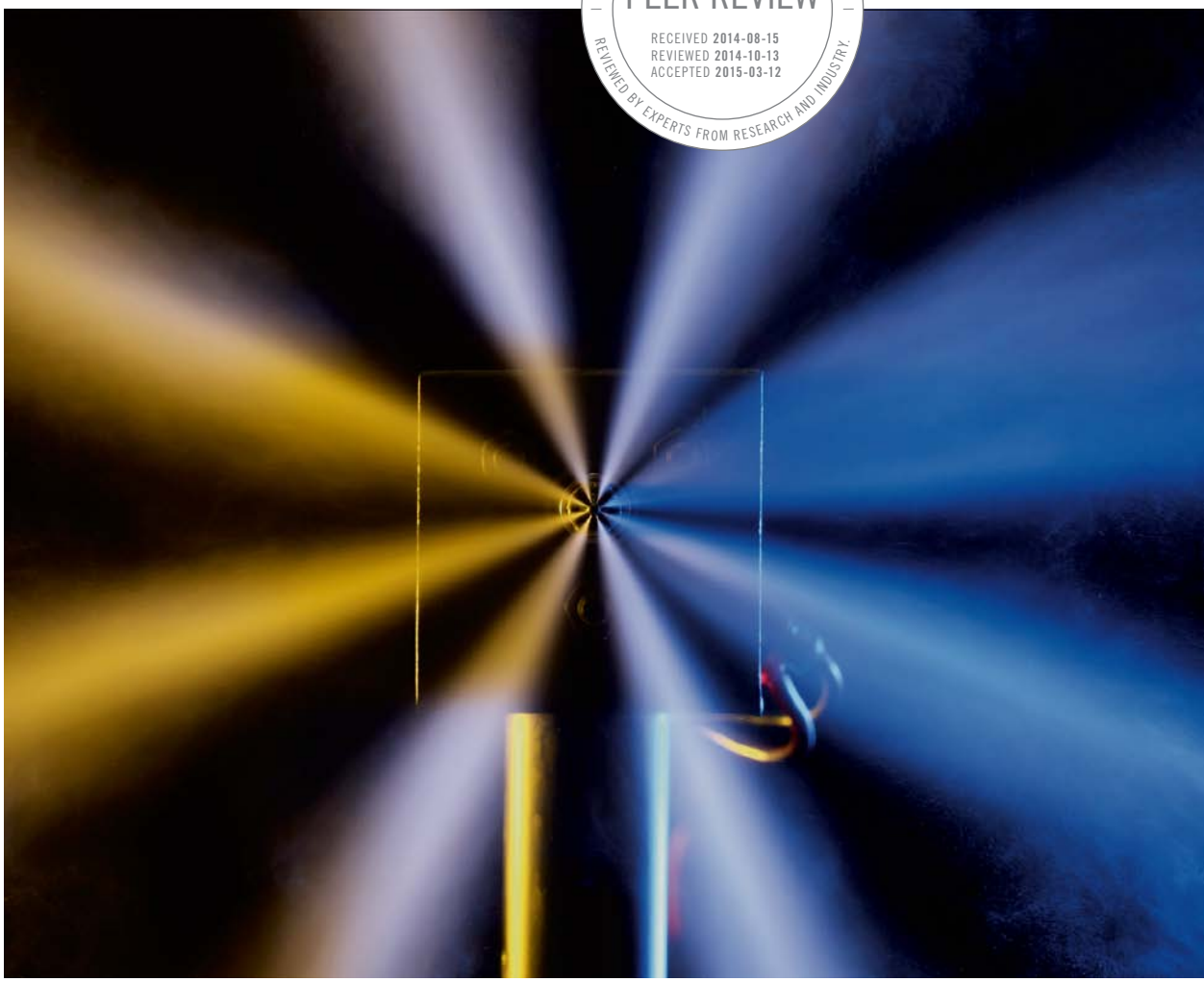

1 INTRODUCTION AND AIM OF THE WORK

It is recognised among experts that direct fuel injection has the greatest potential for future developments, with regard to both petrol engines and diesel engines, in order to meet existing and especially prospective technical requirements of combustion engines. These requirements comprise the reduction of pollutants and noise emissions with consideration of the individual road behaviour, the fuel consumption and, as a result, the CO_2 emissions of the vehicle. A solution to attain the reduction of emissions is the increase of injection pressure in diesel engines. A higher pressure offers a better atomisation quality and a higher spray factor, which leads to a better mixture generation. The higher the pressure, the shorter the injection time, but the pressure increase also renders a lot of problems, in particular the increase in system costs and in its complexity should be stated.

The solution of increasing the pressure is taken from the spray formation mechanism of liquid free jets. It is shown that the single-jet spray injectors currently on the market have properties such as, for instant, small spray taper angles (approximately 20°) and a concentration of the big drops in the centre of the spray. All of this leads to relatively late spray formations, after opening the valve. The increased length of spray formation time can be reduced for single-hole nozzles by raising the injection pressure applied in diesel engines. With a predefined opening time of a valve, the opening time until spray formation is reduced with increasing injection pressure. This leads to the observed continuously increasing injection pressures in diesel engines If, however, the mechanism of the spray production is changed so that the spray generation sets in much earlier, new ways of improving injection systems for diesel engines can be realised, as demonstrated by the authors' work. This paper also reports first experiments that confirm the derived advantages of twin-jet injection systems for diesel engines.

2 SINGLE AND TWIN-JET SPRAY GENERATORS

Ohnesorge [1] and Reitz [2] have shown in works that the decay of single liquid jets can be represented as a function of the Reynolds and Ohnesorge numbers of jets. They undertook similarity studies in order to show that the decay of liquid jets, as outlined in **FIGURE 1**, can generally be depicted in Ohnesorge–Reynolds diagrams. The Ohnesorge numbers characteristic of jets of petrol and diesel fuels, plotted in the diagram, demonstrate the jet formation and disintegration of jets of these fuels. Considering a diesel injector with a drilling diameter of 130 µm, the Reynolds number at which a complete disintegration of the single-jet sprays at the nozzle outlet takes place is approximately Re = 14577. This corresponds to an injection pressure of approximately 860 bar.

For twin-jet sprays,two liquid jets (petrol or diesel), generated by two nozzle apertures, are superimposed on each other at an angle of about 30 to 70° in order to generate a different kind of spray development (see Durst et al. [3]). If a dimensional analysis similar to that of the single jet is used, twin-jet sprays can also be plotted in an Ohnesorge-Reynolds diagram. **FIGURE 2** shows an example for a twin-jet spray with a collision angle of 90°. Now considering a twin-jet diesel injector with a drilling diameter of 130 µm and a collision angle of 90°, the Reynolds number at which a complete disintegration takes place is approximately Re = 841. This corresponds to an injection pressure of approximately 4.32 bar. **FIGURE 2** in comparison with **FIGURE 1** shows that, for petrol or diesel engines, the spray formation sets in earlier than for single-jet sprays. The relatively long time from the opening of the valve to the onset of spray generation, in the case of single-jet sprays, does not occur with twin-jet sprays. Twin-jet sprays have a shorter length of time between nozzle opening and spray generation. This has considerable advantages for their application in combustion engines. The achievable spray generation time amounts to approximately 25 µs.

3 TWIN-JET SPRAYS AND REQUIREMENTS OF DIESEL INJECTION SYSTEMS

The above mentioned Reynolds numbers of liquid jets, which have to be reached in order to achieve spray generation suitable for single- and twin-jet sprays define the onset times for the spray generations after opening the valve. On the basis of **FIGURE 1** and **FIGURE 2**, these periods of time can be calculated and, consequently, the time differences between single and twin-jet sprays can be demonstrated. This is presented below.

When the valve of an existing diesel engine injector is opened, the pressure on the inside of the injection aperture increases as a function of time until the common-rail pressure is reached. For this reason, the outlet velocity from the injection aperture increases continuously with time and, when it reaches a Reynolds number of Re ≈ 14577, the spray generation for single jet injectors sets in. This is equivalent to a pressure difference of approximately 860 bar

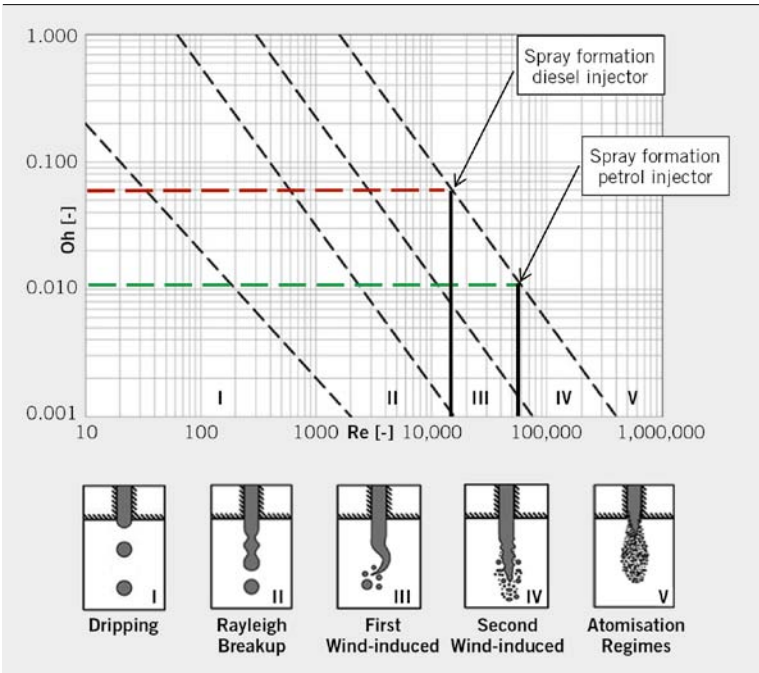

FIGURE 1 Ohnesorge-Reitz diagram for the purpose of generally depicting the decay of liquids

FIGURE 2 Oh-Re diagram for twin-jet sprays indicating the Reynolds numbers for spray formation (collision angle 90°)

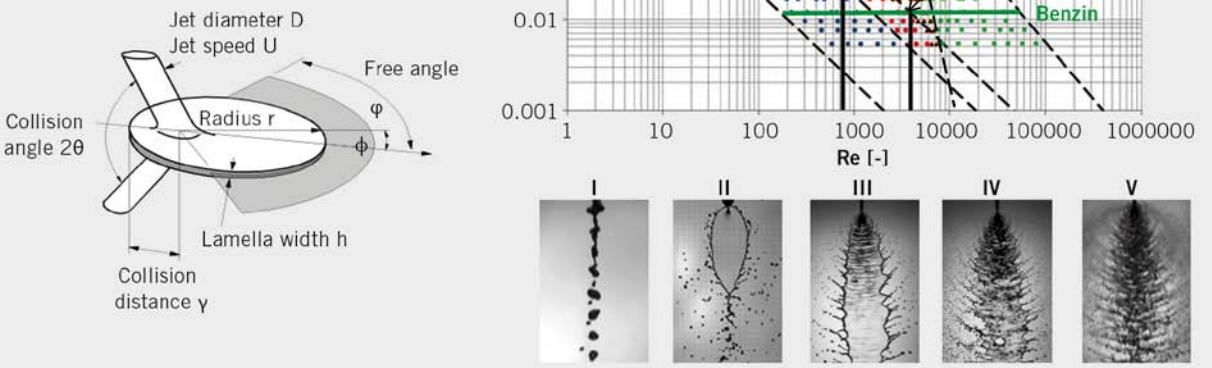

between the admission and the emission of the corresponding injector nozzle aperture, as shown in the previous section.

FIGURE 3 shows pressure gradients within a diesel injector during the opening time at different rail pressures. If an injector with a hole diameter of 130 µm is chosen, an Ohnesorge number of approximately Oh = 0.062 can be achieved for this nozzle–fluid combination with normal winter diesel. The transition line of the Reynolds number for the sprays required for good combustion can be shown by means of a correlation derived from the experimental measurements carried out by the authors for a single-jet spray injector:

Eq. 1	$2 \lg Oh + 2.5 \lg Re \geq 8$

Taking into consideration the pressure gradient, after opening a single jet valve, a "pressure build-up time" for the pressure required for spray generation can be determined. After this time

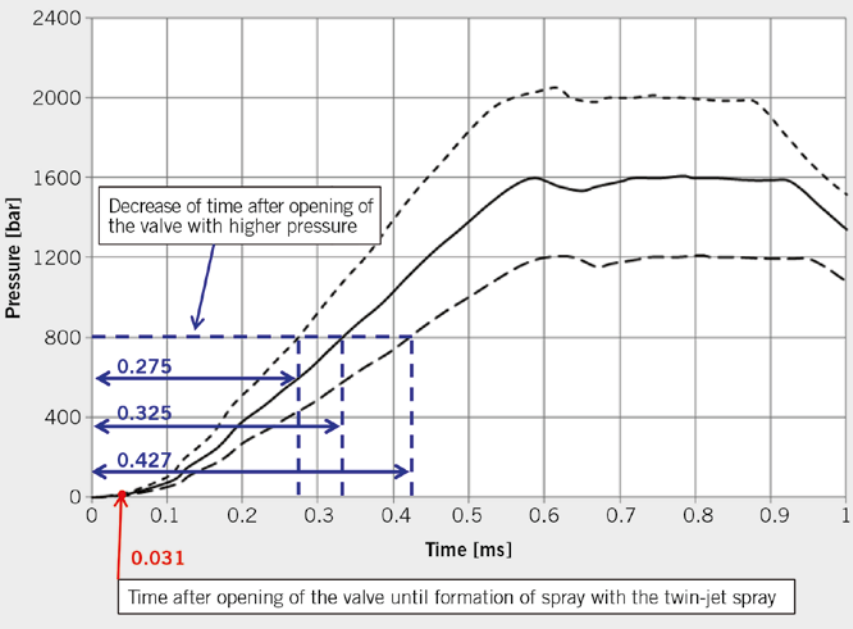

FIGURE 3 Pressure curve on the inside of a diesel injector against point of opening

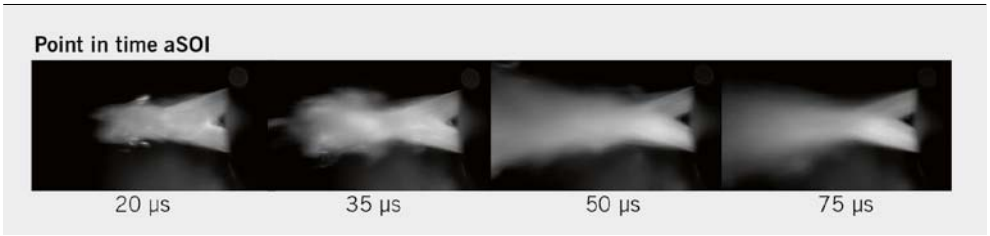

FIGURE 4 High-speed photograph of the opening process with twin-jet spray injector

the resultant spray properties are suitable for diesel combustion engines. These times are plotted in **FIGURE 3** as blue lines for different rail pressures. With increasing rail pressure, the time required to achieve a good spray formation, after opening the valve, decreases considerably. Hence, increasing pressures improve the combustion performance of the diesel engines of today.

The above discussion indicates that the spray development times for an observed single-jet spray injector decrease with increase in rail pressure, from 0.43 to 0.28 ms. If, however, a twin-jet spray injector is used for comparison, it is notable that atomisation sets in much earlier, as illustrated in **FIGURE 3**. It is possible to achieve spray generation sufficient for good combustion at low Reynolds numbers (i.e. in the areas IV and V of the corresponding Ohnesorge-Reynolds diagram), connected with spray onset times of less than 30 µs.

The Reynolds number of twin-jet sprays required for good spray generation can be calculated by means of the following correlation, which was derived from many systematic measurements carried out by the authors:

Eq. 2 $$\mathrm{Re}\cdot Oh \geq \frac{28.4}{\sin}\sqrt{1+\cos}$$

where θ is half the collision angle between the liquid jets of a twin-jet spray. By means of similar calculations to that which led to the times for single-jet spray injectors in **FIGURE 3**, the point in time for the required rail pressure can be determined for twin-jet sprays. For an injector applied by the authors in the diesel sector, a rail pressure sufficient for spray development was calculated to be approximately 4.32 bar. For this reason, the pressure build-up time of the considered twin-jet spray required for atomisation, sufficient for good combustion, is much shorter, as the times plotted in **FIGURE 3** show. This means that after only a very short period of time of about 0.03 ms after opening the valve the twin-jet spray generation is sufficient for good combustion in diesel engines.

The results deduced from **FIGURE 1** and **FIGURE 2** can be derived from the close-ups for the jet and spray development with twin-jet spray injectors. Twin-jet sprays are illustrated in **FIGURE 4**, and these photographs indicate that for this kind of spray generation the spray is formed after only 20 to 35 µs after opening the valve.

The above observations demonstrate furthermore that there are spray generation mechanisms that do not require the high common-rail pressures of existing diesel engines to produce sprays suitable for diesel combustion, after only a short period of time after valve opening. If such spray mechanisms additionally lead to drops that are smaller than those in conventional injectors, then the spray is highly suitable for the injection of diesel fuel into the combustion engine. **FIGURE 5** shows that twin-jet sprays possess small droplet size as required for good diesel combustion.
From further considerations, as to which rail pressure is suitable for both injectors, the measurements of the Sauter mean diameter of liquid droplets produced by twin-jet spray generators, given in **FIGURE 6**, show that values from 400 to 600 bar are sufficient to produce sprays suitable for diesel engine combustion. In the range from 600 to 800 bar, the twin-jet spray shows an increase in d_{32} diameters and after approximately 800 bar d_{32} starts to decrease

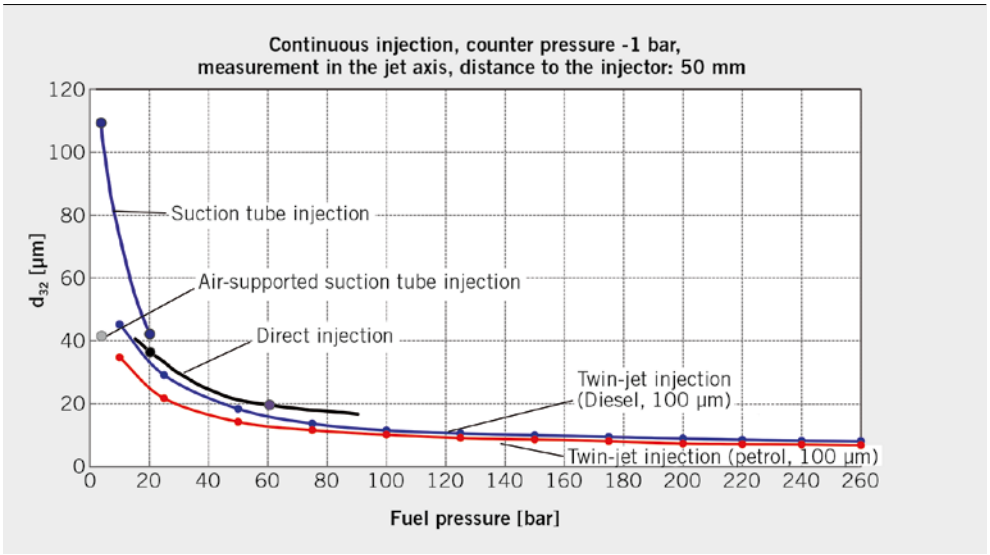

FIGURE 5 Droplet size distributions for different methods of spray generation

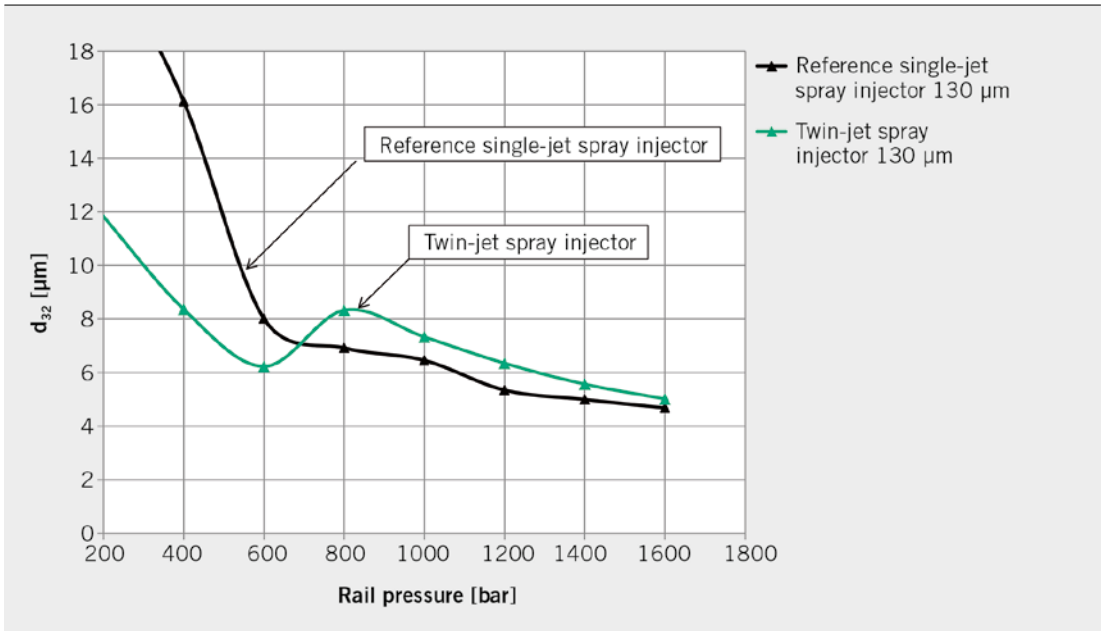

FIGURE 6 Sauter mean diameter of twin-jet sprays as a function of the injection pressure

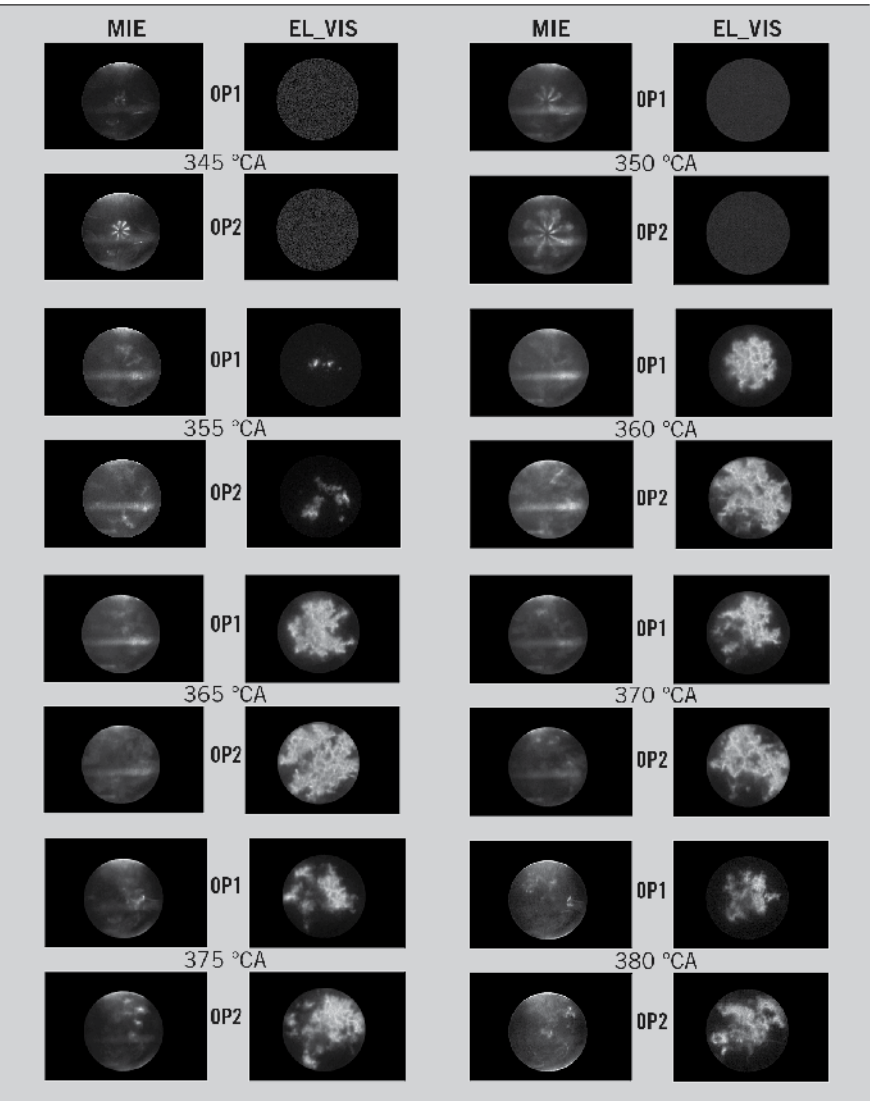

FIGURE 7 Mie and EL_VIS photograph of the combustion process with a twin-jet spray injector

again together with the pressure. The reason for this is that, at a pressure of over 600 bar, spray is already generated within the two jets before their collision. The superimposition of the two jets leads to a higher d_{32} for the entire spray. If the pressure is further increased, to more than 800 bar, d_{32} of the overlapping sprays also decreases. However, the resultant d_{32} diameter is slightly bigger than that of single-jet sprays.

Another important factor in choosing the injector pressure of twin-jet sprays is the injection volume per injection. Under the same injection conditions, twin-jet spray injectors require two drillings to generate a spray lobe. It is possible to derive from the equations that, as a result, these injectors only require $\Delta P/4$ in order to reach the same injection volume as single-jet spray injectors at ΔP. The above discussion shows that a pressure in the range of 400 to 600 bar is sufficient to provide the required amount of fuel for diesel engine combustion without an increase in the diameter of the injection aperture and using the same injection times.

Eq. 3

$$\dot{M}_{ES} = \frac{\pi D^2}{4} C_{dis} \sqrt{\frac{2\Delta P}{\rho}} \Delta t = 2 \dot{M}_{ZS}$$

The production of twin-jet spray injectors has been launched by the authors and cooperating companies in several projects. The steels required for injection pressures of 400 to 600 bar allow mechanical drilling to produce prototypes of twin-jet diesel injectors. The injectors utilised for testing purposes were manufactured correspondingly. Second, "wire-cut electric discharge machining (EDM)" can be applied for the manufacture of suitable injectors, as used in the ongoing operations at FMP Technology. Furthermore, the company has access to a drilling system working with picosecond lasers, so that it can be expected that the FMP

FIGURE 8 Drillings of a twin-jet prototype for testing purposes

OP	Rotational speed [rpm]	Injection pressure [bar]	SOI [°CA]	T_{gas} [K]	P_{gas} [bar]
1	1500	100	340	298	1
2		200			

TABLE 1 Parameters of the investigations of the engine

developments can be continued towards the serial production. It is some long-term experiments and extensive usage of twin-jet injectors in diesel combustion engines that still need to be carried out.

The twin-jet spray method has already been described by the authors, see [3, 4], but at the time of publication no experimental data were available that would demonstrate the use of this method in diesel combustion engines. Since then, the authors have been able to carry out investigations on single cylinder engines. The results obtained in these experiments are depicted as a time sequence of photographs taken inside of a "glass engine". The parameters applied in these investigations are indicated in **TABLE 1**. The measurement technique utilised was the Mie light scattering method for the purpose of visualising liquid fuels and flame properties in the spectral range of light (EL_VIS), in order to detect the combustion. The diesel fuel was injected into a transparent test engine under the conditions mentioned tabulated in **TABLE 1**, and the photographs were taken using two optical systems.

It can be deduced from the discussion, **TABLE 1**, and from the previous publication [4] that twin-jet sprays form so-called spray fans, i.e. no round spray jets are developed, but rather a two-dimensional spray distribution, which lead only to elliptical jet shapes under high pressure. Therefore, the oxygen required for combustion can easily reach the centre of the spray, where it mixes with the fuel in order to provide the mixture necessary for combustion.

Moreover, twin-jet sprays stand out owing to their small droplet sizes in the spray, which are already developed at small injection pressures. For this reason, it is possible to obtain very good combustion conditions with twin-jet injectors. With injection pressures of only 400 to 600 bar, very good conditions are obtained for diesel engine combustion. In addition, the combustion initialised in such a way is advantageous because it progresses from the inside of the cylinder to the outside, i.e. the combustion, in its ignition phase, is not initialised by a large part of the combustion chamber, but begins with a small flame that spreads to the outside at a high combustion speed. **FIGURE 7** shows combustion tests in a one cylinder diesel engine at reduced injection pressure. The complete combustion can be observed within a crank angle of 35°, both at 100 and 200 bar. Contrary to this, the mixture generated at 100 bar with a multi-hole single-jet injector cannot be ignited.

4 CONCLUSION

The investigations described in this paper show that single-jet sprays need a long period of time, after opening of the injector valve, to generate a spray, in some cases 200 to 400 µs. The pressure in the pre-chamber of the injection jet has to be increased to about 800 bar before the spray formation leads to a suitable droplet size distribution. This is shown with the help of the Ohnesorge-Reitz diagram, which can be used for both petrol and diesel engine injection. By means of the twin-jet spray technique, the common rail pressure required for good spray formation can be reduced to approximately 30 µs. At the same time, the pressure build-up phase can be abbreviated yielding faster spray formation after opening the injector valve. The present results indicate that the application of twin-jet spray injectors has great advantages for diesel engine combustion, and, therefore, it is suggested that they be utilised in such systems. **FIGURE 8** shows that prototypes of twin-jet injectors can be manufactured. Efforts are currently being made to prepare them for serial production.

REFERENCES

[1] Reitz, R.D.; Bracco, F.V.: Mechanisms of breakup of round liquid jets. In: The Encyclopedia of Fluid Mechanics (1986), No. 3, Chapter 10, pp. 233-249
[2] Ohnesorge, W.: Die Bildung von Tropfen an Düsen und die Auflösung flüssiger Strahlen. In: Zeitschrift für angewandte Mathematik der Mechanik (1931), No. 16, pp. 355-358
[3] Durst, F.; Han, Y.; Handtmann, A.; Zeilmann, M.: Experimental and theoretical investigations of Twin-Jets. In: ICLASS 2012, 12th Triennial International Conference on Liquid Atomization and Spray Systems (2012), Heidelberg, Germany
[4] Durst, F.; Handtmann, A.; Weber, M.; Schmid, F.: Twin-Jet nozzle injectors for gasoline engines. In: MTZ (2012), No. 6, pp. 34-40